

12



RADC-TR-85-255
Final Technical Report
January 1986

AD-A165 280

LUMPED-ELEMENT AND LEAKY-WAVE ANTENNAS FOR MILLIMETER WAVES

Polytechnic Institute of New York

A. A. Oliner

DTIC
SELECTED
MAR 18 1988
S D

APPROVED FOR PUBLIC RELEASE; DISTRIBUTION UNLIMITED

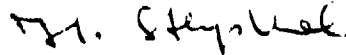
DTIC FILE COPY

ROME AIR DEVELOPMENT CENTER
Air Force Systems Command
Griffiss Air Force Base, NY 13441-5700

This report has been reviewed by the RADC Public Affairs Office (PA) and is releasable to the National Technical Information Service (NTIS). At NTIS it will be releasable to the general public, including foreign nations.

RADC-TR-85-255 has been reviewed and is approved for publication.

APPROVED:



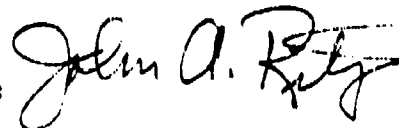
HANS P. STEYSKAL
Project Engineer

APPROVED:



ALLAN C. SCHELL
Chief, Electromagnetic Sciences Division

FOR THE COMMANDER:



JOHN A. RITZ
Plans & Programs Division

If your address has changed or if you wish to be removed from the RADC mailing list, or if the addressee is no longer employed by your organization, please notify RADC (EEA) Hanscom AFB MA 01731. This will assist us in maintaining a current mailing list.

Do not return copies of this report unless contractual obligations or notice on a specific document requires that it be returned.

PAGES _____
ARE
MISSING
IN
ORIGINAL
DOCUMENT

REPORT DOCUMENTATION PAGE

| | | | | | | |
|---|-------|---|--|--|----------------------------------|-------------------------------|
| 1a. REPORT SECURITY CLASSIFICATION UNCLASSIFIED | | | 1b. RESTRICTIVE MARKINGS N/A | | | |
| 2a. SECURITY CLASSIFICATION AUTHORITY N/A | | | 3. DISTRIBUTION / AVAILABILITY OF REPORT Approved for public release; distribution unlimited | | | |
| 2b. DECLASSIFICATION / DOWNGRADING SCHEDULE N/A | | | 4. PERFORMING ORGANIZATION REPORT NUMBER(S) N/A | | | |
| 4. PERFORMING ORGANIZATION REPORT NUMBER(S) N/A | | | 5. MONITORING ORGANIZATION REPORT NUMBER(S) RADC-TR-85-255 | | | |
| 6a. NAME OF PERFORMING ORGANIZATION Polytechnic Institute of New York | | 6b. OFFICE SYMBOL (if applicable) | | 7a. NAME OF MONITORING ORGANIZATION Rome Air Development Center (EPA) | | |
| 6c. ADDRESS (City, State, and ZIP Code) 333 Jay Street Brooklyn NY 11201 | | | 7b. ADDRESS (City, State, and ZIP Code) Hanscom AFB MA 01731 | | | |
| 8a. NAME OF FUNDING / SPONSORING ORGANIZATION Rome Air Development Center | | 8b. OFFICE SYMBOL (if applicable) EEA | | 9. PROCUREMENT INSTRUMENT IDENTIFICATION NUMBER F19628-81-K-0044 | | |
| 8c. ADDRESS (City, State, and ZIP Code) Hanscom AFB MA 01731 | | | 10. SOURCE OF FUNDING NUMBERS | | | |
| | | | PROGRAM ELEMENT NO. 62702F | PROJECT NO. 2305 | TASK NO. J3 | WORK UNIT ACCESSION NO. 30 |
| 11. TITLE (Include Security Classification) LUMPED-ELEMENT AND LEAKY-WAVE ANTENNAS FOR MILLIMETER WAVES | | | | | | |
| 12. PERSONAL AUTHOR(S) A.A. Oliner | | | | | | |
| 13a. TYPE OF REPORT Final | | 13b. TIME COVERED FROM _____ TO _____ | | 14. DATE OF REPORT (Year, Month, Day) January 1986 | | 15. PAGE COUNT |
| 16. SUPPLEMENTARY NOTATION N/A | | | | | | |
| 17. COSATI CODES | | | 18. SUBJECT TERMS (Continue on reverse if necessary and identify by block number) | | | |
| FIELD | GROUP | SUB-GROUP | Millimeter waves Leaky wave antennas | | | |
| 09 | 01 | | Antennas Transverse equivalent network | | | |
| 09 | 05 | | Groove guide Nonradiative dielectric (NRD) guide | | | |
| 19. ABSTRACT (Continue on reverse if necessary and identify by block number) | | | | | | |
| <p>Some millimeter wave antennas can be scaled from their microwave frequency counterparts, but others cannot because of two main problems; the small wavelengths, which require small waveguide dimensions and pose fabrication difficulties, and higher metal loss. This contract was concerned with those antennas that cannot be scaled successfully, and it concentrated on novel leaky wave antennas. The first of the problems mentioned above was overcome by choosing structures with longitudinally continuous apertures, and the second by basing the antennas on low-loss waveguides. Two such waveguides were selected: the groove guide, and nonradiative dielectric (NRD) guide.</p> <p>Six different leaky wave antennas were analyzed on this program, with two treated in special detail. Three different mechanisms for producing leakage were employed: asymmetry, fore-shortening the structure's cross section, and using leaky higher modes. The different mechanisms also lead to different polarizations of the radiated fields.</p> <p style="text-align: right;">(Cont'd on reverse)</p> | | | | | | |
| 20. DISTRIBUTION / AVAILABILITY OF ABSTRACT <input checked="" type="checkbox"/> UNCLASSIFIED/UNLIMITED <input type="checkbox"/> SAME AS RPT. <input type="checkbox"/> DTIC USERS | | | | 21. ABSTRACT SECURITY CLASSIFICATION UNCLASSIFIED | | |
| 22a. NAME OF RESPONSIBLE INDIVIDUAL Hans P. Stevskal | | | 22b. TELEPHONE (Include Area Code) (617) 861-2052 | | 22c. OFFICE SYMBOL RADC (EPA) | |

UNCLASSIFIED

Accurate theoretical analyses were conducted for each of the antenna structures. Transverse equivalent networks were established, the elements of which were derived in closed form, so that the dispersion relations were also. Numerical values for the propagation characteristics were obtained as a function of various geometric parameters, to aid in the design of antennas based on these leaky structures. Special design considerations, including optimization procedures, were also developed where possible. In the case of the foreshortened top antenna based on NRD guide, detailed measurements were also taken, which showed very good agreement with our theory.

This comprehensive final report contains detailed discussions on all of these antennas, including the derivations of the theoretical expressions and typical numerical results.

UNCLASSIFIED

TABLE OF CONTENTS

| | <u>Page</u> |
|---|-------------|
| <u>PART I. BACKGROUND AND EARLY WORK</u> | |
| A. INTRODUCTION | 1 |
| 1. Scope of Program | 1 |
| 2. Mechanisms Used to Produce Leakage | 6 |
| 3. List of Publications and Presentations | 8 |
| B. LOW-LOSS WAVEGUIDES | 10 |
| 1. General Remarks | 10 |
| 2. NRD Guide | 11 |
| 3. Groove Guide | 15 |
| C. SOME GENERAL PROPERTIES OF LEAKY WAVE ANTENNAS | 19 |
| D. IMPROVED SOLUTION FOR THE DOMINANT MODE OF OPEN GROOVE GUIDE | 22 |
| <u>PART II. ANTENNAS BASED ON GROOVE GUIDE</u> | |
| A. THE ASYMMETRIC STRIP ANTENNA | 35 |
| 1. Summary of Principal Features | 36 |
| 2. Discussion of Comprehensive Report | 41 |
| B. THE LEAKY MODE SPECTRUM OF GROOVE GUIDE | 43 |
| 1. Summary of Principal Features | 45 |
| 2. Derivations for the $n = 3$ (Odd) Leaky Mode | 55 |
| (a) Wavenumber Considerations to Demonstrate Leakage | 55 |
| (b) The Mode Functions and the Field Components | 57 |
| (c) Turns Ratios for the Step Junction | 60 |
| (d) The Coupling Network at the Step Junction | 60 |
| (e) The Dispersion Relation | 63 |

| | <u>Page</u> |
|--|-------------|
| 3. Derivations for the $n = 2$ (Even) Leaky Mode | 64 |
| (a) Wavenumber Considerations to Demonstrate Leakage | 64 |
| (b) The Mode Functions and the Field Components | 65 |
| (c) Turns Ratios for the Step Junction | 69 |
| (d) The Coupling Network at the Step Junction | 69 |
| (e) The Dispersion Relation | 71 |
| C. ANTENNAS BASED ON THE $n = 2$ LEAKY MODE | 72 |
| 1. Antenna of Simple Configuration | 72 |
| 2. Antenna with Added Strips | 77 |
| D. ALTERNATIVE THEORETICAL APPROACH FOR THE $n = 2$ LEAKY MODE ANTENNA | 82 |
| <u>PART III. ANTENNAS BASED ON NRD GUIDE</u> | 95 |
| A. THE FORESHORTENED-TOP ANTENNA: ACCURATE ANALYSIS AND NUMERICAL RESULTS | 101 |
| 1. Summary of Principal Features | 102 |
| 2. Derivations of the Constituents of the Transverse Equivalent Network | 107 |
| (a) The Modes Employed | 108 |
| (b) The Air-Dielectric Interface | 112 |
| (c) The Radiating Open End | 116 |
| (1) Summary of Weinstein's Formulation | 117 |
| (2) Analytic Continuations | 120 |
| (d) The Dispersion Relation for the Leaky Mode | 124 |
| 3. Numerical Results | 125 |
| B. THE FORESHORTENED-TOP ANTENNA: PERTURBATION ANALYSES | 131 |
| 1. Procedure Based on the Transverse Equivalent Network | 132 |
| 2. Simpler, Reflection Coefficient, Procedure | 137 |
| 3. Comparisons with Accurate Analysis | 141 |

| | <u>Page</u> |
|--|-------------|
| C. THE FORESHORTENED-TOP ANTENNA: MEASUREMENTS | 149 |
| 1. Measurement Procedure | 152 |
| 2. Measurements Taken by Yoneyama | 159 |
| 3. Comparisons with Theory | 162 |
| D. NEW ASYMMETRIC ANTENNA | 170 |
| 1. Principle of Operation | 171 |
| 2. Analysis and Numerical Results | 173 |

REFERENCES

179

APPENDICES

APPENDIX A: THE DOMINANT MODE PROPERTIES OF OPEN
GROOVE GUIDE: AN IMPROVED SOLUTION
by A. A. Oliner and P. Lampariello

APPENDIX B: A NEW LEAKY WAVE ANTENNA FOR MILLIMETER
WAVES BASED ON THE GROOVE GUIDE
by P. Lampariello and A. A. Oliner



| | |
|---------------------|-------------------------------------|
| Accession For | |
| NTIS CRA&I | <input checked="" type="checkbox"/> |
| DTIC TAB | <input type="checkbox"/> |
| Unannounced | <input type="checkbox"/> |
| Justification | |
| By | |
| Distribution / | |
| Availability Codes | |
| Dist | Avail and/or Special |
| A-1 | |

PART I. BACKGROUND AND EARLY WORK

A. INTRODUCTION

1. Scope of Program
2. Mechanisms Used to Produce Leakage
3. List of Publications and Presentations

B. LOW-LOSS WAVEGUIDES

1. General Remarks
2. NRD Guide
3. Groove Guide

C. SOME GENERAL PROPERTIES OF LEAKY WAVE ANTENNAS

D. IMPROVED SOLUTION FOR THE DOMINANT MODE OF OPEN GROOVE GUIDE

A. INTRODUCTION

1. Scope of Program

Antennas for millimeter waves fall into two broad categories: those that can be successfully scaled from their microwave frequency counterparts, and those that cannot. In the first category, one would place reflectors, lenses and horns. The small size in fact enhances their attractiveness, since higher directivity can be achieved with small size. The second category includes such antennas as slot arrays, leaky wave antennas, and phased arrays. This contract is concerned with antennas in the second category.

Millimeter wave antennas present particular challenges because of two main problems. The first problem relates to the small wavelengths involved, requiring antennas of smaller size. For certain types of antennas this feature is a boon, but for others it presents a greater difficulty of fabrication. The second problem is higher metal loss. For components which are about a wavelength long, the higher loss does not produce much of a problem, so that useful millimeter wave integrated circuitry can be designed up to 100 GHz or so using such relatively lossy guides as microstrip or finline. For antennas that employ traveling waves, on the other hand, the antenna lengths may be typically 20 to 100 wavelengths long, and the waveguide loss may compete with the leakage, or radiation, loss, thereby distorting or upsetting the antenna design.

The smaller size and higher loss can cause problems for antennas in the second category mentioned above, so that direct scaling from known microwave designs is not suitable for such antennas. It is therefore necessary to seek novel structures or modifications of known structures as the basis for new antennas. This recognition has furnished the motivation for the research program on this contract.

The contract proposal contained many suggestions for such new antennas, including lumped-element radiators that could serve as elements in phased

arrays, and new types of leaky wave antennas. The title of the contract reflects this broad scope of possible new antenna structures. Of the various possible directions we could pursue, we chose first to explore novel antennas of the leaky wave type. This choice was dictated in part by our past experience with such antennas and in part because leaky wave antennas form a natural class of antennas for millimeter waves, in view of the small size of waveguides in the millimeter wavelength range. In addition, such antennas can be used as elements in a phased array in which the array is comprised of leaky wave line sources all parallel to each other and fed from one end, with phase shifts between them to produce scanning in the cross plane.

We were successful almost immediately in our study of novel leaky wave antennas. Because of the results achieved, and the further promise evident, we wrote in Quarterly Status Report No. 5: "...the studies so far have turned out to be very productive, with several new antennas emerging from them. Because of the success achieved already, and because of the indications that additional antennas with different properties are also possible, we feel that it is best for us to continue along these lines rather than to diversify and explore other structures." In this context, we discussed this matter with the contract's Scientific Program Officer, Dr. Hans Steyskal, and he gave his approval for this change in the stress, and therefore in the scope, of this contract's activities. Despite the original title, therefore, this Final Report does not cover any lumped-element investigations, but describes the accomplishments in connection with several new types of leaky wave antennas.

On the other hand, it should be noted that the original proposal addressed only theoretical investigations, and did not contain any experimental phase. In the course of the studies on one of these new leaky wave antennas, however, it became desirable to take measurements of the leakage constant. Approval was also given by Dr. Steyskal to modify the scope of the contract to add this experimental phase, since such measurements would improve the content and quality of the scientific program. The need for such measurements, and details regarding both the measurement method and

the results of those measurements, are contained in Part III, Section C, of this Final Report.

Leaky wave antennas for the millimeter wave range face the two main problems mentioned earlier. The first relates to the small wavelengths involved, which require small waveguide dimensions and pose fabrication difficulties. The second problem is higher metal loss; for antennas which are many wavelengths long, the leakage (which results in radiation) may compete with the intrinsic waveguide loss, and the antenna design can be adversely affected. We overcome the first of these problems by considering leaky wave structures with longitudinally-continuous apertures, and the second by basing the antennas on low-loss waveguides. These are the two principal features that characterize all of the new antennas discussed here.

Of the possible low-loss waveguides that have been proposed over the years, we have selected two on which to base our new leaky wave antennas: the groove guide and the nonradiative dielectric (NRD) guide. In order to assist the reader who may not be familiar with the properties of these two waveguides, we present in Sec. B of Part I some general remarks about low-loss millimeter waveguides, and then some specific background on NRD guide and groove guide and their relations to H guide.

A leaky wave antenna is basically an open waveguide possessing a mechanism that permits a slow leakage of power along the length of the waveguide. This slow leakage is characterized by a phase constant β and a leakage constant α , and these quantities are the end products of any analysis of a leaky wave structure. The relations between β and α and the properties of an actual leaky wave antenna, such as the angle of maximum radiation, the beam width, and the side lobe distribution, are standard. For the convenience of the reader, some general properties of leaky wave antennas, and their relations to β and α , are summarized in Sec. C of Part I.

Several different mechanisms have been introduced to produce the necessary leakage. These mechanisms include asymmetry, foreshortening of the structure, and leaky higher modes. The first two approaches apply to antennas based on both the groove guide and the NRD guide, but the third one is suitable only for the groove guide. The polarization of the radiated fields can also be changed according to the mechanism selected. Further details regarding these different mechanisms are presented in subsection 2 of this Introduction.

For each of the leaky structures analyzed, we have developed the appropriate transverse equivalent network, and we have derived accurate, yet closed-form, expressions for each constituent of the networks. As a result, the dispersion relation for the propagation properties (α and β) for each antenna is also obtained in closed form. Calculations were then made which show that the antennas are feasible, and they also indicate how the propagation properties depend on the frequency and on various geometric parameters. From this information, optimum designs for each antenna type can be deduced.

Six different leaky wave antenna structures have been analyzed on this program (four based on groove guide and two on NRD guide), but not all have received equal treatment in depth. The two which have received the greatest attention have been the asymmetric strip antenna based on groove guide and the foreshortened-top antenna using NRD guide. Complete analyses have been obtained for all six structures, however, and derivations as well as some numerical data are presented here for each.

This Final Report is divided into three parts, as may be seen from the Table of Contents. Part I is devoted to introductory remarks, such as those above, and some background material to place the studies in better perspective. Comments were made above with respect to Secs. B and C of Part I. Also included in Part I is Sec. D, which is of a different nature. As the first stage in the analysis of the asymmetric strip antenna based on groove guide, we found it desirable to obtain an improved solution for

the properties of the dominant (bound) mode of groove guide. That solution was later incorporated into the transverse equivalent network for the asymmetric strip antenna. That early study on this program was very thorough and very successful, and it constitutes a contribution in its own right. A short version of that work appears in a symposium digest, and a longer version has been accepted for publication. Since this work represents an accomplishment on this program, it must be included here, but since it is not directly an antenna study (although it underlies it) it is placed into Part I. Actually, the short version appears as Sec. D, and the longer paper constitutes Appendix A.

Parts II and III are devoted to the various leaky wave antennas based on groove guide and on NRD guide, respectively. The order of the presentations and the detailed listings of the contents are presented both in the overall Table of Contents and in the partial ones appearing at the beginning of each part. We shall not repeat them here. As an aid to the reader, however, summaries are presented at the beginnings of Parts II and III, indicating what is included and what is important. Further summaries, containing increased levels of detail, are to be found at the beginning of each section. It is recommended that these summaries be read first to obtain a good idea of the overall effort and to learn where to look for what.

Earlier on this contract, an Interim Scientific Report was issued, and a comprehensive report was submitted on the new asymmetric strip leaky wave antenna based on groove guide. Since this latter report has not yet appeared, it is included in this Final Report as Appendix B. It is included here for two reasons: first, for completeness, and, second, because heavy reference is made to portions of it in connection with other, later studies, and this material would otherwise need to be repeated.

The various investigations on this contract have also resulted in a number of publications and presentations at professional society meetings, with short papers appearing in the proceedings or digests associated with

those meetings. In many cases those short papers represent excellent introductions to the work and summaries of the results obtained. Because of their utility in this connection, use has been made here of such short papers, and they have been incorporated in context in Parts II and III. Five such short papers are included, two in Sec. A, 1 and two in Sec. B, 1 of Part II, and one in Sec. A, 1 of Part III. A complete list of the publications and presentations appears in subsection 3 of this Introduction.

The author of this Final Report has been the Principal Investigator of this program. General technical assistance has been provided by Prof. S. T. Peng, and detailed contributions have been made by Dr. P. Lampariello, now an Associate Professor at the University of Rome, Italy, and previously a NATO Postdoctoral Fellow who spent a year with us at the Polytechnic Institute of New York, Dr. A. Sanchez, a Ph.D. student who received his doctorate in June 1983, and Mr. Q. Han, another student. Dr. Lampariello contributed to the various antennas based on groove guide contained in Part II, and Dr. Sanchez conducted the theoretical analyses for the foreshortened-top antenna described in Part III (and most of these analyses were incorporated into his Ph.D. thesis), and Mr. Han performed the measurements discussed in Part III.

2. Mechanisms Used to Produce Leakage

Several different mechanisms have been introduced to produce the required leakage from the waveguide mode that is ordinarily purely bound. In all cases, however, these mechanisms involve continuous apertures, making the antennas relatively simple to fabricate.

One mechanism, that was employed for antennas based on both the groove guide and the NRD guide, is asymmetry. Many open waveguides have modes that are purely bound when the structure is symmetrical; the introduction of asymmetry produces mode conversion to another mode that then leaks power away. This concept was first employed, to my knowledge, by W. Rotman in

his invention of the asymmetric trough guide antenna [1] in the late 1950's. The revival here of that concept was made first to the asymmetric strip leaky wave antenna based on groove guide. That antenna was analyzed in great detail, and the results are contained in Sec. A of Part II. An asymmetric leaky wave structure in NRD guide was analyzed only late in the contract period, but results for it are presented in Sec. D of Part III. It is to be stressed that many different means may be used to produce the leakage, and that the specific structures discussed here were selected in part because they were amenable to closed-form analysis. A second example of an asymmetric structure based on groove guide is the very simple one treated in Secs. C and D of Part II, obtained by bisecting the basic groove guide vertically, and a third example also presented in Sec. C, is a modification of that structure employing added strips in order to increase the leakage constant.

A second mechanism involves foreshortening part of the guiding structure to permit an evanescent field to see free space before the field decays to negligible values. This mechanism was examined in great detail in connection with an antenna based on NRD guide, and discussed thoroughly in Secs. A, B and C of Part III. Section A describes the antenna and presents the derivations in the analyses, Sec. B presents two different perturbation procedures which simplify the analysis, and Sec. C contains the results of measurements (which agreed very well with our theory). This same mechanism can be employed with groove guide, but we did not pursue it there because it would not yield something basically different.

A third mechanism, that was relevant to groove guide, is based on the fact that higher modes in groove guide are leaky. We prove this statement, and derive expressions for leaky structures based on the first higher odd mode and then the first higher even mode. These analyses are described in Sec. B of Part II.

Different mechanisms can also lead to different polarizations for the radiated fields. The asymmetry mechanism, because of the mode conversion

to a TEM-like mode, results in horizontal polarization. The mechanism based on foreshortening maintains the polarization of the exciting mode, which here implies vertical polarization, whether for groove guide or NRD guide. The leaky higher mode mechanism for groove guide results in vertical polarization for the first higher odd mode and horizontal polarization for the first higher even mode.

3. List of Publications and Presentations

This list is arranged chronologically.

1. P. Lampariello and A. A. Oliner, "A Novel Leaky-Wave Antenna for Millimeter Waves Based on the Groove Guide," Digest of IEEE International Symposium on Antennas and Propagation, pp. 652-655, Albuquerque, NM (May 24-28, 1982).
2. A. A. Oliner and P. Lampariello, "Theory and Design Considerations for a New Millimeter-Wave Leaky Groove Guide Antenna," Proc. 12th European Microwave Conference, pp. 367-371, Helsinki, Finland (September 13-17, 1982).
3. P. Lampariello and A. A. Oliner, "Bound and Leaky Modes in Symmetrical Open Groove Guide," Proc. Fourth National Meeting on Electromagnetic Applications, pp. 217-220, Florence, Italy (October 4-6, 1982).
4. A. A. Oliner and P. Lampariello, "A Novel Leaky-Wave Antenna for Millimetre Waves Based on the Groove Guide," Electronics Letters, Vol. 18, No. 25/26, pp. 1105-1106 (December 9, 1982).
5. P. Lampariello and A. A. Oliner, "Theory and Design Considerations for a New Millimetre-Wave Leaky Groove Guide Antenna," Electronics Letters, Vol. 19, No. 1, pp. 18-20 (January 6, 1983).
6. A. A. Oliner and P. Lampariello, "Leaky Modes of Symmetrical Groove Guide," Digest of IEEE International Microwave Symposium, pp. 390-392, Boston, MA. (May 31 - June 3, 1983).
7. P. Lampariello and A. A. Oliner, "Bound and Leaky Modes in Symmetrical Open Groove Guide," Alta Frequenza, Vol. 52, No. 3, pp. 164-166 (May-June 1983).
8. A. Sanchez and A. A. Oliner, "Accurate Theory for a New Leaky-Wave Antenna for Millimeter Waves Using Nonradiative Dielectric Waveguide," Proc. URSI International Symposium on Electromagnetic Theory, pp. 397-400, Santiago de Compostela, Spain (August 23-26, 1983).

9. P. Lampariello and A. A. Oliner, "The Leaky Mode Spectrum of Groove Guide," Proc. URSI International Symposium on Electromagnetic Theory, pp. 545-548, Santiago de Compostela, Spain (August 23-26, 1983).
10. A. A. Oliner and P. Lampariello, "Simple and Accurate Expression for the Dominant Mode Properties of Open Groove Guide," Digest of IEEE International Microwave Symposium, pp. 62-64, San Francisco, CA. (May 30 - June 1, 1984).
11. A. Sanchez and A. A. Oliner, "Microwave Network Analysis of a Leaky-Wave Structure in Non-radiative Dielectric Waveguide," Digest of IEEE International Microwave Symposium, pp. 118-120, San Francisco, CA. (May 30 - June 1, 1984).
12. A. Sanchez and A. A. Oliner, "Accurate Theory for a New Leaky-Wave Antenna for Millimeter Waves Using Nonradiative Dielectric Waveguide," Radio Science, accepted for publication.
13. A. A. Oliner and P. Lampariello, "The Dominant Mode Properties of Open Groove Guide: An Improved Solution," Trans. IEEE on Microwave Theory Tech., accepted for publication.

B. LOW-LOSS WAVEGUIDES

1. General Remarks

About 25 years ago, the advantages of millimeter waves began to be understood, and serious attention was paid for a few years to means for overcoming the new challenges that these higher frequencies had posed. One of these challenges related to waveguiding structures. It was recognized that coaxial or rectangular waveguide would have appreciable loss at these higher frequencies, and thought was given to devising new waveguides with lower loss, particularly in connection with long runs of waveguide. Several new waveguiding structures were invented during this period in response to this challenge, and among these were the H guide and the groove guide.

After a few years, interest in these new waveguides declined, in part because practical sources of millimeter wave power were not available, and in part because there were no real needs yet for these smaller wavelengths. Within the past decade, however, sources have become plentiful, and needs have multiplied. There is great interest today in millimeter waves, and attention has again been paid to new types of waveguide.

The primary drive now with respect to these waveguides is not long runs of them, however, but their utility and ease of fabrication with respect to building components, particularly in an integrated circuit sense. Some of these waveguides, such as microstrip line and finline, are in fact not low-loss guides at all, but they satisfy these component needs. Most components are short, having lengths only of the order of a wavelength, so that the loss in the line exerts only a small effect on the component's performance. For leaky wave antennas, however, which may typically be $20 \lambda_0$ to $100 \lambda_0$ in length, where λ_0 is the free space wavelength, the intrinsic loss in the waveguide, due to the losses in the metal walls or the dielectric medium, can be comparable to the leakage loss and therefore compete with it, distorting the antenna performance. The problem is particularly severe for antennas with narrow beams, since then a long aperture

is required, and the leakage per unit length (which produces the radiation) must be kept small.

For leaky wave antennas, therefore, it is necessary to concentrate on low-loss waveguides. (We recognize, of course, that leaky wave antennas are comprised of waveguides that are perturbed to produce continuous leakage of power along their lengths.) A common characteristic of many low-loss waveguides is that the electric field of the mode that is used is maintained parallel to the waveguide walls almost everywhere. The reason for this field orientation is that the metal wall losses decrease as the frequency is increased if the electric field is parallel to the walls, but increase with increasing frequency if the electric field is perpendicular to the walls. The two low-loss waveguides on which leaky wave antennas have been based in this study are the groove guide and the nonradiative dielectric (NRD) guide, which is a recent variant of H guide. In both of these waveguides, the electric field is purposely polarized parallel to the waveguide walls for the above reason.

These two waveguides will be described below in more detail, but it should be mentioned here that both waveguides are outgrowths of the H guide originally devised and discussed by F. Tischer. The groove guide was invented by T. Nakahara as a means to overcome the dielectric loss in H guide without increasing its metal wall loss appreciably, and its field confinement behavior strongly resembles that of H guide. NRD guide was proposed by T. Yoneyama and S. Nishida, and it is similar to H guide except for the plate spacing, which is made less than a half wavelength to eliminate radiation from discontinuities. Fuller explanations of these points are made in context below.

2. NRD Guide

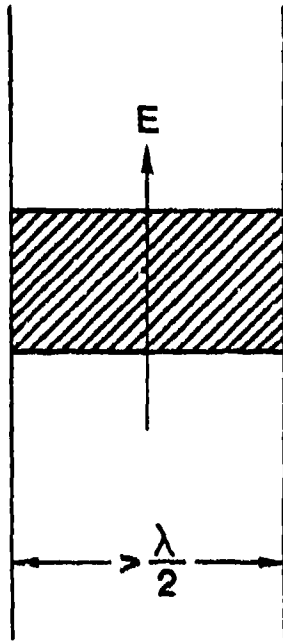
Although this study began with an analysis of groove guide, and in fact Part II deals with leaky wave antennas based on groove guide, we shall here consider NRD guide next because it is so closely related to

H guide, and, as mentioned above, both NRD and groove guide were basically outgrowths of H guide. We begin, therefore, with a summary of the properties of H guide.

The cross section of the basic form of H guide is shown on the left side of Fig. 1.1. It is seen to consist of two vertical metal walls, with a thin dielectric strip placed between them. The electric field orientation is vertical, so that it is almost everywhere parallel to the metal walls. The function of the dielectric strip is to concentrate the field vertically, so that the field in the air regions above and below the dielectric strip is evanescent vertically away from the strip. The field distribution is reminiscent of that of the TE_{10} mode in rectangular waveguide, in which the electric field is vertical, and the variation horizontally is sinusoidal. Although the presence of the dielectric strip introduces additional field components so that the mode becomes hybrid in the longitudinal direction, the vertical field is still a dominant feature. The guide structure looks like a rectangular waveguide loaded in the middle with dielectric, and without its top and bottom walls since they are no longer needed because the fields are now vertically evanescent in the air regions.

The purpose of this structure was to eliminate all metal walls at which electric fields could terminate perpendicular to the walls. Thus, the top and bottom walls of rectangular waveguide were removed, and the dielectric strip was introduced to confine the field vertically. As mentioned above, the metal losses increase with increasing frequency when the electric field lines are perpendicular to the metal walls. From the standpoint of metal losses, therefore, H guide is still useful at the high frequency end of the millimeter wave range. At this end, however, the dielectric losses become more significant, and groove guide was proposed as a way out of this predicament.

In this section, however, we are concerned with what NRD guide is and how it differs from H guide. The cross section of NRD (nonradiative dielectric) waveguide is shown on the right side of Fig. 1.1. It is seen



- lower loss
- must maintain uniform
- hard to build components

H Guide



- still low loss
- no radiation or leakage from bends or junctions
- easy to build components

NRD Guide

Fig. 1.1 Comparisons between H guide and NRD (nonradiative dielectric) guide

to be identical with H guide except that the spacing between the metal plates is less than one half free space wavelength in contrast to H guide, where the spacing is deliberately made greater than half a wavelength to further decrease the wall losses. This seemingly trivial modification makes an enormous practical difference. (It is of passing interest that both T. Yoneyama, one of the original proposers of NRD guide, and J.A.G. Malherbe, who claims to have independently invented it but did not publish in time, told me at the 1984 International Microwave Symposium in San Francisco that they had devised the NRD guide by some totally different route, and only afterwards realized its simple relation to H guide.)

H guide was originally conceived to be useful for long runs of guide, so the objective would be to achieve as low an attenuation as possible. For this reason, the spacing between the plates was made wide, certainly greater than a half a wavelength. As long as the guide was uniform and straight, the dominant mode was purely bound no matter what the plate spacing was, but any discontinuity present, such as a bump or some junction connected with a component, even if it maintained the required symmetry, could excite the first higher mode between parallel plates. When the plate spacing is greater than half a free space wavelength, this first higher mode is above cutoff, so that power can leak away from the H guide by means of this parallel plate mode. Because of this feature, it was difficult to build components in H guide, and that guide type was deemed impractical (except for long runs).

T. Yoneyama and S. Nishida [2] of Tohoku University in Japan proposed that the plate spacing in H guide be reduced to less than a half wavelength so that the first higher mode in parallel plate guide would remain below cutoff. In that way, all junctions or other discontinuities that maintained the symmetry of the dominant mode would be reactive and the radiation problem faced by H guide would be eliminated. Components could then be constructed readily, and the guide would become practical. Although the structural change is simple, the practical implications of it are so widespread that the authors felt it best to give the guide a new name: NRD guide.

Soon thereafter, Yoneyama and Nishida quickly and easily built a variety of components [3], paralleling structures common in microstrip line, and demonstrating that these components could be arranged in integrated circuit fashion. A page from one of their earlier papers [3] is reproduced here as Fig. 1.2, showing how simple it is to build such components as filters and ring resonators. Since that time (late 1981), they built and analyzed many other components, such as bends [4], couplers [5], more filters [6], etc..

To our knowledge, no antennas have been designed that are based on NRD guide. Our study, described in detail in Part III, is the first in this direction.

3. Groove Guide

Groove guide was invented by T. Nakahara [7] as a way to overcome the dielectric loss in H guide without significantly affecting the metal losses. The waveguide is shown in Fig. 1.3, and is seen to consist only of metal. Instead of the dielectric in H guide, the center region of groove guide is made wider than the upper and lower outer regions. The fields in the vertical direction then have a trigonometric dependence in the grooved region, but are exponentially decaying (evanescent) in the narrower regions above and below. The fields are therefore confined to the central grooved region in a manner similar to those in the central dielectric region of H guide.

A sketch of the electric field lines in the cross section of groove guide, and an approximate plot of the vertical component of the electric field, consistent with the discussion above, are shown in Figs. 1.4 (a) and (b).

The dominant mode in groove guide is seen from Fig. 1.3 to be an even closer relative to the TE_{10} mode in rectangular waveguide than the

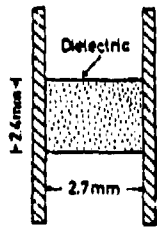


Fig. 1 NRD-guide

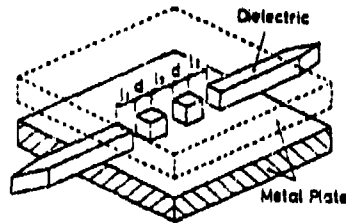


Fig. 5 Filter

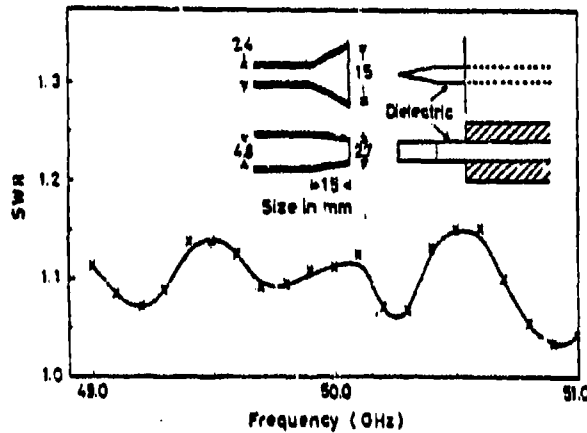


Fig. 2 SWR of Transition

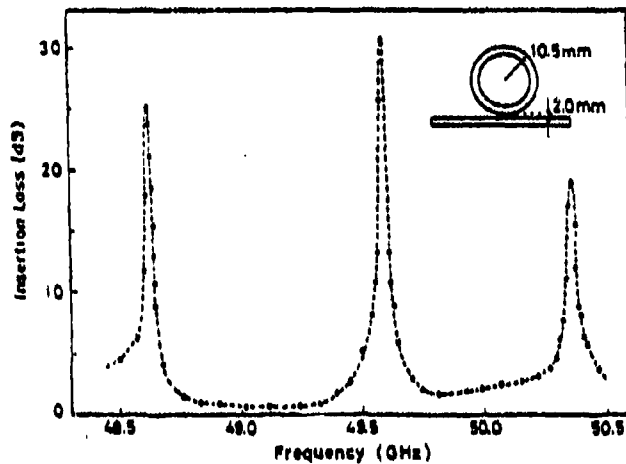


Fig. 4 Insertion Loss of Ring Resonator

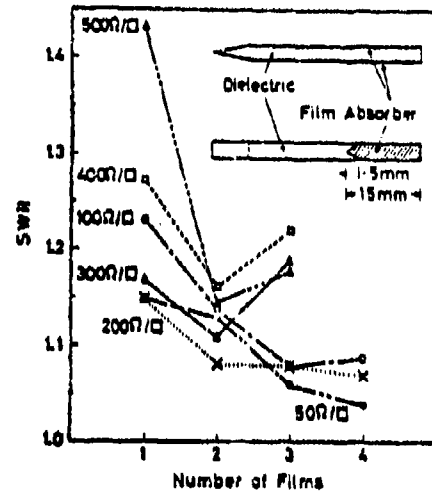


Fig. 3 SWR of Terminator

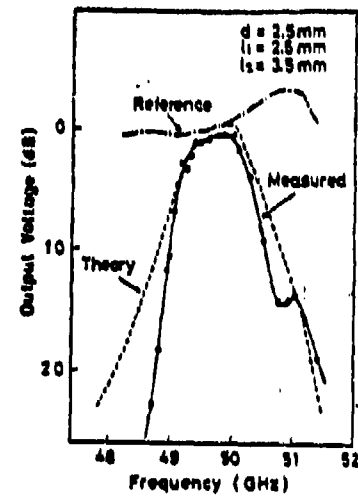


Fig. 6 Frequency Response of Filter

Fig. 1.2 Page from paper by T. Yoneyama and S. Nishida [3], showing how components such as filters and ring resonators can be constructed simply in NRD guide.

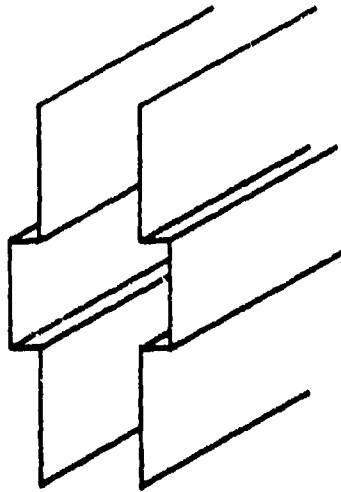


Fig. 1.3 The open groove guide, comprised of two parallel metal plates whose central regions are grooved outwards.

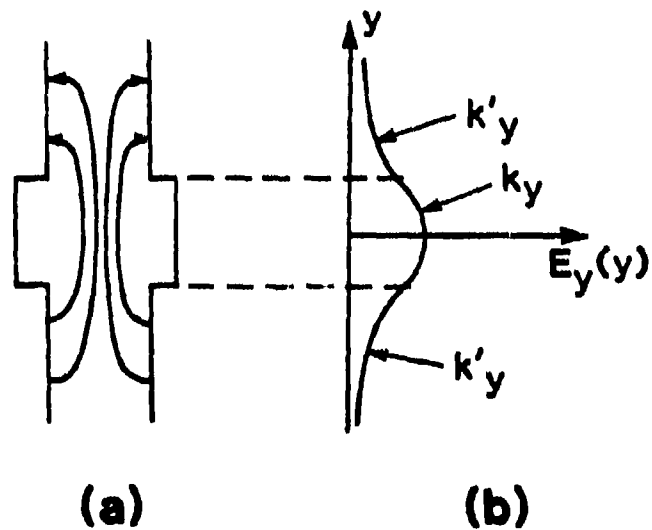


Fig. 1.4 The electric field of the dominant mode in open groove guide. (a) A sketch of the electric field lines in the cross section, (b) An approximate plot of the vertical component E_y as a function of vertical position y , showing that the guided mode is bound transversely to the central grooved region.

H guide is. The groove guide indeed looks like rectangular waveguide without most of its top and bottom walls; since the fields are evanescent above and below the central grooved region, we may say that the top and bottom metal walls have been replaced by reactive walls. The electric field is also primarily vertical for the groove guide, as sketched in Fig. 1.4(a), but the mode is not hybrid in the longitudinal direction as it was in H guide.

The top and bottom of groove guide are still primarily open, so that the electric field is still essentially parallel to the side walls, resulting in lower loss at the higher frequencies. However, one does not get something for nothing; the elimination of the dielectric losses was obtained at the expense of small sections of metal walls (in the central grooved section) that are perpendicular to the electric field. Those small sections contribute terms to the metal losses that increase with frequency. Hence, no guide is perfect as regards attenuation at the higher frequencies, although groove guide does rather well in this connection, with the metal losses first decreasing and eventually increasing as the frequency continues to be increased.

After Nakahara returned to Japan, he continued to explore the properties of open groove guide [8,9] with N. Kurauchi, and a bit later H. Shigesawa and K. Takiyama [10,11] of Japan studied the closed groove guide, where the top and bottom ends were closed off by metal plates. Following Nakahara's original work, independent investigations were conducted in the U.S.A. by F. J. Tischer [12] and by J.W.E. Griemsmann [13], and later by N. Y. Yee and N. F. Audeh [14]. Interest in the groove guide then declined for a few years, along with the millimeter wave field as a whole, but then, in the mid 1970's, it was revived and developed further by D. J. Harris and colleagues [15,16] in Great Britain (Wales). Harris at first studied various basic properties, mostly experimentally, but later he concentrated on the feasibility of certain basic components for groove guide. Other recent work included that of J. Meissner, who investigated the coupling [17] between groove guides, and the radiation losses of bends [18].

The investigations on this contract, presented in detail in Part II, represent the first contributions to antennas based on the groove guide.

C. SOME GENERAL PROPERTIES OF LEAKY WAVE ANTENNAS

A leaky wave antenna is basically an open waveguide possessing a mechanism which permits a slow leakage of power along the length of the waveguide. The leaky wave that exists at the opening along the length of the waveguide provides the aperture field distribution of the antenna, and the length of the waveguide over which the leaky wave contains significant power defines the antenna aperture length. It is customary to retain a length for which 90% or 95% of the power can leak away; the remaining 10% or 5% is absorbed in a load placed at the end of the waveguide.

The rate of leakage per unit length along the waveguide is given by the attenuation constant α of the complex propagation constant $k_z (= \beta - j\alpha)$ of the leaking waveguide mode. If the value of α is small, the antenna aperture will be long, and the far field radiation pattern will possess a narrow beam. If α is large, the power is radiated more rapidly along the antenna length and a wider radiated beam will be obtained.

The design of a leaky wave antenna proceeds by first specifying the desired performance characteristics of the antenna: the angle of maximum radiation, the beam width, and the side lobe properties. The angle θ_m that the maximum of the main beam makes with the normal to the antenna

aperture (broadside direction) is given approximately by

$$\sin \theta_m = \beta/k = \lambda/\lambda_g \quad (1.1)$$

where β is the phase constant of the complex propagation constant k_z . The beam width $\Delta\theta$ is related linearly to the reciprocal of the aperture length L , and a rule of thumb for $\Delta\theta$ is

$$\Delta\theta = \frac{\lambda}{L \cos \theta_m} \quad (1.2)$$

Relation (1.1) above is summarized pictorially in Fig. 1.5.

For the side lobe properties, it is well known that the antenna

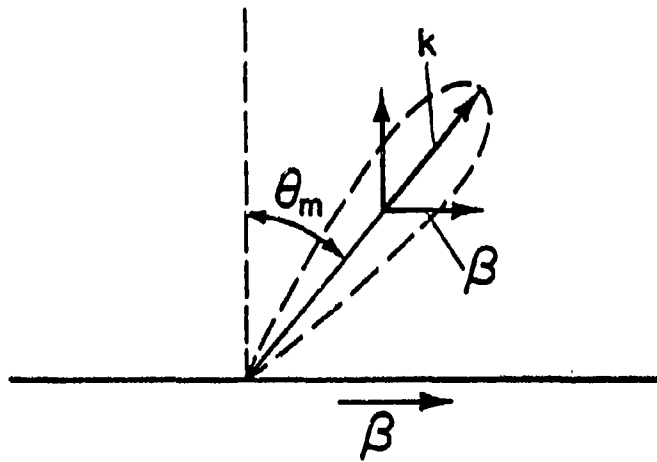


Fig. 1.5 Pictorial representation for $\sin \theta_m \approx \beta/k$, where θ_m is the angle that the maximum of the radiated beam makes with the normal to the antenna aperture surface, and β is the phase constant of the leaky wave that travels along the aperture surface.

aperture distribution must be tapered in a specified fashion in order to achieve the desired side lobe requirements. The necessary tapers corresponding to various side lobe specifications appear in standard antenna texts. When the aperture distribution is tapered, relation(1.2) for the beam width is affected somewhat numerically, but not more than $\pm 25\%$ depending on the taper, so that (1.2) remains a useful and reasonably accurate indication of the beam width.

When the geometry of the waveguide is uniform along its length, the aperture distribution consists of a slow exponential decay. To produce the taper needed for the side lobe requirements, it is necessary to vary the α of the waveguide along the length L , and therefore to vary the transverse dimensions in some fashion along the waveguide length. The phase constant β is maintained constant along the length so that all parts of the antenna aperture radiate at the same angle θ_m . The relation between $\alpha(z)$, where z is the longitudinal coordinate, and the desired taper along z of the antenna aperture distribution is also available in the literature.

The dispersion relations for the leaky structures yield the values of α and β corresponding to specific geometrical parameters in the cross section. That relation must be used in a specific design to produce the $\alpha(z)$ needed while maintaining $\beta(z)$ constant. Part of the design considerations to be discussed in this Final Report are aimed at recommending which geometrical parameter or parameters should be varied to change α but not β .

The analyses in this report discuss the behavior of the leaky structures when the cross section is maintained constant, and they stress the variation of β and α with frequency and with various dimensional parameters. If we assume, as is common, that the antenna aperture of length L radiates 90% of the power (with the remaining 10% absorbed by a load), then the power level at the end of the antenna aperture is 10 dB down from its value at the beginning. In the numerical values that follow, we shall present the α value in the form α/k in nepers, so that the value of α in dB per wavelength is $2\pi(8.686)(\alpha/k) = 54.6 (\alpha/k)$. The antenna length L in free space wavelengths is then approximately

$$\frac{L}{\lambda} = \frac{10}{54.6} \frac{1}{\alpha/k} = \frac{0.18}{\alpha/k} \quad (1.3)$$

The precise value of L will depend on how the aperture distribution is tapered. If the percentage of power radiated is different from 90%, the length L in (1.3) will differ somewhat numerically, but may be readily computed.

In summary, the values of β/k and α/k that are presented in this report permit us to determine readily the values θ_m from (1.1), the aperture length L from (1.3), and the beamwidth $\Delta\theta$ from (1.2).

D. IMPROVED SOLUTION FOR THE DOMINANT MODE OF OPEN GROOVE GUIDE

It was mentioned in the Introduction (Sec. A, 1) that an improved solution was derived for the properties of the dominant mode in groove guide. Although this investigation was motivated by the need for a better solution for use in the transverse equivalent network of the asymmetric strip leaky wave antenna, discussed in Sec. A of Part II, it represented a complete and thorough investigation on its own, and is of interest in its own right. The improved solution is notable in that it is compact, simple, accurate, has all its elements in closed form, and yields better agreement with measurements than any previous solution.

A talk on this new solution was presented recently at the IEEE International Microwave Symposium, held at San Francisco, CA, on May 30-June 1, 1984. The title and authors of this talk are: "Simple and Accurate Expression for the Dominant Mode Properties of Open Groove Guide," by A. A. Oliner and P. Lampariello. A short paper summarizing the study appeared in the Digest of that symposium on pp. 62-64, and it is reproduced here in this section.

In addition, a more complete version was written up to be issued as a report on this contract. After it was ready, it was recommended that it should be issued as a paper rather than a report, and it was subsequently sent to the IEEE MTT Transactions. It has been accepted for publication, but since it is not yet available either as a report or a paper it is included here as Appendix A. The title and authors are: "The Dominant Mode Properties of Open Groove Guide: An Improved Solution," by A. A. Oliner and P. Lampariello.

Summary of Principal Features

SIMPLE AND ACCURATE EXPRESSION FOR THE
DOMINANT MODE PROPERTIES OF OPEN GROOVE GUIDE

by A. A. Oliner and P. Lampariello

SIMPLE AND ACCURATE EXPRESSION FOR THE DOMINANT MODE PROPERTIES OF OPEN GROOVE GUIDE

A. A. Oliner* and P. Lampariello**

*Polytechnic Institute of New York
Brooklyn, New York 11201

**Universita' di Roma "La Sapienza"
00184 Rome, Italy

Abstract

Groove guide, one of several low-loss waveguides proposed some years ago for use at millimeter wavelengths, is again receiving attention in the literature. A new transverse equivalent network and dispersion relation for the properties of the dominant mode are presented here which are extremely simple in form and yet very accurate. Comparisons with accurate published measurements indicate better agreement with this new theory than with any previous theory.

A. INTRODUCTION

Groove guide is one of a group of low-loss waveguiding structures proposed some years ago for use at millimeter wavelengths. Results for the propagation characteristics of the dominant mode in groove guide have been published previously. There exist theoretical expressions which are simple but approximate, more accurate expressions which involve infinite sums and are messy to compute from, and careful measured results. We present here a new expression for the propagation constant of groove guide, which is very accurate, yet in closed form and simple. The microwave network approach used in the derivation of the new expression is summarized, and then comparisons are made with previously published theoretical and experimental results. It will be seen that the new expression provides excellent agreement with measurement, and in fact better agreement than with any previous theoretical data.

The motivation for obtaining an improved expression for the propagation constant of groove guide, and in the process a transverse equivalent network which is simple and whose constituents are all in closed form, is that groove guide appears to be an excellent low-loss waveguide upon which can be based a number of novel leaky-wave antennas for the millimeter wavelength range. The results of this paper then form an important step in the analysis of such antennas. One antenna in this class has been described recently [1, 2].

The cross section of groove guide is shown in Fig. 1, and an indication of the dominant mode electric field lines present in its cross section is given in Fig. 2(a). One should first note that the structure resembles that of rectangular waveguide with most of its top and bottom walls removed. The groove guide can therefore be excited by

providing a smooth tapered transition between it and a feed rectangular waveguide. Furthermore, if symmetry is maintained, many components can be designed for groove guide which are analogues of those in rectangular guide.

The greater width in the middle, or central, region was shown by T. Nakahara [3-5], the inventor of groove guide, to serve as the mechanism that confines the field in the vertical direction, much as the dielectric central region does in H guide. The field thus decays exponentially away from the central region in the narrower regions above and below, as shown in Fig. 2(b). If the narrower regions are sufficiently long, it does not matter if they remain open or are closed off at the ends.

The theoretical approach to the propagation constant of the dominant mode taken by most of the previous investigators has been to produce a first-order result by taking only the dominant transverse mode in each region of the cross section, and then obtaining the dispersion relation on use of the transverse resonance condition. That procedure, which neglects the presence of all higher transverse modes, is equivalent to accounting for the step junction between the central and outer regions by employing a transformer only, and by ignoring the junction susceptance entirely. With that approximation, a simple dispersion relation is obtained, which produces reasonably good agreement with measured data when the step discontinuity is small. More accurate theoretical phrasings were presented in some references by accounting for the susceptance by taking an infinite number of higher modes on each side of the step junction and then mode matching at the junction. The resulting expressions involve matrices which, even after the necessary truncation, are messy to compute from. When only one or two higher modes are included, the improvement in accuracy is quite small and the added complexity in calculation is substantial.

The approach in this paper is to establish a proper transverse equivalent network, identify the appropriate transverse mode (which is hybrid), obtain an accurate expression in closed form for the step junction susceptance, and then apply the transverse resonance condition to the now-complete transverse equivalent network, which yields the relevant dispersion relation for the propagation constant. This dispersion relation is simple, in

closed form, and very accurate, as demonstrated by comparison with measured data from references 4 and 5.

B. THE TRANSVERSE EQUIVALENT NETWORK

The complete transverse equivalent network for the groove guide is derived by starting with a proper phrasing of the problem and then by putting together all the constituent elements. The essential new constituent in the transverse equivalent network is a simple closed form expression for the step junction susceptance.

To begin with, however, we must identify the correct mode in the y direction (see Fig. 2). We first note that with respect to the z (longitudinal) direction the overall guided mode is a TE (or H) mode; that is, there exists only a component of H in the z direction. This result is to be expected since the groove guide consists of a perfectly conducting outer structure filled with only a single dielectric material (air). In the y direction, however, there exist both E_y and H_y components, so that the mode is hybrid in that direction.

Since the groove guide is uniform in the z direction, and its field has only an H_z component, the hybrid mode in the y direction is seen to be what is called by some an H -type mode with respect to the z direction, and by others an LSE mode with respect to the z direction. We prefer the former notation, and we shall designate the mode in the y direction as an $H^{(y)}$ -type mode. Altschuler and Goldstone [6] discuss such modes in detail and present the field components for them and the characteristic admittances for transmission lines representative of them. For this mode, we find that the characteristic admittance is given by

$$Y_0 = \frac{k_0^2 - k_y^2}{\omega \mu k_y} \quad (1)$$

where k_y is the propagation constant of the transmission line.

The step junction is a lossless asymmetric discontinuity, and it therefore requires three real quantities for its characterization. It has been found by experience, however, that for most situations the network conveniently reduces to a shunt network comprised of a shunt susceptance B and a transformer with turns ratio n .

Employing the mode functions for the $H^{(z)}$ -type mode mentioned above, the turns ratio n can be derived in the usual manner to yield

$$n = \left[\frac{a'}{a} \right]^{3/2} \frac{4}{\pi} \frac{\cos \frac{\pi a'}{2a}}{1 - (a'/a)^2} \quad (2)$$

To our knowledge, an expression for the shunt susceptance for the step junction subject to the excitation shown in Fig. 2(a) is not available in the

literature. By a simple additional step, however, we can adapt an available, but not widely known, result to our discontinuity of interest.

The available result is a symmetric discontinuity which is contained in Vol. 8 of the MIT Radiation Laboratory Series [7] and is presented there as an illustration of how Babinet's principle may be used creatively. That result, combined with appropriate stored power considerations, permits us to obtain the following result for the step junction discontinuity susceptance:

$$\frac{B}{Y_0} = 0.55 k_y \frac{2a}{\pi} \cot^2 \frac{\pi a'}{2a} \quad (3)$$

The resulting transverse equivalent network becomes that shown in Fig. 3, where bisection has been employed, and where the network has been placed horizontally for convenience. The expressions for parameters B , n and Y_0 (and therefore Y_0') are given respectively by (3), (2), and (1). The form of the network and the expressions for its constituents are seen to be eminently simple, and yet they characterize the structure very accurately.

Once the network in Fig. 3 becomes available, the determination of the dispersion relation for the lowest mode becomes an essentially trivial task. By applying the transverse resonance condition, we obtain

$$\cot k_y \frac{b}{2} = \frac{1}{n^2} \frac{k_y}{|k_y'|} + k_y 0.55 \frac{2a}{\pi} \cot^2 \frac{\pi a'}{2a} \quad (4)$$

The early first-order solution derived by various authors corresponds precisely to the first two terms in (4). The third term in (4) represents a particularly simple and convenient way to take into account the influence of all the higher modes, which the first-order solution admittedly neglects.

C. NUMERICAL RESULTS; COMPARISON WITH MEASUREMENTS

We next verify the accuracy of these new theoretical results, as embodied in dispersion relation (4) and the simple transverse equivalent network shown in Fig. 3. Toward this end, we present now a comparison between our theoretical numbers and the careful experimental results of Nakahara and Kurauchi [4,5] (referred to below as N-K).

In Fig. 9 of reference 5 and Fig. 10 of reference 4, N-K present the results of careful measurements on a variety of groove guides. They give the measured values of λ_c as a function of a' for groove guides of different cross sections, and they show how these values compare with curves obtained using first-order theory. All of these data, plus our theoretical numbers, are contained in Figs. 4(a) and 4(b) presented here; the first-order theory is represented by dashed lines, our more accurate theory by solid lines, and the measured data as discrete points. The cross sections corresponding to each set of curves are

shown as insets.

It is seen that our theoretical curves agree very well with the measured values in almost all cases. On the other hand, the first-order theoretical values are systematically somewhat below both our theory and the measured data. It appears, therefore, that the first-order theory represents a rather good approximation, considering its simplicity, and that the new theory using (4) is indeed significantly more accurate.

D. REFERENCES

1. A. A. Oliner and P. Lampariello, "A Novel Leaky-Wave Antenna for Millimetre Waves Based on the Groove Guide," *Electronics Letters*, Vol. 18, No. 25/26, pp. 1105-1106; December 9, 1982.
2. P. Lampariello and A. A. Oliner, "Theory and Design Considerations for a New Millimetre-Wave Leaky Groove Guide Antenna," *Electronics Letters*, Vol. 19, No. 1, pp. 18-20; January 6, 1983.
3. T. Nakahara, Polytechnic Institute of Brooklyn, Microwave Research Institute, Monthly Performance Summary, Report No. PIBMRI-875, pp. 17-61; 1961.
4. T. Nakahara and N. Kurauchi, "Transmission Modes in the Grooved Guide," *J. Inst. of Electronics and Commun. Engrs. of Japan*, Vol. 47, No. 7, pp. 43-51; July 1964.
5. T. Nakahara and N. Kurauchi, "Transmission Modes in the Grooved Guide," *Sumitomo Electric Technical Review*, No. 5, pp. 65-71; January 1965.
6. H. M. Altschuler and L. O. Goldstone, "On Network Representations of Certain Obstacles in Waveguide Regions," *IRE Trans. Microwave Theory Tech.*, Vol. MTT-7, pp. 213-221; April 1959.
7. C. G. Montgomery, R. H. Dicke and E. M. Purcell, *Principles of Microwave Circuits*, Vol. 8 in the MIT Radiation Laboratory Series, McGraw-Hill Book Co., New York, 1948. See Eq. (22) on p. 176.

ACKNOWLEDGMENT

The research described in this paper was conducted under Contract No. F19628-81-K-0044 with the Rome Air Development Center, Hanscom Field, Massachusetts.

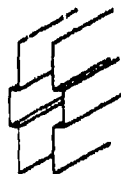


Fig. 1. The open groove guide.

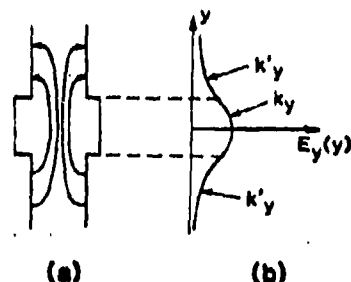


Fig. 2 The electric field of the dominant mode in open groove guide. (a) A sketch of the electric field lines in the cross section, (b) An approximate plot of the vertical component E_y as a function of y , showing that the guided mode is bound transversely to the central grooved region.

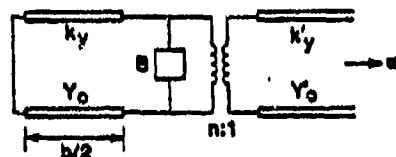


Fig. 3 Complete transverse equivalent network for open groove guide, for the excitation indicated in Fig. 2(a).

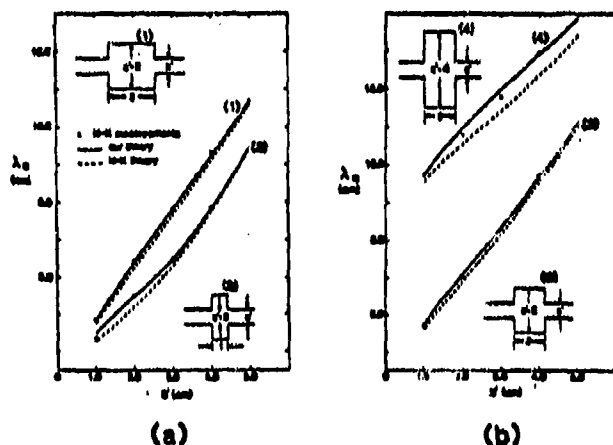


Fig. 4 Comparisons between measured and theoretical values of the cutoff wavelength λ_c for groove guides of various cross sections. The solid lines represent our improved theory, the dashed curves are the first-order theoretical values, and the points are the measured results of N-K [4, 5]. The insets indicate the cross-sectional geometries for each measured point, where the numbers are in cm.

PART II. ANTENNAS BASED ON GROOVE GUIDE

- A. THE ASYMMETRIC STRIP ANTENNA
 - 1. Summary of Principal Features
 - 2. Discussion of Comprehensive Report

- B. THE LEAKY MODE SPECTRUM OF GROOVE GUIDE
 - 1. Summary of Principal Features
 - 2. Derivations for the $n = 3$ (Odd) Leaky Mode
 - (a) Wavenumber Considerations to Demonstrate Leakage
 - (b) The Mode Functions and the Field Components
 - (c) Turns Ratios for the Step Junction
 - (d) The Coupling Network at the Step Junction
 - (e) The Dispersion Relation
 - 3. Derivations for the $n = 2$ (Even) Leaky Mode
 - (a) Wavenumber Considerations to Demonstrate Leakage
 - (b) The Mode Functions and the Field Components
 - (c) Turns Ratios for the Step Junction
 - (d) The Coupling Network at the Step Junction
 - (e) The Dispersion Relation

- C. ANTENNAS BASED ON THE $n = 2$ LEAKY MODE
 - 1. Antenna of Simple Configuration
 - 2. Antenna with Added Strips

- D. ALTERNATIVE THEORETICAL APPROACH FOR THE
 $n = 2$ LEAKY MODE ANTENNA

II. ANTENNAS BASED ON GROOVE GUIDE

Two basic low-loss waveguides for millimeter waves were described in Sec. B of Part I; they were both used in this study as the basis for new types of leaky wave antennas for application to millimeter wavelengths. The first of these waveguides is the groove guide, and the various antennas based on it that were analyzed and evaluated in this study are discussed in this part of the Final Report.

Two different leakage mechanisms were employed in these antennas. The first mechanism is asymmetry; the structure proposed and analyzed based on this mechanism utilized an added anymmetric strip to produce the controlled leakage. The second mechanism makes use of the fact that all of the higher modes of groove guide are leaky; only the dominant mode is purely bound. New antennas become possible based on the $n = 2$ (even) and $n = 3$ (odd) higher modes, and they radiate in different polarizations, according to the basic mode.

The asymmetric strip antenna is the one that was analyzed in the greatest detail, and on which we have the largest amount of numerical performance data. The study of that structure also emerged with various optimization considerations. Two short papers were written that summarized the principal features of this antenna; both appeared in Electronics Letters. Just prior to their publication, two talks were presented at professional society meetings on the same basic material; they were given at the IEEE International Symposium on Antennas and Propagation at Albuquerque, New Mexico, in May 1982, and at the European Microwave Conference at Helsinki, Finland, in September 1982. The first talk covered the principles of operation of the antenna, and the second one stressed the design considerations. The two short papers followed a similar format.

The studies on the asymmetric strip antenna are covered in Sec. A below. In Sec. A, 1, we include the two short papers that appeared in Electronics Letters, because they represent an excellent summary of the principal features relating to the antenna, including the principle of operation, the transverse equivalent network, selected numerical results, and some remarks

concerning dimensional optimization. Those papers contain no derivations, however, and they omit many of the numerical results. Because there was much more to present, a comprehensive report was written that contains much additional information. Since this comprehensive report has not as yet been issued by the Air Force, it is included in this Final Report as Appendix B, so that it becomes available to those who wish to see it at this time. In addition, we refer to its contents several times in connection with some of the derivations presented below. A few remarks concerning this comprehensive report are presented as Sec. A, 2.

The second mechanism that serves as a basis for groove-guide leaky wave antennas, as indicated above, is that all higher modes on groove guide are leaky. Although it was known that higher odd modes were leaky, we showed that the leakage statement was also valid for higher even modes. More important, however, is the fact that, before our studies, no analysis had been made to determine the amount of the leakage. We derived appropriate transverse equivalent networks, and determined not only the amount of the leakage but also some of its parametric dependences. These studies on the leaky mode spectrum of groove guide are presented in Sec. B.

In Sec. B. 1, we include two short published papers on this topic that summarize the most important features of this work. These papers contain discussions on the physical basis for this higher-mode leakage, the transverse equivalent networks, and some numerical results, together with a discussion on why the curves of α and β as a function of frequency and dimensional aspect ratio behave physically as they do. The first of these papers was published in Alta Frequenza in 1983, and the second appeared in the Proceedings of the URSI Symposium on Electromagnetic Theory, held in Spain in August, 1983. Their contents differ in the following way: although there is clearly some overlap, the first paper treats only the odd higher modes, comments on the dominant mode, and presents data as a function of frequency. The second paper presents an overview, but is concerned primarily with a comparison between the behaviors of the odd and the even higher modes.

Before these short papers appeared, two talks were given on their contents. These talks were presented at the Fourth National Meeting on Electromagnetic Applications at Florence, Italy, in October 1982, and at the IEEE International Microwave Symposium at Boston, Mass., in June 1983. The first of these talks led to the above-mentioned paper in Alta Frequenza, and the second constituted an overview comparing the properties of the odd and even higher modes.

The derivations of the expressions for the constituents of the transverse equivalent networks are not included in these paper or talks, because of the limited space and time available. They are therefore presented here in Secs. B, 2 and B, 3 for the $n = 3$ and $n = 2$ leaky higher modes, respectively.

The mid-plane of the groove guide for the $n = 2$ higher mode is an electric wall, from symmetry. By bisecting that structure, and placing a metal wall at the mid-plane, we obtain an asymmetric antenna of simple cross section. It is interesting that this latter structure can be viewed as leaky either because of asymmetry or because the field distribution is that of the first higher even mode, which is leaky. Either way, the structure is an interesting candidate for a millimeter wave leaky wave antenna because of its simplicity. Comments on the performance of this structure, and its limitations, appear in Sec. C, 1. The principal limitation is that its leakage constant is lower than that found for the other antennas.

For this reason, small strips were added at the sites of the step junctions in the cross section. This modified structure was analyzed; a higher leakage constant is obtained, of course, but at the expense of some added fabrication difficulty. In Sec. C, 2, we present the modified structure, the derivation for its properties, some numerical values for α and β , and suggestions regarding its fabrication.

The calculations in Sec. C, 1 also indicate that for maximum radiation the cross section dimensions resembled a small tee stub on a vertical guide.

Our theory is probably no longer accurate in that range of groove dimensions, so that these numerical results may no longer be reliable. It was therefore necessary to view the structure differently, and to derive a new theoretical result.

This new theoretical approach is discussed in Sec. D. The structure was viewed as a tee stub on a parallel plate guide, rather than as a modified groove guide, in this range of dimensions. A transverse equivalent network was derived consistent with this point of view, and expressions for its parameters were obtained. Numerical values for the leakage constant obtained via this approach were substantially larger than those obtained previously.

This transverse equivalent network is valid in the horizontal direction, whereas that for the groove guide approach applied to the vertical direction. The theories are therefore totally different, both in appearance and in substance. The derivations involved in this new approach are described in Sec. D, 1, and the numerical results, together with a discussion of their limitations, are contained in Sec. D, 2. Recommendations for future work are also included there.

A. THE ASYMMETRIC STRIP ANTENNA

As indicated above, the studies conducted on this antenna have been summarized in two short papers, described in two talks at professional society meetings, and written up in substantial detail in a comprehensive report. The two short papers, both of which appeared in *Electronics Letters*, represent an excellent summary of the antenna's principal features. For this reason, they are reproduced here in Sec. A, 1. The first paper presents the structure of the antenna, its principle of operation, and a typical set of numerical results as regards dimensions and antenna performance. The second paper summarizes the transverse resonance analysis, including the transverse equivalent network, and then discusses design considerations in the context of some numerical results.

The comprehensive report, which contains much more information, including derivations and additional numerical results, is reproduced as Appendix B, but is discussed briefly in Sec. A, 2.

1. Summary of Principal Features

- (a) NOVEL LEAKY-WAVE ANTENNA FOR MILLIMETRE
WAVES BASED ON GROOVE GUIDE

by A. A. Oliner and P. Lampariello

- (b) THEORY AND DESIGN CONSIDERATIONS FOR A
NEW MILLIMETRE-WAVE LEAKY GROOVE-GUIDE
ANTENNA

by P. Lampariello and A. A. Oliner

NOVEL LEAKY-WAVE ANTENNA FOR MILLIMETRE WAVES BASED ON GROOVE GUIDE

Indexing terms: Antennas, Leaky-wave antennas, Millimetre waves, Groove guide

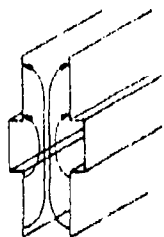
A new type of leaky-wave antenna, with a simple longitudinally continuous configuration, is described. The antenna is based on the groove guide, a low-loss waveguide for millimetre waves.

Introduction: The groove guide was one of several waveguiding structures proposed for millimetre-wave use about 20 years ago in order to overcome the higher attenuation occurring at these higher frequencies. Although these new low-loss waveguides were introduced many years ago, they were not pursued beyond some initial basic studies because they were not yet needed. Now, however, millimetre waves are again becoming important, and attention is again being paid to new types of waveguide. Among these are dielectric strip waveguides of different types, the H-guide in several forms, and the groove guide.

The present letter describes a novel type of leaky-wave antenna which is based on the groove waveguide. Although lossy waveguides may be acceptable for components only a wavelength or so long, they are not suitable for leaky-wave antennas, which may typically be $20\lambda_0$ to $100\lambda_0$ in length, where λ_0 is the free-space wavelength. For these antennas, therefore, it is necessary to employ a low-loss waveguide, and the groove guide satisfies that requirement. The antenna involves a simple longitudinally continuous structure; as a result, it should be easy and cheap to fabricate, and can probably be made by a simple extrusion process. In view of the small size of waveguiding structures at millimetre wavelengths, leaky-wave antennas form a natural class of antennas for these waveguides.

The antenna has been analysed in an almost rigorous manner, and a closed-form expression has been derived for the dispersion relation for its complex propagation constant. From numerical calculations, we find that excellent control can be effected over the leakage constant α , so that radiation patterns can be designed in a systematic way.

Basic groove waveguide: The cross-section of the groove waveguide is shown in Fig. 1, together with an indication of the



0077

Fig. 1 Cross-section of symmetrical, nonradiating groove waveguide. Ends can either be left open, as shown, or be closed off

electric field lines present. One should note that the structure resembles that of a rectangular waveguide with most of its top and bottom walls removed. Since the attenuation associated with those walls increases as the frequency is increased, whereas the attenuation due to the presence of the side walls (with the electric field parallel to the walls) decreases with increasing frequency, the overall attenuation of the groove waveguide at higher frequencies is much less than that for a rectangular waveguide. The reduced attenuation loss will therefore interfere negligibly with the leakage loss of the novel antenna to be described.

The greater width in the middle, or central, region was shown by T. Nakahara,^{1,2} the inventor of the groove guide, to serve as the mechanism that confines the field in the vertical direction, much as the dielectric central region does in the

H-guide. The field thus decays exponentially away from the central region in the narrower regions above and below. If the narrower regions are sufficiently long, it does not matter if they remain open or are closed off at the ends.

Work on the groove guide progressed in Japan^{2,3} and the United States^{4,5} until the middle 1960s, but then stopped until it was revived and developed further by D. J. Harris and his colleagues in Wales (see, for example, References 7 and 8). To our knowledge, the present letter represents the first contribution to antennas based on the groove waveguide.

Operating principle of new leaky-wave antenna: The new leaky-wave antenna is shown in Fig. 2. The basic difference between the structures in Figs. 1 and 2 is that in Fig. 2 a continuous metal strip of narrow width has been added to the guide in asymmetrical fashion. Without that strip, the field of the basic mode of the symmetrical groove waveguide is evanescent vertically, so that the field has decayed to negligible values as it reaches the open upper end. The function of the asymmetrically placed metal strip is to produce some amount of net horizontal electric field, which in turn sets up a mode akin to a TEM mode between parallel plates. The field of that mode propagates all the way to the top of the waveguide, where it leaks away. It is now necessary to close up the bottom of the waveguide, as seen in Fig. 2, to prevent radiation from the bottom, and (nonelectrically) to hold the structure together. Of course, the upper walls could end as shown in Fig. 2 or they could attach to a ground plane.

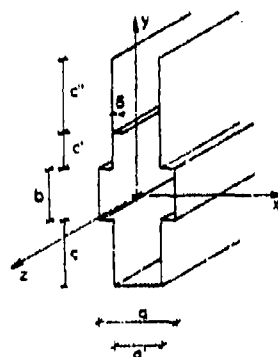


Fig. 2 Cross-section of novel leaky-wave antenna, where leakage is produced by introduction of an asymmetric continuous metal strip

We now have available a leaky-wave line-source antenna of simple construction. The value of the propagation wave number β of the leaky wave is governed primarily by the properties of the original unperturbed groove guide, and the value of the attenuation constant α is controlled by the width and location of the perturbing strip.

Typical set of numerical results: ... with any leaky-wave antenna, one can, by suitably changing the dimensions and the frequency, obtain a variety of scan angles and leakage constants. Let us choose as a typical case $d/a = 0.70$, $b/a = 0.80$, $c/a = 1.215$, $c'/a = 0.145$, $c''/a = 1.50$, $\delta/a = 0.21$ and $\lambda_0/a = 1.20$. For this particular set of dimensions, our calculations yield $\beta/k_0 = 0.749$ and $\alpha/k_0 = 6.24 \times 10^{-3}$. This value of leakage constant α yields a leakage rate of about 0.34 dB per wavelength, resulting in an antenna about $30\lambda_0$ long if, as is customary, 90% of the power is to be radiated, with the remaining 10% dumped into a load. The resulting beam width of the radiation is approximately 2.9°, and the beam radiates at an angle of about 49° to the normal. At a frequency of 50 GHz, for example, dimension a would be 0.50 cm and the antenna would be 18 cm long.

We have described here a new type of leaky-wave antenna suitable for millimetre waves. It is based on the groove guide, which is a low-loss waveguide, so that the waveguide attenuation will interfere negligibly with the leakage process. The structure is simple and longitudinally continuous, rendering it attractive for fabrication at the small wavelengths in the millimetre-wave range.

Acknowledgment: This work has been supported in part by the Air Force Rome Air Development Center at Hanscom AFB, under contract no. F19628-81-K-0044, and in part by the University of Rome.

A. A. OLINER

28th October 1982

Polytechnic Institute of New York
333 Jay Street
Brooklyn, NY 11201, USA

P. LAMPARIELLO

Istituto di Elettronica
Università di Roma
via Eudossiana 18
00184 Roma, Italy

References

- 1 Polytechnic Institute of Brooklyn, Microwave Research Institute, Monthly Performance Summary, Report PIBMRI-875, 1961, pp. 17-61

- 2 NAKAHARA, T., and KURAUCHI, N.: 'Transmission modes in the grooved guide', *J. Inst. Electron. & Commun. Eng. Jpn.*, 1964, 47, pp. 43-51; *Sumitomo Electr. Tech. Rev.*, 1965, pp. 65-71
- 3 SHIGESAWA, H., and TAKIYAMA, K.: 'Transmission characteristics of the close grooved guide', *J. Inst. Electron. & Commun. Eng. Jpn.*, 1967, 50, pp. 127-135; 'On the study of a close grooved guide', *Sci. & Eng. Rev. Doshisha Univ.*, 1968, 9, pp. 9-40
- 4 TISCHER, F. J.: 'The groove guide, a low-loss waveguide for millimeter waves', *IEEE Trans.*, 1963, MTT-11, pp. 294-296
- 5 GRIEMSMANN, A. W. B.: 'Groove guide', Proc. Symposium on quasi-optics, Polytechnic Press of Polytechnic Institute of Brooklyn, 1964, pp. 565-578
- 6 YEE, H. Y., and AUDEH, N. P.: 'Wave propagation in groove guides', Proc. National Electronics Conf., 1965, 21, pp. 18-23
- 7 HARRIS, D. J., and LEE, K. W.: 'Groove guide as a low-loss transmission system for short millimetric waves', *Electron. Lett.*, 1977, 13, pp. 775-776
- 8 HARRIS, D. J., and MAK, S.: 'Groove-guide microwave detector for 100 GHz operation', *ibid.*, 1981, 17, pp. 516-517

0013-5194/82/251105-02\$1.50/0

Reprinted from *ELECTRONICS LETTERS* 9th December 1982 Vol. 18, No. 25/26 pp. 1105-1106

REPRINTED WITH PERMISSION FROM IEEE - REPRODUCTION DOES NOT CONSTITUTE ANY
COPYRIGHT VIOLATION.

THEORY AND DESIGN CONSIDERATIONS FOR A NEW MILLIMETRE-WAVE LEAKY GROOVE-GUIDE ANTENNA

Indexing terms: Antennas, Leaky-wave antenna, Millimetre waves, Groove guide

A transverse equivalent network is presented for a new type of leaky-wave antenna based on the groove guide and suitable for millimetre waves. Employing this network, the antenna's performance characteristics are explained and systematic design considerations are deduced.

Introduction: A recent paper¹ discussed a new type of leaky-wave antenna for millimetre waves based on the groove guide. The operating principle underlying the new antenna was presented there, together with background relating to the basic groove guide and the presentation of a typical set of numerical performance data.

As stated there, the antenna is created by the introduction into the basic groove guide of an additional longitudinally continuous metal strip. The strip is introduced in *asymmetrical* fashion so as to produce some net horizontal electric field. In effect, a new *transverse mode* is created thereby, which propagates all the way to the top of the waveguide, where it leaks away, thus transforming the initially bound mode into a leaky one.

The leaky-wave antenna has been analysed by deducing the proper *transverse equivalent network*, deriving simple closed-form expressions for the various parameters of this network, and then obtaining the dispersion relation for the complex propagation constant of the leaky mode from the lowest resonance of the transverse equivalent network. The resulting expression for the complex propagation constant is also in closed form, and is judged by us to be very accurate.

From this expression, numerical calculations were made of the antenna's performance characteristics, and their dependence on the various dimensional parameters of the antenna. From these results we noted certain radiation peculiarities, due to the presence of a transverse standing wave, and we were then able to deduce systematic design considerations which permit one to *optimise* the antenna performance.

In this letter we first present the transverse equivalent network and discuss the transverse modes which are coupled by the added continuous strip. Then, utilising this transverse equivalent network, we explain the performance behaviour obtained as the values of dimensional parameters are varied,

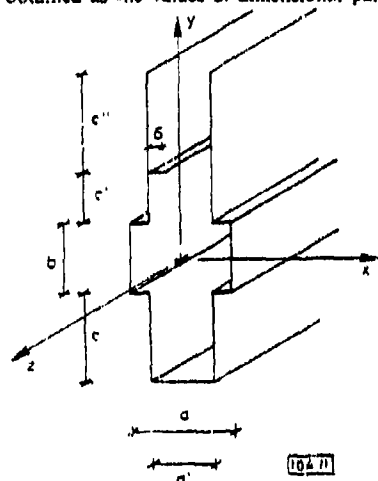


Fig. 1 Cross-section of novel leaky-wave antenna, where leakage is produced by introduction of an asymmetric continuous metal strip

and finally we outline the design considerations for optimisation, again employing the transverse equivalent network.

Transverse resonance analysis of the new antenna: The basic structure of the new leaky-wave antenna is given in Fig. 1. As discussed in Reference 1, it is the added continuous strip of width δ that introduces asymmetry into the basic groove guide

and creates the leakage. The strip therefore gives rise to an additional transverse mode and couples that mode to the original transverse mode which by itself would be purely bound.

The transverse equivalent network for the cross-section of the structure shown in Fig. 1 must therefore be based on these two transverse modes, which propagate in the y direction and are coupled together by the narrow asymmetrical strip. These coupled transverse modes then combine to produce a net TE longitudinal mode (in the x direction) with a complex propagation constant $\beta - j\alpha$.

In view of the uniformity of the structure along z , the appropriate transverse modes are the $i = 0$ and $i = 1$ H -type (or LSE) modes with respect to the z direction. The complete equivalent network based on these transverse modes is given in Fig. 2. In the network, which has been placed on its side for clarity, the $i = 1$ transmission lines represent the original mode with a half-sine-wave variation in the x direction in Fig. 1, and the $i = 0$ transmission lines represent the new mode which has no variation with x . In the central region, corresponding to the unprimed parameters, both the $i = 1$ and $i = 0$ transmission lines are above cutoff; in the outer (primed) regions, however, the $i = 1$ transmission lines are below cutoff but the $i = 0$ ones are above cutoff, leading to standing waves in sections c, c' and c'' , and to radiation via G_H .

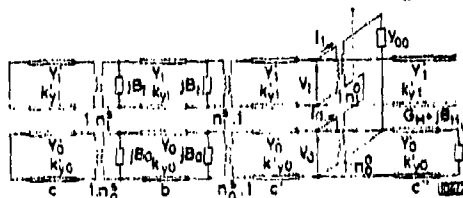


Fig. 2 Transverse equivalent network for structure whose cross-section is shown in Fig. 1

For clarity, the network is placed horizontally rather than vertically.

Although the fields in the $i = 1$ transmission line of length c' are evanescent, c' is sufficiently short that the added strip located at c' can convert some of the $i = 1$ mode power into the $i = 0$ mode. The amount of power converted per unit length clearly depends on the length c' and the width δ of the strip. Particular note should be made of the simple form of the network at c' which couples the two transmission lines. That form and the expressions for the elements in that network were derived using small obstacle theory in a multimode context; it was necessary to extend the formulations available in the literature because one of the constituent transmission lines ($i = 1$) is below cutoff.

Space does not permit listing the expressions for the various constituents of this network, nor the final expression for β and α , but they, together with their derivations, will soon be presented for publication. It should be mentioned, however, that the theoretical expressions for the individual constituents, as well as for β and α , are in closed form.

Design considerations: In order to systematically design radiation patterns, one must be able to taper the antenna aperture amplitude distribution while maintaining the phase linear along the aperture length, i.e. one must be able to vary α while keeping β the same. Fortunately, several parameters can be varied that will change α while affecting β hardly at all; the best ones are δ and c , if c is long enough.

Since the $i = 0$ transverse mode is *above* cutoff in both the central and outer regions of the guide cross-section, however, a *standing wave* effect is present in the $i = 0$ transmission line. As a result, a short circuit can occur in that transmission line at the position of the coupling strip of width δ , and the value of α then becomes zero. Hence, we must choose the dimensions to avoid that condition, and in fact to optimise the value of α .

In the design, one first chooses the width a and adjusts a' and b to achieve the desired value of β/k_0 , which is determined essentially by the $i = 1$ transverse mode. That value of β/k_0 immediately specifies the angle of the radiated beam. It is then recognised that the value of α can be increased if the coupling strip width δ is increased, or if the distance c' between the step

junction and the coupling strip is decreased, since the coupling strip is excited by the $i = 1$ transverse mode, which is evanescent away from the step junction in the outer regions. After those dimensions are chosen, the length c must be determined such that the standing-wave effect mentioned above optimises the value of α . If c is sufficiently long, it will affect only the $i = 0$ transmission line and influence β negligibly. The length c also affects α strongly and β weakly, and it also must be optimised because another, although milder, standing wave exists between the coupling strip and the radiating open end.

We have obtained numerical values in graphical form of the variation of α and β with each of these dimensional parameters, so that design optimisation can proceed in systematic fashion. However, we present here, in Figs. 3a and b, respectively, only a curve of α/k_0 as a function of c' (Fig. 3a), and the value of $c + c'$ (Fig. 3b) that must be selected so as to achieve the optimised value of α given in Fig. 3a. In effect, therefore, Fig. 3b indicates the value of c required once α (via c') is specified. It is interesting to note that $c + c'$ is almost constant for optimisation.

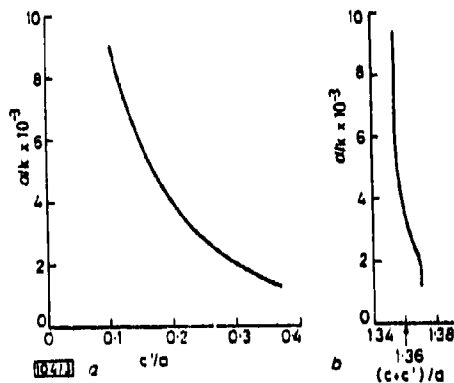


Fig. 3

- a Leakage constant α/k_0 of leaky-wave antenna shown in Fig. 1 as a function of distance c'/a of perturbing strip from step junction
 b Optimum value of leakage constant α/k_0 as a function of $(c + c')/a$ required for optimisation

It is important to realise that the dimensions for optimisation are *independent of frequency*, since the transverse-wave numbers are all frequency-independent. Of course, when the frequency is altered the values of β and α will change, but the dimensional optimisation is undisturbed. In fact, for the dimensions discussed above, the radiated beam can be scanned with frequency from about 15° to nearly 60° from the normal before the next mode begins to propagate.

The new leaky-wave antenna suitable for millimetre waves, for which the transverse resonance analysis and design considerations are presented here, is therefore capable of straightforward understanding and systematic design. It is also sufficiently flexible with respect to the dimensional parameters which can be varied that a reasonably wide range of pointing angles and beam widths can be achieved with it.

Acknowledgment: This work has been supported in part by the Air Force Rome Air Development Center at Hanscom AFB, under contract F19628-81-K-0044, and in part by the University of Rome.

P. LAMPARIELLO

Istituto di Elettronica
 Università di Roma
 via Eudossiana 18
 00184 Roma, Italy

A. A. OLINER

Polytechnic Institute of New York
 333 Jay Street
 Brooklyn, NY 11201, USA

15th November 1982

Reference

- OLINER, A. A., and LAMPARIELLO, P.: 'A novel leaky-wave antenna for millimetre waves based on the groove guide', *Electron. Lett.*, 1982, 18, pp. 1105-1106

0013-5194/83/010018-03\$1.50/0

Reprinted from *ELECTRONICS LETTERS* 6th January 1983 Vol. 19 No. 1 pp 18-20

REPRINTED WITH PERMISSION FROM IEEE- REPRODUCTION DOES NOT CONSTITUTE ANY COPYRIGHT VIOLATION.

2. Discussion of Comprehensive Report

The two short papers comprising Sec. A, 1 summarize the main features of the asymmetric strip antenna, but they necessarily omit much material because of their limited length. For that reason, a comprehensive report was written to supplement the short papers and present the remaining information. Because this comprehensive report was submitted only a few months ago to the Air Force, and it has not yet been distributed, it is included here as Appendix B. In this way, it is available now as part of the total discussion of the various new antennas based on groove guide. It is also useful to have it available because some of the derivations in Sec. B rely heavily on material contained in this report.

The form of the transverse equivalent network was presented in Sec. A, 1, in the second paper, but no expressions were given for the constituent elements of this network, and, of course, no derivations were included of these expressions. Accordingly, detailed derivations of the various expressions are presented in this comprehensive report; in fact, about half of the report is devoted to these derivations. The considerations include, first, the transverse modes that must be used to cope with their hybrid nature in the transverse direction, and then the representations for the discontinuity structures present in the cross section, including the step junction, the asymmetric strip, and the radiating open end. Special attention must be paid to the asymmetric strip, that couples the incident bound $i = 1$ transverse mode to the radiating $i = 0$ transverse mode. That structure was analyzed using small obstacle theory in a multimode context, but it was also necessary to extend the available theory to include the fact that one of the modes is below cutoff. All these considerations are treated in detail.

Many additional numerical results are presented near the end of the report so that one has available the dependence of the phase constant β and the leakage constant α on each of the possible geometric parameters. For the design of leaky wave antennas, one wants to be able to vary α

without affecting β , and vice versa. These results offer guidance in that context, and, of course, recommendations are given as well. These recommendations are also to be taken in connection with the optimization and other design considerations presented there.

Section E, 1 of this report contains some general rules regarding the behavior of leaky wave antennas in general. As mentioned in Part I, this section, with minor changes, has been reproduced as Sec. C of Part I because it is relevant to all the leaky wave antennas treated here, and is of basic general interest.

Lastly, it should be remarked that the asymmetric strip antenna is an example of how the initially bound dominant mode of groove guide can be transformed into a leaky mode by the introduction of asymmetry. The asymmetry could be introduced in many different ways, depending on convenience. This structure was chosen because it was amenable to accurate analysis, as well as being reasonably simple in structure.

B. THE LEAKY MODE SPECTRUM OF GROOVE GUIDE

It turns out that only the dominant mode of groove guide is purely bound, and that all higher modes are leaky. Nakahara and Kurauchi [9] had shown toward the end of an article many years ago that the odd higher modes were leaky but they gave no indication of the magnitude of that leakage. We extended their result to show that all higher even modes are also leaky, and we derived appropriate transverse equivalent networks for the first higher ($n = 3$) odd mode and first higher ($n = 2$) even mode, and computed from them the extent of the leakage and its dependence on frequency and dimensional ratios.

As mentioned earlier, these studies have been summarized in two short papers and in two talks before professional society symposia. The two papers summarize the main features of the studies, and they present the physical basis for the higher-mode leakage, the form of the transverse equivalent networks (but no expressions or derivations), and some numerical results with physical discussion. The two papers overlap somewhat in content, but differ in stress in addition to other content. The first paper, which appeared in Alta Frequenza in 1983, treats only the odd higher modes, contains remarks about the dominant mode, and includes explanations of why the curves of α and β behave physically the way they do as a function of frequency and dimensions. The second paper is concerned primarily with a comparison between the odd and the even higher modes, with respect to the behavior of α and β and the difference in polarization of the radiation.

Because these two short papers furnish an excellent summary of the conclusions reached by these studies, they are reproduced here as Sec. B, 1.

The expressions for the constituents of the transverse equivalent networks, and the derivations of those expressions, are presented in Secs. B, 2 and B, 3 for the first higher odd mode, $n = 3$, and the first higher even mode, $n = 2$, respectively.

It should, of course, be understood that these two leaky modes furnish the basis for two new leaky wave antennas. The leakage from the $n = 3$ mode occurs in the form of the $n = 1$ mode, with E parallel to the walls. If the structure is maintained vertical, the radiation will then be vertically polarized. Since the leakage from the $n = 2$ mode occurs in the form of the TEM, or $n = 0$, mode, the radiation from that antenna will be horizontally polarized.

1. Summary of Principal Features

(a) BOUND AND LEAKY MODES IN
SYMMETRICAL OPEN GROOVE GUIDE

by P. Lampariello and A. A. Oliner

(b) THE LEAKY MODE SPECTRUM OF GROOVE GUIDE

by P. Lampariello and A. A. Oliner

Bound and leaky modes in symmetrical open groove guide

Paolo Lamparello

DIPARTIMENTO DI ELETTRONICA, UNIVERSITÀ DI ROMA
VIA EUDOSSIANA, 18 - 00184 ROMA

Arthur A. Oliner

POLYTECHNIC INSTITUTE OF NEW YORK
333 JAY STREET - BROOKLYN, N.Y. 11201

Abstract. It is shown that on symmetrical open groove guide, which was proposed some years ago as a low-loss waveguide for millimeter waves, the dominant mode is purely bound but all higher modes are leaky. Analytical expressions and numerical values are obtained for the propagation characteristics of the dominant and first higher modes, including the leakage constant for the latter.

1. INTRODUCTION

Groove guide is one of several waveguiding structures proposed for millimeter wave use about 20 years ago in order to overcome the higher attenuation occurring at these higher frequencies. Although these new low-loss waveguides were introduced many years ago, they were not pursued beyond some initial basic studies because they were not yet needed. Now, however, millimeter waves are again becoming important, and attention is again being paid to new types of waveguide. Among these are dielectric strip waveguides of different types, H guide in several forms, and groove guide.

2. THE DOMINANT MODE OF GROOVE WAVEGUIDE

The basic form of open symmetrical groove guide is shown in Fig. 1, together with an indication of the electric field lines present for the lowest mode. One should note that the structure resembles that of rectangular waveguide with most of the top and bottom walls removed. The attenuation associated with those walls increases as the frequency is increased, whereas the attenuation due to the side walls (with the electric field parallel to the walls) decreases with increasing frequency. Therefore, the overall attenuation for groove guide at higher frequencies is very much less than that for rectangular waveguide.

The greater width in the middle region was shown by T. Nakahara [1,2], the inventor of groove guide, to serve as the mechanism that confines the field in the vertical direction, much as the dielectric central region does in H guide. The field thus decays exponentially away from the central region in the narrower regions above and below. Work on the groove guide progressed in Japan [2,3] and in the United States [4-6] until the middle 1960's, but then stopped until it was revived and developed further by D.J. Harris and co-workers [7,8] in Wales.

It has been shown in the previous publications that the dominant mode in groove guide is a TE mode in the longitudinal direction whose theoretical propagation characteristics agree reasonably well with measurements. The first portion of the present investigation involves the derivation of an improved dispersion relation for the dominant mode which is more accurate than any given previously and is a closed-form transcendental relation that does not require any summation of terms. This result, simple in form and accurate, agrees better with measured data [3] than any earlier theoretical results over a wide range of parameter values.

The earlier theories either neglect entirely the susceptance contribution from the step junction in Fig. 1, or they perform mode matching there so that the dispersion relation involves infinite sums which produce a complicated dispersion relation even after truncation. Our approach was to derive a simple but accurate expression for the susceptance of the step junction, extrapolating from a little-known but available result for a closely related discontinuity. An accurate transverse equivalent network then becomes available in which all the elements are represented by simple closed-form expressions.

3. PHYSICAL BASIS FOR LEAKAGE OF HIGHER MODES

The second portion of our study, which involves the major contribution, relates to the leaky wave nature of the higher modes of groove guide. The leaky wave nature of these modes was originally noted by Nakahara and Kurauchi [2], and was brought to our attention by Prof. D.J. Harris. By examining the simple relations among various wavenumbers, Nakahara and Kurauchi concluded that the dominant mode is always bound, and that *all higher modes are leaky*. These considerations show *whether* or not the particular mode is leaky, but they do not indicate the *magnitude* of the leakage.

Our first step was to verify these original conclusions and, by extension, to obtain additional information on the propagating or evanescent nature of various field components. We then derived a transverse equivalent network that takes into account the coupling between the dominant and the first higher transverse modes. This network is shown in Fig. 2.

To understand the propagation behavior of the first higher longitudinal mode, we first recognize that the cross section dimensions must be large enough to permit both the dominant and the first higher longitudinal modes to propagate. Looking in the y direction in the structure of Fig. 1, we observe that at the step junction an $i = 1$ transverse mode will couple to all other transverse modes of the same symmetry; i.e., it will couple to all $i = 3, 5, 7, \dots$ transverse modes. In the transverse equivalent network of Fig. 2, the $i = 1$ and $i = 3$ transverse modes are separated out, and separate transmission lines are furnished for each of them. It is necessary to derive expressions for all the parameters of the network in Fig. 2, and we have obtained simple closed-form expressions for all of them. The coupling susceptance between the transmission lines was derived using small obstacle theory in a multimode context.

When the groove guide is excited in dominant mode

fashion, the $i = 1$ transmission line is propagating in the central region of width a , but evanescent in the outer narrower regions of width a' . Also, it can be shown that the $i = 3$ transmission line is below cutoff everywhere, so that the dominant longitudinal mode is purely bound. On the other hand, when the groove guide is excited in the first higher longitudinal mode, corresponding to the $i = 3$ transverse mode, the $i = 3$ transmission line is propagating in the central region but evanescent in the outer regions. But, the $i = 1$ transmission line can now be shown to be propagating in both the central and the outer regions. The result is that the first higher mode is leaky, but with the interesting feature that the energy that leaks has the variation in x of the dominant mode, not of the first higher mode.

These coupled transverse modes therefore combine to produce a net TE longitudinal mode (in the z direction) with a complex propagation constant, $\beta + j\alpha$. From the transverse equivalent network of Fig. 2 one can readily derive the dispersion relation in the form of a transcendental relation all of whose constituents are in a simple closed form. The leakage constant α can be found readily from this dispersion relation.

4. NUMERICAL RESULTS

We now present some numerical results for the behavior of the phase constant β and the attenuation constant α of the leaky mode that results when the groove guide is excited in the first higher longitudinal mode (the $i = 3$ transverse mode). In Figs. 3(a) and 3(b) we plot the variation of β and α as a function of frequency. We see from Fig. 3(a) that β is almost linear with frequency at the higher frequencies, but shows substantial curvature near cutoff. The variation of α with frequency, in Fig. 3(b), is seen to be almost hyperbolic at the higher frequencies; nearer to cutoff, α is seen to rise substantially.

These variations follow directly from the simple wavenumber relationships. By taking the real part, and noting that the transverse wavenumbers are independent of frequency, we find that β is approximately linearly proportional to the frequency when α is small, which occurs for the higher frequencies. Such behavior is in agreement with that in Fig. 3(a). When we take the imaginary part, we find that the product $\alpha\beta$ should remain independent of frequency. In the frequency range for which β is proportional to frequency, we thus find that α must vary as the reciprocal of the frequency, in agreement with Fig. 3(b).

The variations of β and α with the dimension b , which is the height of the central region, are presented in Figs. 4(a) and 4(b). The behavior of α , in Fig. 4(b), is particularly interesting. We observe that the curve seems to be comprised of a basic envelope which decreases monotonically as b increases, modified by a series of nulls which depress the envelope curve periodically. The basic envelope shape can be understood physically when we recognize that the k_{y3} dependence (of the exciting mode) in the central region varies with b . When b is large, $k_{y3}b$ is larger and the variation of the field in the y direction in the central region approximates a half-period sine wave in shape. Thus, the field at the step junctions is substantially lower than the field at the middle of the central region. As a result, the interaction between the $i = 1$ and $i = 3$ modes is substantially

reduced, and the value of α becomes much lower. When b is small, $k_{y3}b$ is small, and the field variation in the central region becomes only a fraction of the half-period sine wave, so that the field at the step junctions is nearly the same as that in the middle of the central region. Then, the interaction between the $i = 1$ and $i = 3$ modes is increased, and α increases.

The cause of the nulls in Fig. 4(b) may be understood by reference to the transverse equivalent network in Fig. 2. A standing wave in the vertical direction is present in the $i = 1$ mode in the central region. When the electrical length of that standing wave is a multiple of π , it is seen from Fig. 2 that a short circuit will appear across the terminals in the $i = 1$ transmission line that connect the $i = 1$ line with the exciting $i = 3$ line. No power is then coupled into the $i = 1$ line from the $i = 3$ line, and no leakage occurs for those values of b . Of course, as b approaches zero those terminals are again short-circuited and the leakage vanishes, as seen in Fig. 4(b).

It is therefore found that the value of the leakage constant α varies with frequency and is strongly dependent on the dimension b ; we also see that α can vary from zero to significant values.

Manuscript received on February 16, 1983.

REFERENCES

- [1] Polytechnic Institute of Brooklyn, Microwave Research Institute, Monthly Performance Summary, Report PIBMRI-873, p. 17-61, 1961.
- [2] T. Nakahara, N. Kurauchi, *Transmission Modes in the Grooved Guide*, "J. Inst. of Electronics and Commun. Engrs. of Japan", July 1964, vol. 47, n.7, p. 43-51. Also in "Sumitomo Electric Technical Review", January 1965, n.3, p. 65-71.
- [3] H. Shigesawa, K. Takiyama, *Transmission Characteristics of the Close Grooved Guide*, "J. Inst. of Electronics and Commun. Engrs. of Japan", November 1967, vol. 50, n.11, p. 127-135. Also in *On the Study of a Close Grooved Guide*, "Science and Engineering Review of Doshisha University", Japan, May 1968, vol. 9, n.1, p. 9-40.
- [4] P.J. Tischer, *The Groove Guide, a Low-loss Waveguide for Millimeter Waves*, "IEEE Trans. on Microwave Theory Tech.", September 1963, vol. MTT-11, p. 291-296.
- [5] J.W.E. Gilemsmann, *Groove Guide*. In: Proc. Sympos. on Quasi-Optics, Polytechnic Press of Polytechnic Institute of Brooklyn, 1964, p. 565-578.
- [6] N.Y. Yee, N.P. Audeh, *Wave Propagation in Groove Guide*. In: Proc. National Electronics Conf., 1965, vol. 21, p. 18-23.
- [7] D.J. Harris, K.W. Lee, *Groove Guide as a Low-Loss Transmission System for Short Millimetric Waves*, "Electron. Lett.", 8 December 1977, vol. 13, n. 25, p. 775-776. Professor Harris and his colleagues have published many papers on this topic, of which this is one of the first. One of their latest works is given as ref. 8.
- [8] D.J. Harris, S. Mak, *Groove-Guide Microwave Detector for 100 GHz Operation*, "Electron. Lett.", 23 July 1981, vol. 17, n.15, p.516-517.

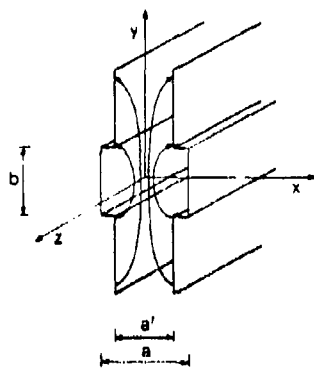


Fig. 1 - Cross section of symmetrical, nonradiating groove waveguide. The ends can either be left open, as shown, or be closed off.

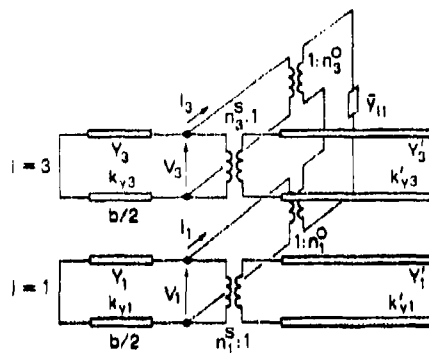


Fig. 2 - Transverse equivalent network for the structure whose cross section is shown in Fig. 1. (For clarity, the network is placed horizontally rather than vertically, and it represents the bisected structure, taking advantage of symmetry.)

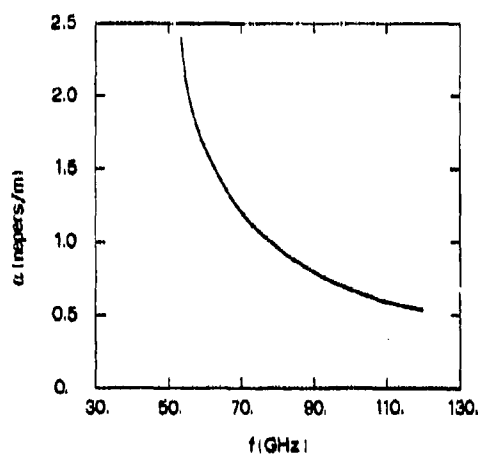
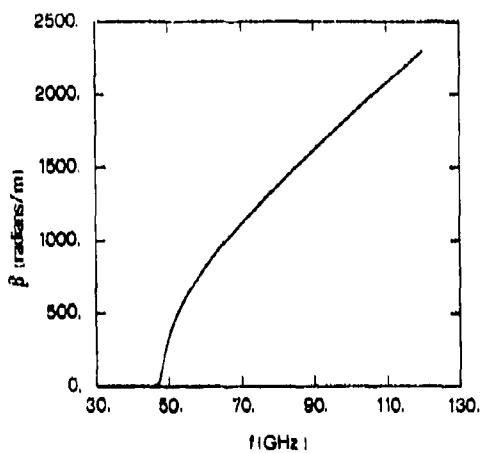


Fig. 3 - The variations with frequency of the phase constant β and the leakage (or attenuation) constant α of the leaky mode that results when the groove guide is excited in the first higher longitudinal mode ($a/a = 0.7$, $b/a = 0.4$).

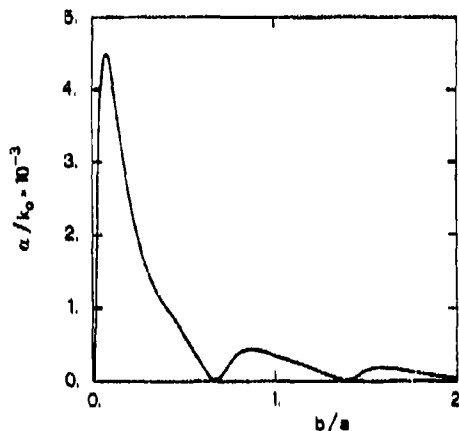
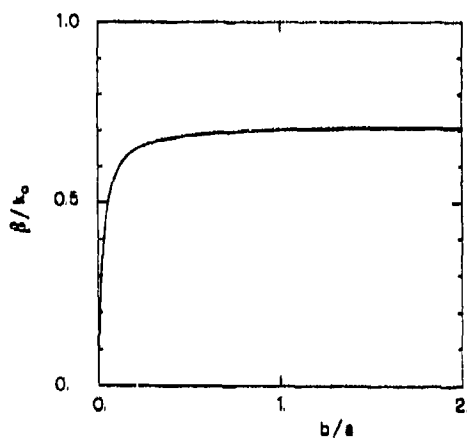


Fig. 4 - The variations of the phase constant β and the leakage constant α , both normalized to the free space wavenumber k_0 , of the leaky mode as a function of the height b of the central region in the groove guide, normalized to the width a ($f = 64$ GHz, $a/a = 0.7$).

THE LEAKY MODE SPECTRUM OF GROOVE GUIDE

LAMPARIELLO P. (*) - OLINER A.A. (**)

* Dipartimento di Elettronica, Università di Roma, Via Eudossiana 18 - 00184 Roma, Italy

** Polytechnic Institute of New York, 333 Jay Street - Brooklyn, N.Y. 11201, U.S.A.

ABSTRACT. - The mode spectrum of open symmetrical groove guide, a low-loss waveguide proposed some years ago for millimeter wavelengths and of interest again today, is investigated quantitatively. The dominant mode is purely bound, as is well known, but we find that *all higher modes are leaky*. We first verified an early prediction that all the *odd* higher modes leak, and we find that all *even* higher modes do also. The leakage for the lowest odd and even leaky modes is obtained quantitatively by deriving accurate transverse equivalent networks, all of whose elements are in closed form.

INTRODUCTION

Groove guide is one of a group of waveguiding structures proposed 20 or more years ago for use at millimeter wavelengths. Those waveguides were not pursued beyond some initial basic studies because they were not yet needed, and because adequate sources for millimeter waves were not yet available. Today, such sources are readily available, and the many advantages of millimeter waves are becoming increasingly appreciated.

It was also recognized some years ago that the shorter wavelengths associated with millimeter waves produce problems relating to the small size of components and the high attenuation of the waveguides. New types of waveguide were therefore proposed for which the attenuation per unit length would be substantially lower than that for customary waveguides, and for which, in some cases, the cross section dimensions were greater. Groove guide is one of the waveguides in that category, and attention is again being paid to it in the context of components for it and new leaky-wave antennas which are based on it.

The basic form of open symmetrical groove guide is shown in Fig. 1, together with an indication of the electric field lines present for the lowest mode. One should note that the structure resembles that of rectangular waveguide with most of the top and bottom walls removed. The attenuation associated with those walls increases as the frequency is increased, whereas the attenuation due to the side walls (with the electric field parallel to the walls) decreases with increasing frequency. Therefore, the overall attenuation for groove guide at higher frequencies is very much less than that for rectangular waveguide.

The greater width in the middle region was shown by T. Nakahara, [1961, 1964] the inventor of groove guide, to serve as the mechanism that confines the field in the vertical direction, much as the dielectric central region does in H guide. The field thus decays exponentially away from the central region in the narrower regions above and below. Work on the groove guide progressed in Japan [T. Nakahara - N. Kurauchi, 1964; H. Shigesawa - K. Takiyama, 1967] and in the United States [F.J. Tischer, 1963; J.W. Griesmann, 1964; N.Y. Yee - N.F. Audoh, 1965] until the middle 1960's, but then stopped until it was revived and developed further in the 1970's by D.J. Harris and co-workers [D.J. Harris - K.W. Lee, 1977; D.J. Harris - S. Mak, 1981] in Wales.

It has been shown in the previous publications that the dominant mode in groove guide is a TE mode in the longitudinal direction whose theoretical propagation characteristics agree reasonably well with measurements. Little is known, however, about the nature of the *higher modes*. The only reference in the literature relates to the *odd* higher modes, and it corresponds to a small section in a paper by Nakahara and Kurauchi [1964]. By examining the simple

relations among various wavenumbers, these authors obtained the very interesting conclusion that the dominant mode is always bound, and that all odd higher modes are *leaky*. These considerations show *whether* or not the particular mode is leaky, but they do not indicate the *magnitude* of the leakage.

A recent publication [P. Lampariello - A.A. Oliner, 1982] summarized an investigation by the present authors which verified these qualitative conclusions, and developed an accurate closed-form dispersion relation for the magnitude of the leakage for the first higher *odd* mode. Some new results are now presented for the lowest leaky *even* mode, together with some of the earlier material for the first higher *odd* mode so that comparisons can be made between them.

HIGHER ODD MODES

After verifying the original [T. Nakahara - N. Kurauchi, 1964] qualitative conclusions for these odd higher modes, we derived a *transverse equivalent network* that takes into account the coupling between the dominant and the first higher odd transverse modes; this network is shown in Fig. 2. From the dispersion relation that follows from this equivalent network, we have obtained quantitative values of the propagation behavior, including the leakage constant.

Let us recognize that we are investigating the case for which the cross section dimensions are large enough to permit both the dominant and the first higher odd longitudinal modes to propagate. Looking in the *y* direction of Fig. 1, we then see that the guide can be initially excited such that the incident power is basically either in the $i = 1$ transverse mode, for which the *x* dependence is a half sine wave, or in the $i = 3$ transverse mode, for which the *x* dependence contains three half sine waves. These excitations result in the $n = 1$ and $n = 3$ longitudinal modes, respectively. In either case, we observe that at the step junction an $i = 1$ or $i = 3$ transverse mode will couple to all other transverse modes of the same symmetry; for example, the $i = 3$ mode will couple to all of the $i = 1, 5, 7, \dots$ transverse modes. In the transverse equivalent network of Fig. 2, the $i = 1$ and $i = 3$ transverse modes are separated out, and separate transmission lines are furnished for each of them. It is necessary to derive expressions for all the parameters of the network in Fig. 2, and we have obtained simple closed-form expressions for all of them. The coupling susceptance between the transmission lines was derived using small obstacle theory in a multimode context.

When the groove guide is excited in *dominant mode* fashion, the $i = 1$ transmission line is propagating in the central region of width *a*, but evanescent in the outer narrower regions of width *a'*. Also, it can be shown that the $i = 3$ transmission line is below cutoff

everywhere, so that the dominant longitudinal mode is purely bound. On the other hand, when the groove guide is excited in the first higher odd longitudinal mode, corresponding to the $i = 3$ transverse mode, the $i = 3$ transmission line is propagating in the central region but evanescent in the outer regions. But, the $i = 1$ transmission line can now be shown to be propagating in both the central and the outer regions. The result is that the first higher odd mode is leaky, but with the interesting feature that the energy that leaks has the variation in x of the dominant mode, not of the first higher mode.

These coupled transverse modes combine to produce a net TE longitudinal mode (in the z direction) with a complex propagation constant, $\beta - j\alpha$. From the transverse equivalent network of Fig. 2 one can readily derive the dispersion relation in the form of a transcendental relation all of whose constituents are in a simple closed form. The leakage constant α can be found readily from this dispersion relation.

NUMERICAL RESULTS FOR FIRST HIGHER ODD MODE

We now present some numerical results for the behavior of the phase constant β and the attenuation constant α of the leaky mode that results when the groove guide is excited in the first higher odd longitudinal mode (the $i = 3$ transverse mode). We have obtained numerical values for the variation of β and α as a function of frequency, of the relative width a'/a , and of the aspect ratio b/a . Only the last-mentioned variation will be discussed here, because of space limitations.

The variations of β and α with the dimension b , which is the height of the central region, are presented in Fig. 3 (a) and 3 (b). The behavior of α , in Fig. 3 (b), is particularly interesting. We observe that the curve seems to be comprised of a basic envelope which decreases monotonically as b increases, modified by a series of nulls which depress the envelope curve periodically. The basic envelope shape can be understood physically when we recognize that the $k_y b$ dependence (of the exciting mode) in the central region varies with b . When b is large, $k_y b$ is large and the variation of the field in the y direction in the central region approximates a half-period sine wave in shape. Thus, the field at the step junctions is substantially lower than the field at the middle of the central region. As a result, the interaction between the $i = 1$ and $i = 3$ modes is substantially reduced, and the value of α becomes much lower. When b is small, $k_y b$ is small, and the field variation in the central region becomes only a fraction of the half-period sine wave, so that the field at the step junctions is nearly the same as that in the middle of the central region. Then, the interaction between the $i = 1$ and $i = 3$ modes is increased, and α increases.

The cause of the nulls in Fig. 3 (b) may be understood by reference to the transverse equivalent network in Fig. 2. A standing wave in the vertical direction is present in the $i = 1$ mode in the central region. When the electrical length of that standing wave is a multiple of π , it is seen from Fig. 2 that a short circuit will appear across the terminals in the $i = 1$ transmission line that connect the $i = 1$ line with the exciting $i = 3$ line. No power is then coupled into the $i = 1$ line from the $i = 3$ line, and no leakage occurs for those values of b . Of course, as b approaches zero those terminals are again short-circuited and the leakage vanishes, as seen in Fig. 3 (b).

HIGHER EVEN MODES

The results described above apply to the spectrum of odd higher modes. We have also examined the spectrum of even higher modes. We find there that qualitatively the same leakage behavior is obtained, but that certain interesting differences appear in the dependence of the leakage constant on the dimensional parameters.

When an odd higher mode is incident in the symmetrical groove guide shown in Fig. 1, the yz plane which bisects the structure vertically, becomes an open-circuit wall (or magnetic wall). Because of the symmetry of the step junctions, all of the transverse modes excited at those step junctions also possess the open circuit bisec-

tion property. Thus, when the $i = 3$ transverse mode is incident, the step junctions couple it to the $i = 1, 5, 7, \dots$ modes, and we saw above that the $i = 1$ transverse mode, being above cutoff transverse in the outer region of width a' , causes the resulting $n = 3$ longitudinal mode to be leaky. Now, when an even higher mode is incident, say the $i = 2$ transverse mode, the bisecting yz plane becomes a short-circuit wall (or electric wall). The transverse modes excited by the symmetrical step junctions are now the $i = 0, 4, 6, \dots$ modes. The $i = 4, 6, \dots$ transverse modes all retain the basic E_x nature of the exciting $i = 2$ mode, as do all the odd modes (except for the open or short circuit nature of the bisecting yz plane). The $i = 0$ transverse mode is different in that it resembles a TEM mode between parallel plates.

The transverse equivalent network for the longitudinal $n = 2$ mode thus requires the inclusion of the $i = 2$ and the $i = 0$ transmission lines, coupled together at the step junctions. When the groove guide is bisected horizontally at the xz plane, the simplified bisected transverse equivalent network has exactly the same form as that in Fig. 2 for the first higher odd mode. In fact, the appropriate network is achieved, in form, by simply replacing 3 and 1 everywhere in the network by 2 and 0, respectively. The expressions representing the parameters of the network are different, of course, but we have again derived closed-form results for them.

When the $i = 2$ transmission line is excited we find that in the transverse equivalent network the $i = 2$ transmission line is propagating in the central region of width a , but evanescent in the outer narrower regions of width a' . On the other hand, the $i = 0$ transmission line, which corresponds to a TEM-like transverse mode, is above cutoff in both the inner and outer regions, as we expect. As a result, the $n = 2$ longitudinal mode, which is the first higher even mode, is leaky, but the transverse form of the leakage is TEM-like and not of the form of the exciting $i = 2$ mode.

In a sense, this leakage behavior is similar to that found for $i = 3$ (first higher odd mode) excitation, but the polarization of the electric field of the leakage energy is horizontal here whereas it was vertical there.

NUMERICAL RESULTS FOR FIRST HIGHER EVEN MODE

The variations of β and α with dimension b , the height of the central region, are presented in Figs. 4 (a) and 4 (b) for the $n = 2$ longitudinal mode, which results in leakage with a TEM-like transverse form. The curves in these figures are to be compared with those in Figs. 3 (a) and 3 (b). Although the basic forms of the curves are clearly similar, comparison yields certain interesting differences. (It should be noted that for the $n = 2$ mode curves in Figs. 4 the value of a'/a is 0.6, whereas the a'/a value for the curves in Figs. 3 is 0.7. The reason for the selection of the particular a'/a values is that the leakage constant α reached its maximum in each case for approximately those values of a'/a .)

The most striking difference is that the leakage rate for the even mode is much smaller than that for the odd mode (the ordinate scales have been made equal). One can also note that for the even mode the maximum occurs at a larger value of b . These differences are due primarily to the polarization of the leakage energy. For the odd mode, the leakage occurs via the $i = 1$ transverse mode, which has a predominantly vertical electric field. That field component has a maximum at the horizontal bisecting plane $y = 0$, so that the leakage can remain high even near to $b = 0$. For the even mode, the leakage is due to the $i = 0$ mode, which has a horizontal electric field that goes to zero at the $y = 0$ bisecting plane. Since stronger leakage occurs for smaller values of b , as commented on earlier, a contradiction arises for the even mode case, thus preventing the leakage from reaching large values. The same effect would tend to push the maximum for the even mode to somewhat larger values of b .

It is also seen that the nulls for the two cases in Figs. 3 (b) and 4 (b) occur at different values of b , which is to be expected since the transverse wavenumbers k_{y1} and k_{y0} are different. It is also observed from Figs. 3 (a) and 4 (a) that the value of β is

greater for the even mode, a result consistent with the fact that the $i = 2$ mode is a lower mode than is the $i = 3$ mode, since the exciting mode determines the value of β to a predominant extent.

The expressions for the susceptances in the transverse equivalent networks become less accurate for small values of b/a , which is precisely the range in which the values of α are maximum. The numerical values near the maxima are therefore not as accurate as those for larger values of b/a , but the trends shown in Figs. 3 and 4 should nevertheless be correct.

In summary, this study has shown that the groove guide is an interesting open waveguide, with its dominant mode purely bound, but with all of its higher modes, both even and odd, leaky. Transverse equivalent networks were also derived, which yielded dispersion relations for the β and α of the first higher longitudinal modes of even and odd symmetry; some numerical values of their behavior are presented above, and the even and odd modes are compared.

ACKNOWLEDGMENT

This work has been supported in part by the Air Force Rome Air Development Center at Hanscom Air Force Base, under Contract No. F19623-81-K-0044, and in part by the University of Rome and by the Consiglio Nazionale delle Ricerche of Italy.

REFERENCES

1. J.W.E. Greismann, 1964, "Groove Guide", Proc. Sympos. on Quasi-Optics, Polytechnic Press of Polytechnic Institute of Brooklyn, pp. 565-578.
2. D.J. Harris and K.W. Lee, Dec. 8, 1977, "Groove Guide as a Low-Loss Transmission System for Short Millimetric Waves", Electron. Lett., vol. 13, no. 25, pp. 775-778. Professor Harris and his colleagues have published many papers on this topic, of which this is one of the first. One of their latest works is given as reference 3.
3. D.J. Harris and S. Mak, July 23, 1981, "Groove-Guide Microwave Detector for 100 GHz Operation", Electron. Lett., vol. 17, no. 15, pp. 516-517.
4. P. Lampariello and A.A. Oliner, 1982, "Bound and Leaky Modes in Symmetrical Open Groove Guide", Atti della IV Riunione Nazionale di Elettromagnetismo Applicato, Firenze, Italy, pp. 217-219. To be published in a special issue of Alta Frequenza.
5. T. Nakahara, 1961, Polytechnic Institute of Brooklyn, Microwave Research Institute, Monthly Performance Summary, Report PIBMRI-875, pp. 17-61.
6. T. Nakahara and N. Kurauchi, 1964, "Transmission Modes in the Grooved Guide", J. Inst. Electronics and Commun. Engrs. of Japan, vol. 47, no. 7, pp. 43-51. Also in: 1965, Sumitomo Electric Technical Review, no. 5, pp. 65-71.
7. H. Shigesawa and K. Takiyama, 1967, "Transmission Characteristics of the Close Grooved Guide", J. Inst. of Electronics and Commun. Engrs. of Japan, vol. 50, no. 11, pp. 127-135. Also in: 1968, "On the Study of a Close Grooved Guide", Science and Engineering Review of Doshisha University, Japan, vol. 9, no. 1, pp. 9-40.
8. F.J. Tischer, 1963, "The Groove Guide, a Low-Loss Waveguide for Millimeter Waves", IEEE Trans. on Microwave Theory Tech., vol. MTT-11, pp. 291-296.
9. N.Y. Yee and N.F. Au-deh, 1965, "Wave Propagation in Groove Guides", Proc. National Electronics Conf., vol. 21, pp. 18-23.

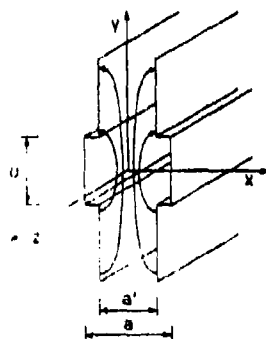


Fig. 1 - Cross section of symmetrical, nonradiating groove waveguide. The ends can either be left open, as shown, or be closed off.

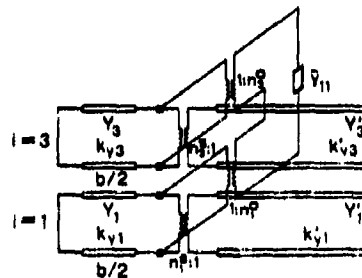


Fig. 2 - Transverse equivalent network, bisected in view of symmetry, for the structure whose cross section is shown in Fig. 1 (for clarity, the network is placed horizontally rather than vertically).

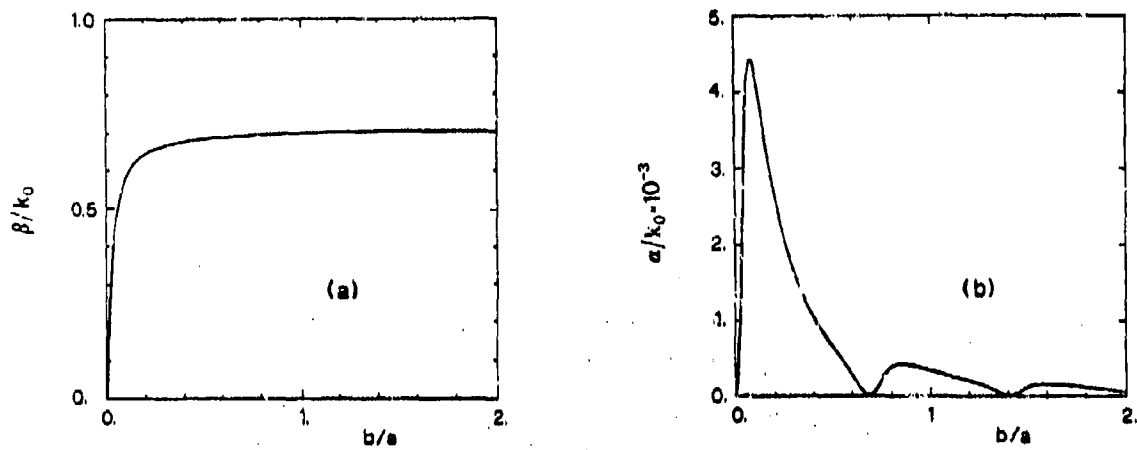


Fig. 3 - The variations of the phase constant β and the leakage constant α , both normalized to the free space wavenumber k_0 , of the first higher *odd* leaky mode as a function of the height h of the central region in the groove guide, normalized to the width a ($f = 64$ GHz, $a'/a = 1.7$).

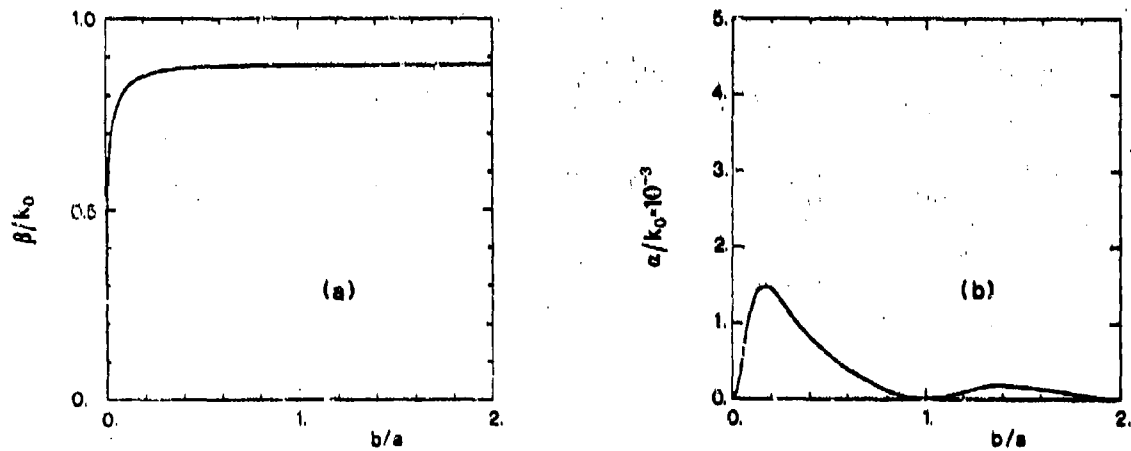


Fig. 4 - The variations of β and α , as in Fig. 3, but for the first higher *even* mode ($f = 64$ GHz, $a'/a = 0.6$). Note that the scales in Figs. 3 and 4 are identical.

2. Derivations for the $n = 3$ (Odd) Leaky Mode

(a) Wavenumber Considerations to Demonstrate Leakage

We shall first present, following Nakahara and Kurauchi [9], the simple wavenumber considerations that indicate under what conditions the $n = 3$ mode is leaky.

When we excite the groove guide in the $n = 3$ mode, the field variation in the x direction, across the guide, possesses three half sine waves, so that $k_{x3} = 3\pi/a$ and $k'_{x3} = 3\pi/a'$. As before, the primed and unprimed quantities refer to the regions of narrower width a' and greater width a , respectively. More precisely, we should say that the $i = 3$ transverse mode has these x variations. If the $n = 3$ longitudinal mode involved only the $i = 3$ transverse mode, then it would be purely bound, with k_{y3} real and k'_{y3} imaginary. Actually, if the groove guide cross section is excited in the $i = 3$ transverse mode, then, when this mode is incident on the step junction between the sections of widths a and a' , an infinite number of odd transverse modes will be excited there, i.e., the $i = 1, 5, 7, 9 \dots$ modes. Let us examine the properties of the $i = 1$ mode.

We may write

$$k_o^2 = k_i^2 + \left(\frac{3\pi}{a}\right)^2 + k_{y3}^2 \quad (2.1)$$

$$k_o^2 = k_i^2 + \left(\frac{3\pi}{a'}\right)^2 - |k'_{y3}|^2 \quad (2.2)$$

since

$$k'_{y3} = -j |k'_{y3}| \quad (2.3)$$

and

$$k_o^2 = k_i^2 + \left(\frac{\pi}{a}\right)^2 + k_{y1}^2 = k_i^2 + \left(\frac{\pi}{a'}\right)^2 + (k'_{y1})^2 \quad (2.4)$$

but we do not yet know the nature of k_{y1} and k'_{y1} . However, from (2.1) and (2.4), we note that

$$k^2_{y1} = k^2_{y0} + \left(\frac{3\pi}{a}\right)^2 - \left(\frac{\pi}{a}\right)^2 = k^2_{y0} + 2\left(\frac{2\pi}{a}\right)^2 \quad (2.5)$$

so that k_{y1} is real, and we also observe that

$$(k'_{y1})^2 = k^2_{y0} + \left(\frac{3\pi}{a}\right)^2 - \left(\frac{\pi}{a'}\right)^2 \quad (2.6)$$

so that

$$(k'_{y1})^2 > k^2_{y0} > 0 \quad (2.7)$$

if

$$\frac{a'}{a} > \frac{1}{3} \quad (2.8)$$

which is always true in any practical groove guide.

We therefore see that, if (2.8) is satisfied, both k_{y1} and k'_{y1} are real; the fact that k'_{y1} is real means that real power is carried away, and the overall mode is leaky. Furthermore, the power that leaks has the x dependence of the $i = 1$ mode, not the $i = 3$ mode.

When these wavenumber properties are viewed in the framework of the transverse equivalent network shown in Fig. 2 of the first paper in Sec. B, 1, their meanings become clearer. For this reason, the transverse equivalent network is repeated here for convenience as Fig. 2.1. Also, the wavenumber statements made at the top of page 2 of that paper are proven by reference to equations (2.1) through (2.8).

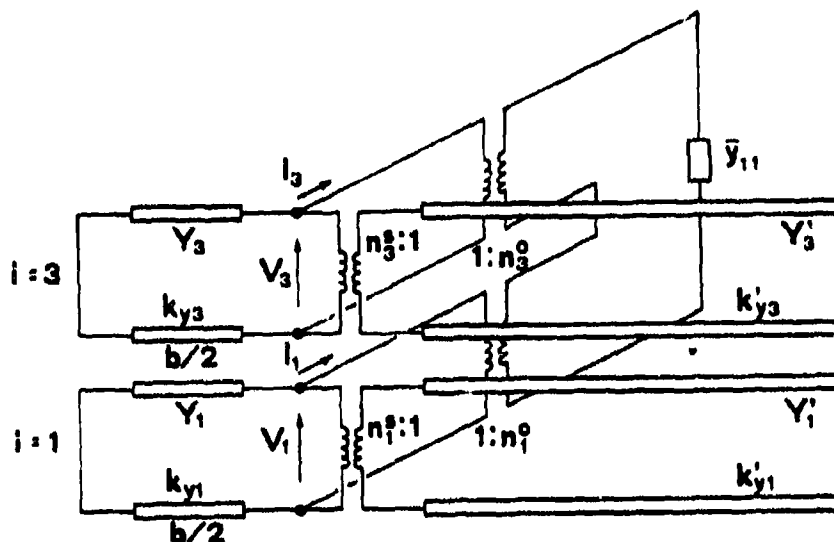


Fig. 2.1 Transverse equivalent network for open symmetrical groove guide, corresponding to excitation in the first higher odd ($n = 3$) longitudinal mode. The network shows the coupling between $i = 1$ and $i = 3$ odd transverse modes, and has been bisected to take advantage of symmetry. The network has also been placed on its side for clarity.

(b) The Mode Functions and the Field Components

Although the net longitudinal mode is a TE mode ($E_z = 0$), the transverse modes are hybrid, possessing five components of field. We take advantage of the fact that $E_z = 0$ by characterizing these transverse modes, which are hybrid in y , as H-type modes with respect to z , or $H^{(z)}$ -type modes. Such modes, with their orthogonality properties, have been discussed in detail by Altschuler and Goldstone [19]. The modes carried by the transmission lines in the transverse equivalent network referred to above are therefore the $i = 1$ and the $i = 3$ $H^{(z)}$ -type modes.

The mode functions and the field components for these modes have been derived, and are listed below. The transmission direction is y for these transverse modes.

For the $i = 1$ transverse mode

$$e_{z1}(x, z) = \sqrt{\frac{2}{a}} \sin \frac{\pi x}{a} e^{-\beta_1 z} \quad (2.9)$$

$$h_{z1}(x, z) = -\sqrt{\frac{2}{a}} \sin \frac{\pi x}{a} e^{-\beta_1 z} \quad (2.10)$$

$$h_{y1}(x, z) = \frac{jk_z}{k_0^2 - k_z^2} \sqrt{\frac{2}{a}} \frac{\pi}{a} \cos \frac{\pi x}{a} e^{-\beta_1 z} \quad (2.11)$$

$$e_{y1}(x, z) = \frac{1}{jk_{y1}} \frac{\partial e_{z1}}{\partial x} = \sqrt{\frac{2}{a}} \frac{\pi}{a} \frac{1}{jk_{y1}} \cos \frac{\pi x}{a} e^{-\beta_1 z} \quad (2.12)$$

$$h_{y1}(x, z) = -\frac{k_{y1} k_z}{k_0^2 - k_z^2} h_{z1} = \sqrt{\frac{2}{a}} \frac{k_{y1} k_z}{k_0^2 - k_z^2} \sin \frac{\pi x}{a} e^{-\beta_1 z} \quad (2.13)$$

$$E_{z1}(x, y, z) = V_1(y) e_{z1}(x, z) \quad (2.14)$$

$$E_{y1}(x, y, z) = Z_1 I_1(y) \frac{1}{jk_{y1}} \frac{\partial e_{z1}(x, z)}{\partial x} \quad (2.15)$$

$$E_{x1}(x, y, z) = 0 \quad (2.16)$$

$$H_{z1}(x, y, z) = I_1(y) h_{z1}(x, z) \quad (2.17)$$

$$H_{y1}(x, y, z) = Y_1 V_1(y) \left[-\frac{k_{y1} k_z}{k_0^2 - k_z^2} \right] h_{z1}(x, z) \quad (2.18)$$

$$H_{x1}(x, y, z) = I_1(y) h_{x1}(x, z) \quad (2.19)$$

with

$$Y_1 = \frac{k_0^2 - k_z^2}{\omega \mu k_{y1}}, \quad Z_1 = \frac{1}{Y_1} \quad (2.20)$$

For the $i = 3$ transverse mode

$$e_{zs}(x, z) = \sqrt{\frac{2}{a}} \sin \frac{3\pi x}{a} e^{-\beta_3 z} \quad (2.21)$$

$$h_{zs}(x, z) = -\sqrt{\frac{2}{a}} \sin \frac{3\pi x}{a} e^{-\beta_3 z} \quad (2.22)$$

$$h_{zs}(x, z) = \frac{j\beta_3}{k_0^2 - k_z^2} \sqrt{\frac{2}{a}} \frac{3\pi}{a} \cos \frac{3\pi x}{a} e^{-\beta_3 z} \quad (2.23)$$

$$e_{ys}(x, z) = \frac{1}{jk_{y3}} \frac{\partial e_{zs}}{\partial x} = \sqrt{\frac{2}{a}} \frac{3\pi}{a} \frac{1}{jk_{y3}} \cos \frac{3\pi x}{a} e^{-\beta_3 z} \quad (2.24)$$

$$h_{ys}(x, z) = -\frac{k_{y3}k_z}{k_0^2 - k_z^2} h_{zs} = \sqrt{\frac{2}{a}} \frac{k_{y3}k_z}{k_0^2 - k_z^2} \sin \frac{3\pi x}{a} e^{-\beta_3 z} \quad (2.25)$$

$$E_{zs}(x, y, z) = V_3(y) e_{zs}(x, z) \quad (2.26)$$

$$E_{ys}(x, y, z) = Z_3 I_3(y) \frac{1}{jk_{y3}} \frac{\partial e_{zs}(x, z)}{\partial x} \quad (2.27)$$

$$E_{zs}(x, y, z) = 0 \quad (2.28)$$

$$H_{zs}(x, y, z) = I_3(y) h_{zs}(x, z) \quad (2.29)$$

$$H_{ys}(x, y, z) = Y_3 V_3(y) \left[-\frac{k_{y3}k_z}{k_0^2 - k_z^2} \right] h_{zs}(x, z) \quad (2.30)$$

$$H_{zs}(x, y, z) = I_3(y) h_{zs}(x, z) \quad (2.31)$$

with

$$Y_3 = \frac{k_0^2 - k_z^2}{\omega \mu k_{y3}}, \quad Z_3 = \frac{1}{Y_3} \quad (2.32)$$

Y_1 and Y_3 are the respective characteristic admittances.

(c) Turns Ratios for the Step Junction

There are two turns ratios for the step junction, one each for the $i = 1$ and $i = 3$ transverse modes. Let us designate them by n_1^s and n_3^s , respectively, where the superscript s denotes "step."

The expression for n_1^s is the same as the one that was derived for the $i = 1$ mode in the asymmetric strip antenna, and it is derived in Appendix B in Sec. C, 2(a) there. The expression for it is given there as eq. (15), which is

$$n_1^s = \left[\frac{a'}{a} \right]^{3/2} \frac{4}{\pi} \frac{\cos \frac{\pi a'}{2a}}{1 - \left(\frac{a'}{a} \right)^2} \quad (2.33)$$

Proceeding in a fashion similar to that described in Appendix B, we find for the $i = 3$ mode, using (2.21) for the required mode function,

$$n_3^s = \left[\frac{a'}{a} \right]^{3/2} \frac{4}{3\pi} \frac{\cos \left[\pi \left(1 + \frac{3a'}{2a} \right) \right]}{1 - \left(\frac{a'}{a} \right)^2} \quad (2.34)$$

(d) The Coupling Network at the Step Junction

The step junction also couples the $i = 1$ and $i = 3$ transverse modes; all the higher modes excited at that junction are lumped into the susceptance element \bar{y}_{11} . The simplified form of the coupling network, shown in Fig. 2.1 emerging at an angle, is consistent with the small obstacle theory used to evaluate the coupling elements.

The viewpoint adopted with respect to the evaluation of the step junction discontinuity susceptance is the following. The step ratio a'/a is usually 0.7 or greater, so that the step is small compared to the actual

guide width itself. The coupling effect is therefore sufficiently small that, for the polarizations involved, a reasonably accurate result should be obtained on use of small obstacle theory. Here, however, we have a step geometry rather than a flat obstacle, but, on use of stored power considerations, we may solve for the y_{11} for the flat obstacle case and then take

$$\bar{y}_{11} = 0.55 y_{11} \quad (2.35)$$

for the susceptance of the step. This procedure was described in detail in Appendix A, in Sec. B, 3 there, where it was applied very successfully. The justifications will therefore not be repeated now.

The remaining consideration is that small obstacle theory requires that the obstacle be far from the walls, in addition to being small, and that here the obstacle is located at the wall. That situation was also present in the asymmetric strip antenna, where the coupling strip was located at the wall. As explained there (Sec. C, 3 in Appendix B) in detail, this difficulty is overcome by employing symmetry. One recognizes that the actual obstacle on the wall in the actual guide is equivalent to a centered obstacle of twice the width in a waveguide of twice the width, with a higher order mode incident such that the mid-plane is an electric wall. The calculations should then reflect this consideration.

The appropriate small obstacle theory has been discussed in some detail in Sec. C, 3 of the report in Appendix B, so that we shall not repeat the details here but instead follow the procedure described there. After reducing the general expression to scalar form, as appropriate to the problem here, we may write, from eq. (25) of Appendix B,

$$y_{ij} = j\omega m (\mu Y_i^* Y_j h_{y'0}^* h_{x'0} - \epsilon \epsilon_{x'0}^* \epsilon_{y'0}) \quad (2.36)$$

For our problem, i and j are 1 and 3, and

$$m = -\frac{\pi}{4}(a-a')^2 \quad (2.37)$$

At the obstacle location, $x = -a/2$, the mode functions (2.9), (2.13), (2.14) and (2.25) reduce to

$$e_{x10} = -\sqrt{\frac{2}{a}} e_{x30} \quad (2.38)$$

$$h_{y10} = -\frac{k_{y1}k_{y3}}{k_0^2 - k_1^2} \sqrt{\frac{2}{a}} = -h_{y30} \frac{k_{y1}}{k_{y3}} \quad (2.39)$$

The z dependence is dropped because of the complex conjugates appearing in (2.36). Finally, we need the characteristic admittances Y_1 and Y_3 , which are given by (2.20) and (2.32), respectively.

Using (2.37) through (2.39) together with (2.20) and (2.32), we find from (2.36),

$$y_{11} = y_{33} = j \frac{\pi}{\omega \mu} \frac{(a-a')^2}{2a} (k_0^2 - k_1^2) \quad (2.40)$$

We also learn from the discussion in Sec. C, 3 of Appendix B that in Sec. C, 3 of Appendix B that the transformer turns ratios n_1^0 and n_3^0 appearing in the coupling network in Fig. 2.1 are related to the susceptance elements y_{11} and y_{33} by

$$y_{11} = y_{11} n_1^0 n_1^0 \quad (2.41)$$

$$y_{33} = y_{11} n_3^0 n_3^0 \quad (2.42)$$

In view of (2.40) together with (2.41) and (2.42), we obtain

$$n_1^o = 1, \quad n_3^o = 1 \quad (2.43)$$

where the superscript o signifies "obstacle."

Based on this approximate theory, the coupling network has become particularly simple, with the turns ratios becoming equal to unity and the susceptance element \bar{y}_{11} being given by (2.35) together with (2.40).

(e) The Dispersion Relation

The theoretical approach employed in this analysis has as its conscious goal a simple approximate transverse equivalent network with closed-form expressions for its constituents. As a result, the dispersion relation that corresponds to a free resonance of this network will be simple in form and have all its elements in closed form. At the same time, the derivations have attempted to maintain reasonable accuracy while striving for simplicity. The principal approximation relates to the coupling network, where the value of susceptance \bar{y}_{11} may be on the low side, with the result that the value of α , and therefore the beam width of the radiation, may be a bit smaller than the actual value.

Almost by inspection of the transverse equivalent network in Fig. 2.1, we may write down the dispersion relation as

$$-j Y_3 \cot k_{y3} \frac{b}{2} + \frac{1}{(n_3^s)^2} Y_3' + \frac{1}{\bar{y}_{11} + \frac{1}{-j Y_1 \cot k_{y1} \frac{b}{2} + \frac{1}{(n_1^s)^2} Y_1'}} = 0 \quad (2.44)$$

where coupling susceptance \bar{y}_{11} is given by (2.35) together with (2.40), characteristic impedances Y_3 and Y_3' by (2.32), Y_1 and Y_1' by (2.20), and turns ratios n_3^s and n_1^s by (2.34) and (2.33), respectively.

3. Derivations for the n = 2 (Even) Leaky Mode

There is much in these derivations that parallels those in Sec. B, 2 above for the n = 3 mode, but there are also important differences. In the derivations below, we point out these differences where they occur.

(a) Wavenumber Considerations to Demonstrate Leakage

We first note that the incident transverse mode is the i = 2 mode, and that it couples at the step junction to the i = 0 mode.

All of the other even modes, i = 4, 6, ..., are also excited, but they only contribute to the reactive content of the step junction. To show that the higher even modes leak, and in particular the n = 2 mode, which is the first higher even mode, we parallel the derivation for the n = 3 case. We should note that Nakahara and Kurauchi [9] did not consider the even higher modes.

To understand the behavior of the i = 0 transverse mode, i.e., whether or not it is above cutoff transversely, we first write

$$k_o^2 = k_i^2 + \left(\frac{2\pi}{a}\right)^2 + k_{y2}^2 \quad (2.45)$$

$$k_o^2 = k_i^2 + \left(\frac{2\pi}{a}\right)^2 - |k_{y2}'|^2 \quad (2.46)$$

since

$$k_{y2}' = -j |k_{y2}'| \quad (2.47)$$

and

$$k_o^2 = k_i^2 + k_{y2}^2 = k_i^2 + (k_{y2}')^2 \quad (2.48)$$

because $k_{x0} = k'_{x0} = 0$. The $i = 0$ transverse mode is akin to a TEM mode traveling at an angle between parallel plates, so that there is no field variation across the plates. From (2.45) and (2.48) we observe that

$$(k'_{y0})^2 = k^2_{y0} = k^2_{y2} + \left(\frac{2\pi}{a}\right)^2 \quad (2.49)$$

From (2.49) we conclude that

$$k^2_{y0} > k^2_{y2} > 0 \quad (2.50)$$

and that

$$(k'_{y0})^2 > k^2_{y2} > 0 \quad (2.51)$$

so that both k_{y0} and k'_{y0} are real. An interesting difference between the even and odd mode cases is that in the even mode case there is no restriction necessary, like (2.8) in the odd mode case.

Since k'_{y0} is always real no matter what the ratio a'/a is, the even modes will be leaky under all conditions. Furthermore, the power that leaks has no x dependence, and it propagates at an angle away from the groove region like a TEM mode.

(b) The Mode Functions and the Field Components

The form of the transverse equivalent network for the $n = 2$ even mode is identical to that for the $n = 3$ odd mode, but the constituent transmission lines are different (now involving the $i = 0$ and $i = 2$ modes), and the expressions for the constituent elements are different, of course. For convenience, the transverse equivalent network is given in Fig. 2.2.

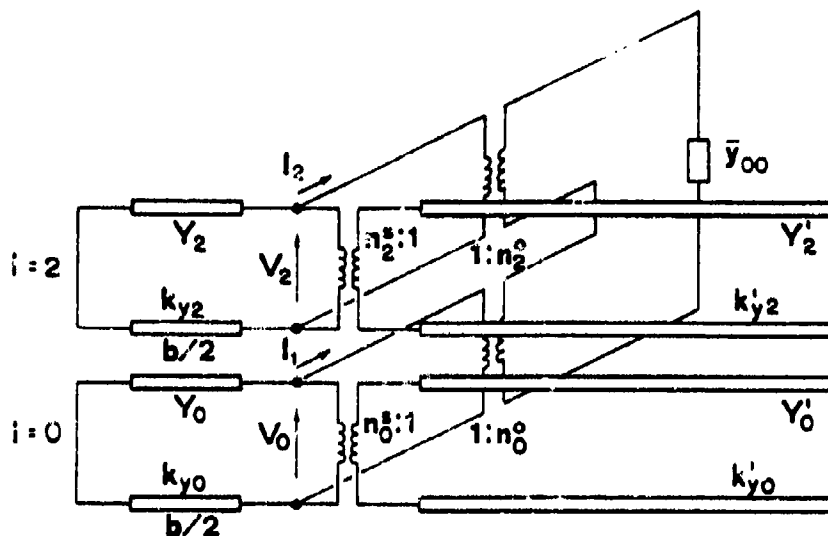


Fig. 2.2 Transverse equivalent network for open symmetrical groove guide, corresponding to excitation in the first higher even ($n = 2$) longitudinal mode. The network shows the coupling between the $i = 0$ and $i = 2$ even transverse modes, and has been bisected to take advantage of symmetry. The network has also been placed on its side for clarity.

The modes carried by the $i = 0$ and $i = 2$ transmission lines in Fig. 2.2 are again $H^{(z)}$ -type modes, and the mode functions and field components for them are now listed below. The transmission direction for these transverse modes is again y .

For the $i = 0$ transverse mode

$$e_{z0}(x, z) = \sqrt{\frac{1}{a}} e^{-j\beta_0 z} \quad (2.52)$$

$$h_{z0}(x, z) = -\sqrt{\frac{1}{a}} e^{-j\beta_0 z} \quad (2.53)$$

$$h_{zo}(x, z) = 0 \quad (2.54)$$

$$e_{yo}(x, z) = 0 \quad (2.55)$$

$$h_{yo}(x, z) = \sqrt{\frac{1}{a} \frac{k_{yo} k_z}{k_o^2 - k_z^2}} e^{-k_z z} = \sqrt{\frac{1}{a} \frac{k_z}{k_{yo}}} e^{-k_z z} \quad (2.56)$$

$$E_{zo}(x, y, z) = V_o(y) e_{zo}(x, z) \quad (2.57)$$

$$E_{yo}(x, y, z) = 0 \quad (2.58)$$

$$E_{zo}(x, y, z) = 0 \quad (2.59)$$

$$H_{zo}(x, y, z) = 0 \quad (2.60)$$

$$H_{yo}(x, y, z) = Y_o V_o(y) \left[-\frac{k_z}{k_{wo}} \right] h_{zo}(x, z) \quad (2.61)$$

$$H_{zo}(x, y, z) = I_o(y) h_{zo}(x, z) \quad (2.62)$$

with

$$Y_o = \frac{k_o^2 - k_z^2}{\omega \mu k_{yo}} = \frac{k_{yo}}{\omega \mu}, \quad Z_o = \frac{1}{Y_o} \quad (2.63)$$

For the $i = 2$ transverse mode

$$e_{x2}(x, z) = \sqrt{\frac{2}{a}} \cos \frac{2\pi x}{a} e^{-jk_z z} \quad (2.64)$$

$$h_{x2}(x, z) = -\sqrt{\frac{2}{a}} \cos \frac{2\pi x}{a} e^{-jk_z z} \quad (2.65)$$

$$h_{y2}(x, z) = -\frac{jk_z}{k_0^2 - k_z^2} \sqrt{\frac{2}{a}} \frac{\pi}{a} \sin \frac{2\pi x}{a} e^{-jk_z z} \quad (2.66)$$

$$e_{y2}(x, z) = j \sqrt{\frac{2}{a}} \frac{2\pi}{k_{y2} a} \sin \frac{2\pi x}{a} e^{-jk_z z} \quad (2.67)$$

$$h_{y2}(x, z) = \sqrt{\frac{2}{a}} \frac{k_{y2} k_z}{k_0^2 - k_z^2} \cos \frac{2\pi x}{a} e^{-jk_z z} \quad (2.68)$$

$$E_{x2}(x, y, z) = V_2(y) e_{x2}(x, z) \quad (2.69)$$

$$E_{y2}(x, y, z) = Z_2 I_2(y) \frac{1}{jk_{y2}} \frac{\partial e_{x2}(x, z)}{\partial x} \quad (2.70)$$

$$E_{z2}(x, y, z) = 0 \quad (2.71)$$

$$H_{x2}(x, y, z) = I_2(y) h_{x2}(x, z) \quad (2.72)$$

$$H_{y2}(x, y, z) = -Y_2 V_2(y) \frac{k_{y2} k_z}{k_0^2 - k_z^2} h_{x2}(x, z) \quad (2.73)$$

$$H_{z2}(x, y, z) = I_2(y) h_{z2}(x, z) \quad (2.74)$$

with

$$Y_2 = \frac{k_0^2 - k_z^2}{\omega \mu k_{y2}}, \quad Z_2 = \frac{r}{Y_2} \quad (2.75)$$

(c) Turns Ratios for the Step Junction

The two turns ratios in Fig. 2.2 for the step junction are n_0^s and n_2^s , for the $i = 0$ and $i = 2$ transmission lines, respectively.

Recognizing that the turns ratio is simply the ratio of voltage terms on each side of the step junction, and following the procedure described in Appendix B, we find for the $i = 0$ mode, using (2.52) for the required mode function,

$$n_0^s = \sqrt{\frac{a'}{a}} \quad (2.76)$$

and for the $i = 2$ mode, using (2.64),

$$n_2^s = \left[\frac{a'}{a} \right]^{1/2} \frac{2}{\pi} \frac{\sin \frac{\pi a'}{a}}{1 - \left(\frac{a'}{a} \right)^2} \quad (2.77)$$

(d) The Coupling Network at the Step Junction

As for the $n = 3$ odd mode case discussed in Sec. B, 2, we employ a simplified form for the coupling network, shown in Fig. 2.2 emerging at an angle, consistent with a small obstacle theory approach. The coupling network couples $i = 0$ and $i = 2$ transmission lines, and the effect of the higher even modes excited at the step junction is lumped into susceptance element \bar{y}_{00} .

The discussion presented in Sec. B, 2 for the coupling network applies here as well, and the procedure outlined there and in Appendix B have been followed in the derivation of the coupling elements. Equation (2.36) is employed here also, except that i and j now correspond to 0 and 2. Polarizability term m is still given by (2.37). At the obstacle location, at $x = -a/2$, the mode functions (2.52), (2.62), (2.56) and (2.68) reduce to

$$e_{y00} = \sqrt{\frac{1}{a}} \quad , \quad e_{y20} = -\sqrt{\frac{2}{a}} \quad (2.78)$$

$$h_{y00} = \sqrt{\frac{1}{a}} \frac{k_z}{k_{y0}} \quad , \quad h_{y20} = -\sqrt{\frac{2}{a}} \frac{k_{y2} k_z}{k_0^2 - k_z^2} \quad (2.79)$$

The z dependence is dropped because of the complex conjugates present in (2.36). We also need the characteristic admittances Y_0 and Y_2 , which are given by (2.63) and (2.75).

Using (2.37), (2.78) and (2.79), together with (2.63) and (2.75), we obtain from (2.36)

$$y_{00} = j \frac{\pi}{\omega \mu} \frac{(a-a')^2}{4a} (k_0^2 - k_z^2) \quad (2.80)$$

and

$$y_{22} = 2 y_{00} \quad (2.81)$$

From the relations

$$y_{00} = y_{00} n_0^2 n_0^2 \quad (2.82)$$

$$y_{22} = y_{00} n_2^2 n_2^2 \quad (2.83)$$

we find that the "obstacle" turns ratios become

$$n_0^2 = 1 \quad , \quad n_2^2 = \sqrt{2} \quad (2.84)$$

Finally, following (2.35), we write

$$\bar{y}_{00} = 0.55 y_{00} \quad (2.85)$$

We now have expressions for all the elements of the complete coupling network, with susceptance element \bar{y}_{00} obtainable from (2.85) and (2.80),

and the "obstacle" turns ratios n_0^o and n_2^o given by (2.84). It is interesting to note a difference here from the n^o terms for the $n = 3$ mode case. There, both turns ratios were equal to unity; here, one of them differs from unity.

(e) The Dispersion Relation

By virtue of the simple form of the transverse equivalent network, the dispersion relation is again simple. It becomes

$$-j Y_2 \cot k_{y2} \frac{b}{2} + \frac{1}{(n_2^s)^2} Y_2' + \frac{(n_2^s)^2}{\frac{1}{\bar{Y}_{00}} + \frac{1}{-j Y_0 \cot k_{y0} \frac{b}{2} + \frac{1}{(n_0^s)^2} Y_0'}} = 0 \quad (2.88)$$

where the coupling susceptance \bar{Y}_{00} is given by (2.80) together with (2.85), characteristic admittances Y_0 and Y_0' by (2.63), Y_2 and Y_2' by (2.75), and turns ratios n_0^s , n_2^s and n_2^o by (2.76), (2.77) and (2.84), respectively.

The general remarks made in connection with the $n = 3$ (odd) mode apply here as well.

C. ANTENNAS BASED ON THE $n = 2$ LEAKY MODE

1. Antenna of Simple Configuration

In Sec. B, 3, we presented derivations of the expressions for the constituents of the transverse equivalent network representative of the $n = 2$ higher mode of groove guide. Some of the properties of this mode were presented in the second of the two short papers in Sec. B, 1.

The $n = 2$ mode, which is leaky, possesses a modal symmetry akin to that of the second mode in rectangular waveguide, i.e., the vertical mid-plane is an electric wall. This modal feature permits us to bisect the groove guide structure vertically, and to then place a metal wall at this bisection plane without disturbing the field distribution. The resulting structure then takes the form shown in Fig. 2.3. That structure is now fed in the groove region in the $i = 1$ transverse mode, which is of course identical with the $i = 2$ mode in the unbisected groove guide. The behavior of the $n = 1$ longitudinal mode in the bisected structure of Fig. 2.3 is thus the same as that of the $n = 2$ mode discussed above in Sec. B for the full symmetrical groove guide.

It is interesting that the structure of Fig. 2.3 may be viewed from two points of view. One is the evolution indicated above from the first higher even mode ($n = 2$) of the symmetrical groove guide, which we have shown in Sec. B is leaky. The second viewpoint is that we have a modified groove guide that supports the dominant mode, which is purely bound in a symmetrical structure, but that the structure has now been made asymmetrical, thereby producing the leakage. The second point of view relates the mechanism of leakage to that employed in Sec. A for the asymmetric strip antenna. From either point of view, however, one readily sees that the bisected structure of Fig. 2.3 has the advantage of possessing a particularly simple configuration.

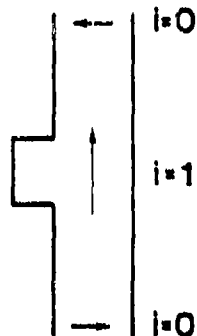


Fig. 2.3 Cross section of groove guide bisected vertically, resulting in a new type of leaky wave line source. Electric field directions are shown for the incident $i = 1$ transverse mode and the leaking $i = 0$ transverse mode.

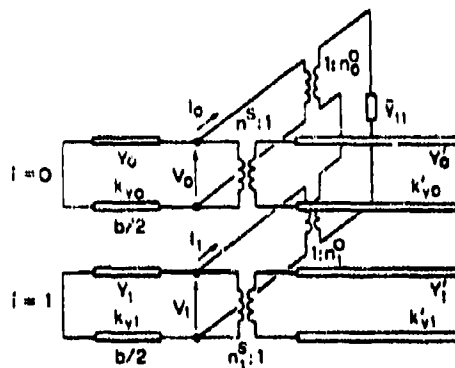


Fig. 2.4 Transverse equivalent network for the structure in Fig. 2.3, but bisected horizontally to take further advantage of symmetry. The network shows how the leaking $i = 0$ transverse mode couples to the incident $i = 1$ transverse mode. (The $i = 1$ mode in the bisected structure in Fig. 2.3 is the same as $i = 2$ mode in the full structure.) As in Fig. 2.2, the network is placed on its side for clarity.

Either mechanism can be employed to explain the leakage, but we already have a solution based on the former mechanism. The transverse equivalent network in Fig. 2.2 is therefore valid here, but we need to change the modal identifications from $i = 2$ to $i = 1$ whenever they appear, in recognition of the fact that the structure of Fig. 2.3 is fed in its dominant mode. Those changes have been made in Fig. 2.4.

A variety of numerical calculations were made for this structure. The values of α and β were determined as a function of frequency, b/a and a'/a , to ascertain how much leakage would be obtained and to seek the cross-sectional aspect ratio that would yield the best performance. Curves of α/k_0 and β/k_0 as a function of b/a were presented in the second of the two short papers in Sec. B, 1, but they will not be repeated here. Those curves hold for a specific ratio of a'/a and for a specific frequency. The a'/a value of 0.60 used there was found to be about optimum, but the value of 64 GHz, corresponding to $a/2 = 0.50$ cm, is quite far from cutoff. If we had made the calculations only somewhat nearer to cutoff, but still not close to it, we could easily have doubled the value α/k_0 . Curves of α/k_0 and β/k_0 as a function of a'/a , for b/a fixed at several different values, show that the leakage constant peaks when a'/a is near to 0.6.

The conclusions that we draw from these calculations are the following.

- 1) The structural aspect ratio that seems to yield the largest value of leakage constant is indicated in Fig. 2.5. Although the structure could be fabricated without difficulty (there would be a metal piece at the bottom to hold the two pieces together and to insure radiation from one end only), it is seen that the two step junctions are pronounced and not far from each other. The theory we employed assumed that the step junctions were effectively isolated from each other, and that small obstacle theory would be appropriate. These optimized dimensions thus correspond to a structure that may be outside of the range of validity of the theory employed.

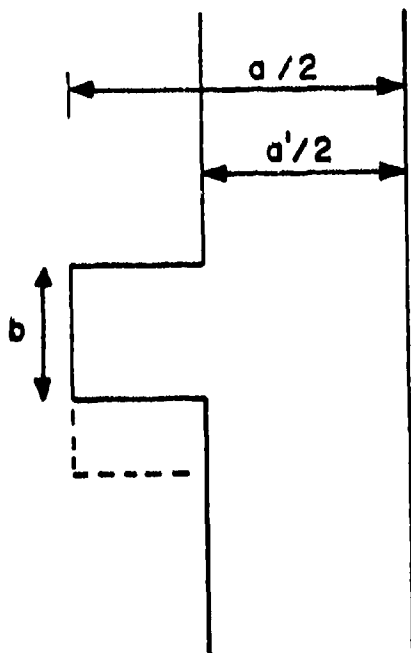


Fig. 2.5 The structural aspect ratio that yields the largest value of leakage constant for this type of leaky wave structure. The dashed line shows the corresponding aspect ratio found by the alternative (tee stub) theory discussed in Sec. D.

For this reason, we used an alternative and very different theoretical approach for this structure, based on a tee stub on a parallel plate guide, and described in Sec. D. The optimum dimensions from that approach were not that much different, it turned out; the a'/a ratio was just about the same, but the b/a ratio was increased somewhat. The altered aspect ratio is shown by the dashed lines in Fig. 2.5.

2) The magnitude of the leakage constant is smaller than we would like. Assuming a slightly lower operating frequency so that the maximum value of α/k_0 would be about 3×10^{-3} , we find via (1.2) and (1.3), that the largest beam width we could achieve is slightly under 2° . Although this result is satisfactory for many applications, greater versatility would be available if the α/k_0 values were larger. The difficulty relating to the low values of leakage constant may relate to the shape of the structure, or it may be due to the use of small obstacle theory beyond its range of applicability, in which case the predicted theoretical values for α would indeed be lower than the true values. Since we did not know the actual reason for the difficulty, we took two parallel paths:

i) We modified the cross section of the structure by adding strips to project from the step junctions in order to increase the value of α ; a discussion of that structure, its analysis, and some numerical results are presented next, in Sec. C, 2.

ii) We pursued the alternative theoretical approach mentioned above, and discussed in Sec. D. We found there that the maximum value obtainable for α is much higher than that found by using small obstacle theory, implying that the small obstacle approach may be inadequate in this range of dimensions.

On the basis of all the studies conducted so far, it seems that the structure of Fig. 2.3, which has the great advantage of structural simplicity, may well yield a practical leaky wave antenna. As we see later, more work needs to be done, and perhaps some measurements of α are in order.

2. Antenna with Added Strips

The analysis we employed (Sec. B, 3) for the leaky structure in Fig. 2.3 indicated a value of leakage constant α that is lower than we would like, as discussed above in Sec. C, 1. On the assumption that the analysis is accurate, we then tried to increase the value of α by modifying the cross section of the structure. We added strips that projected from the step junctions, thereby effectively enhancing the influence of the step junctions in converting power from the $i = 1$ transverse mode into the $i = 0$ transverse mode. The cross section of the resulting structure is shown in Fig. 2.6, where the projecting strips are of width δ .

The transverse equivalent network for this modified structure is taken to be the same in form as that for the structure without added strips, shown in Fig. 2.4. The difference lies in the value of the coupling susceptance \bar{y} , which now has contributions from both sides of the step junction. The modes in the two regions, and the turns ratios n^s , are the same as before the strips were added. We therefore need to discuss the derivations for the susceptance \bar{y} only.

The coupling susceptance \bar{y} can be written as

$$\bar{y} = \frac{1}{2}y_{oo} + \frac{1}{2}y'_{oo} \quad (2.87)$$

where the contributions from each side of the strips are regarded as independent and equal to one half of the susceptance that would be obtained if each of the discontinuities were symmetrical separately. For the unprimed side, of guide width $a/2$, the susceptance element is derived from (2.36) with i and j being equal to 0 and 2, and with the mode functions still given by (2.78) and (2.79). The polarizability term m , taking the added strip length δ into account, now becomes

$$m = -\pi \left(\frac{a-a'}{2} + \delta \right)^2 \quad (2.88)$$

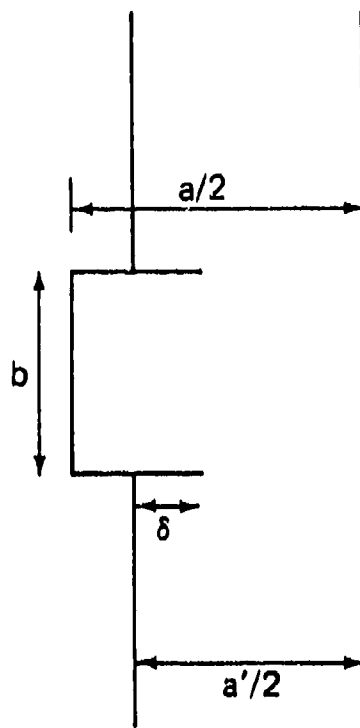


Fig. 2.6 Cross section of proposed new leaky wave groove guide structure with added strips to increase the leakage constant. The added strips enhance the conversion of power from the $i = 1$ to the $i = 0$ mode.

When the mode functions from (2.78) and (2.79), and the characteristic admittances Y_0 and Y_2 from (2.63) and (2.75), together with the new value of m from (2.88), are all placed into (2.36), we obtain

$$V_{22} = 2V_{11} = -j \frac{\pi}{\omega\mu} \frac{2}{a} \left(\frac{a-a'}{2} + \delta \right)^2 (k_0^2 - k_1^2) \quad (2.89)$$

From relations (2.82) and (2.83), which are also still valid here, we find

$$n_1^s = 1 \quad , \quad n_2^s = \sqrt{2} \quad (2.90)$$

as in (2.84).

On the primed side, of guide width $a'/2$, expressions (2.36) for the susceptances, (2.78) and (2.79) for the mode functions, and (2.63) and (2.75) for the characteristic admittances, are all still applicable when the quantities involved become primed, meaning that they correspond to the guide of width $a'/2$, rather than $a/2$. The polarizability m' must be separately specified, however, and it is readily seen to be given by

$$m' = -\pi\delta^2 \quad (2.91)$$

When all of these quantities are appropriately inserted into (2.36), suitably modified, one finds

$$y_{22}^s = 2y_{22}^s = j \frac{\pi}{\omega\mu} \frac{2}{a'} \delta^2 (k_0^2 - k_1^2) \quad (2.92)$$

and, from (2.82) and (2.83), we deduce

$$(n_1^s)' = 1 \quad , \quad (n_2^s)' = \sqrt{2} \quad (2.93)$$

The total coupling susceptance \bar{y} is then seen to become, on use of (2.87) together with (2.89) and (2.92),

$$\bar{y} = j \frac{\pi}{2\omega\mu} (k_0^2 - k_1^2) \left[\frac{\delta^2}{a'} + \frac{1}{a} \left(\frac{a-a'}{2} + \delta \right)^2 \right] \quad (2.94)$$

With the other turns ratios n_0^s and n_2^s given by (2.76) and (2.77), we now have available all the constituents of the transverse equivalent network of the form in Fig. 2.4. We understand that the $i = 2$ quantities used above apply to the second mode in an unbisected groove guide, whereas the $i = 1$ terminology in Fig. 2.4 is intended for the $i = 1$ mode in the bisected structure; they are, of course, equivalent.

The complete transverse resonance condition, or dispersion relation, then becomes

$$-j \cot k_{y2} \frac{b}{2} + \frac{1}{(n_2^e)^2} \frac{k_{y2}}{k_{y2}'} + \frac{-j \frac{b}{\pi} \frac{1}{\left[\left(\frac{a-a'}{2} + \delta \right)^2 \frac{1}{a} + \delta^2 \frac{1}{a'} \right]} + \frac{-j \frac{k_{y2}}{k_0} \cot k_{y0} \frac{b}{2} + \frac{1}{(n_0^e)^2} \frac{k_{y2}}{k_0'}}{2} = 0 \quad (2.95)$$

A variety of numerical calculations were made for α and β as a function of the dimensional parameters. It is no longer feasible to specify a single optimum set of dimensions as a larger δ obviously means a larger maximum value of α . But the values of a'/a and b/a also strongly affect the results. It turns out that a value of δ/a as small as 0.05 can double the value of α in many cases. With $\delta/a = 0.10$ or 0.15, the value of α can be increased five-fold. One of the curves of δ/k_0 vs. b/a is shown in Fig. 2.7.

It is clear that, if the value of α is really too low, the addition of small strips in the manner shown in Fig. 2.6 can greatly increase the value of α . Small values of δ can have an important influence on the leakage constant. The structure is harder to fabricate than the one without added strips, of course, but there may be simple ways to include the added strips. One way is to make the structure in two parts (assuming an ultimate direct connection on the bottom). One part consists of the vertical stub section of height b plus the horizontal parts of the groove region, including the added strips, which are made as a direct extension of the length $(a-a')/2$; this part resembles a squarish "c" or a "u" on its side. The other part is the rest of it that holds the first part in place.

At any rate, the key question is whether or not the added strips are needed in the first place, i.e., whether or not the value of α is really low. The alternative theoretical approach in Sec. D discusses this question, and concludes that α can be quite high if required even without the added strips.

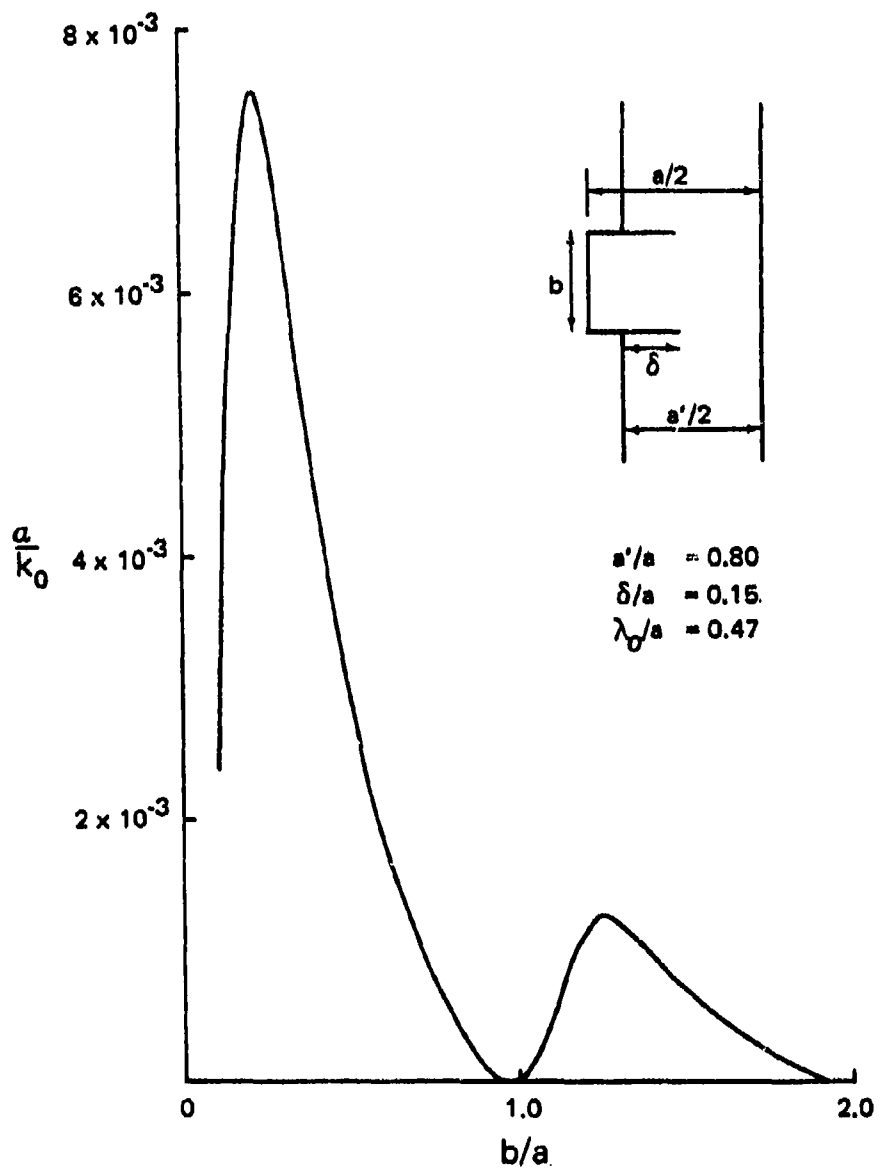


Fig. 2.7 Curve of leakage constant α as a function of the dimensional ratio b/a for the structure with added strips given in Fig. 2.6. The dimensional parameters are indicated in the inset.

D. ALTERNATIVE THEORETICAL APPROACH FOR THE $n = 2$ LEAKY MODE ANTENNA

The aspect ratio of the optimized leaky structure shown in Fig. 2.5 suggests that it resembles a tee stub on a parallel plate guide. From that standpoint, it is easier to understand the behavior if we rotate the structure through 90° , as shown in Fig. 2.8.

The structure is excited in the stub guide, of width b and length $(a-a')/2$, in the TEM mode. Of course, we impose a variation with x , which is the axial (longitudinal) direction, as always, so that the wave is really a TEM wave at an angle. Because of the symmetry, the field incident from the stub guide leaks into the two "main" arms of the parallel plate guide in antisymmetric fashion, as shown in Fig. 2.8 for the electric field. The dimensions of the main guide, of width $a'/2$, are such that only the TEM mode (at an angle) can propagate, and all the other modes are below cutoff.

This approach and the previous one used for groove guide are completely different. For example, the upper and lower stubs in the bisected groove guide are now the arms of the main parallel plate guide. Also, the transmission line representing the wider guide region was in the same direction as the other transmission lines in the groove guide approach, but here it is perpendicular to them. The domains of validity for each approach are therefore different; the approaches are complementary rather than overlapping.

In principle, and conceptually, the stub guide approach is simpler. What is needed is only an accurate representation for the tee junction itself. There is no need for H-type modes, etc., and only one mode is required, rather than two. One possible transverse equivalent network that is representative of the structure is shown in Fig. 2.9. The transmission line representative of the stub guide has length $(a-a')/2$, and the main guide arms are infinitely long. Each transmission line corresponds to the transverse wavenumber k_{y0} in the y direction, where

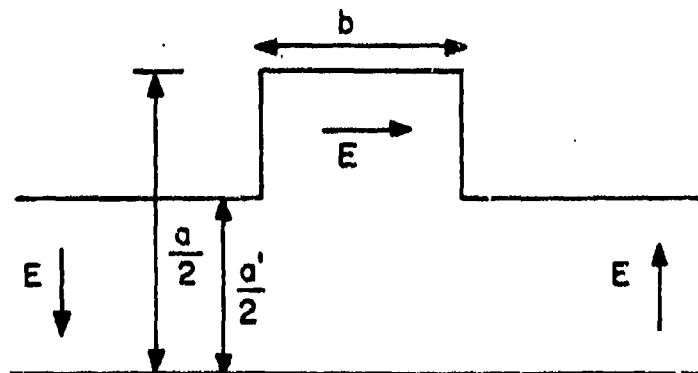


Fig. 2.8 The bisected groove guide structure in Fig. 2.3 (or 2.5) rotated through 90° so that it can be viewed more easily as an E plane tee stub on a parallel plate waveguide.

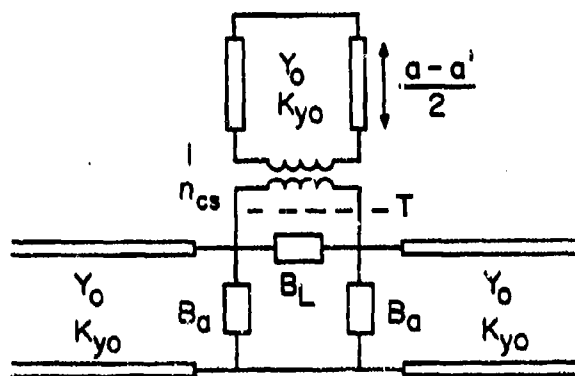


Fig. 2.9 A transverse equivalent network corresponding to the structure in Fig. 2.8, containing one form of network representation for the tee junction itself.

$$k_{y_0}^2 = k_0^2 - k_z^2 \quad (2.98)$$

since there is no variation in x (across the widths) in these TEM modes at an angle.

The first representation for the tee junction that we tried was the one given in the Waveguide Handbook [20], Sec. 6.1, pp. 337-341. The structure corresponds directly, and the network representation is close to that shown in Fig. 2.9 but not quite the same. Since we must take a resonance of the transverse equivalent network in order to obtain the dispersion relation for the longitudinal leaky mode that results, we require analytical expressions for the elements of the tee junction. The problem with the representation in the Waveguide Handbook is that the analytical expressions are valid only in the static limit, $b/\lambda_g = 0$. The curves given there are accurate away from that limit, however, so that we can assess the numerical error in, say, the most important susceptance element, B_b/Y_0 , in their network (similar, but not identical, to B_L/Y_0 in Fig. 2.9). For $2b/\lambda_g = 0.6$, a typical case, for the ratio of stub guide width to main guide width (b'/b in their notation, $b/2a'$ in ours) equal to unity, we find that $B_b/\lambda_0 = 1.36$, instead of 0.86 when the static limit is used. For a narrower stub guide, say, $b/2a' = 0.67$, the comparison is $B_b/Y_0 = 0.84$ vs. 0.66, which is not as bad. For narrower stub guides, therefore, the Waveguide Handbook expressions should yield results that are reasonably reliable. On the other hand, the geometric aspect ratio is less interesting in that range.

Nevertheless, we obtained some numerical values that were surprising when we compared them with corresponding previous results. Three examples are:

| $\frac{b}{a}$ | $\frac{2b}{a}$ | <u>Stub Guide Method</u> | | <u>Groove Guide Method</u> | |
|---------------|----------------|--|---------------------|--|---------------------|
| | | $\frac{\alpha}{k_0}$ ($\times 10^{-2}$) | $\frac{\beta}{k_0}$ | $\frac{\alpha}{k_0}$ ($\times 10^{-2}$) | $\frac{\beta}{k_0}$ |
| 0.40 | 1.33 | 4.94 | 0.847 | 0.082 | 0.865 |
| 0.20 | 0.67 | 4.36 | 0.872 | 0.145 | 0.845 |
| 0.10 | 0.33 | 2.50 | 0.878 | 0.134 | 0.812 |

In these numerical examples, we compare corresponding sets of values computed using the Waveguide Handbook analytical expressions for the first set of numbers and the expressions in Sec. B, 3 for the second set. We note that the α/k_0 values are the ones that seem very different, the stub guide method yielding results more than ten times the earlier numbers. It is true that for smaller values of b/a the groove guide results are not reliable, and that for larger values of b/a the static limit expressions from the Waveguide Handbook are inaccurate, so that the above comparison cannot be trusted. We therefore sought better network representations for the tee junction.

The next representation chosen is that shown in Fig. 2.9. It is adapted from the one given in an old comprehensive report [21] on equivalent circuits for slots in rectangular waveguide. That report contained the output of a group comprised of J. Blass, L. B. Felsen, H. Kurss, N. Marcuvitz and A. A. Oliner. This representation, and expressions for its elements, are given on pp. 122-125 of [21]. The earlier work applied to a more complicated structure in which a slot was present at the stub junction plane, and these expressions were found to be accurate for most of the range of slot dimensions when the ordinary rectangular guide aspect ratio was used. For our case, the "slot" is wide open, but we need to modify the guide dimensional ratios.

A symmetrical tee network requires four independent parameters for its characterization, but only three appear in Fig. 2.9. If one employs

the transformer format, an additional series element is present just above the transformer; however, we have found that the reactance of that series element is essentially zero, and that the element can be neglected. Of the three remaining elements, the expression for the turns ratio n_{cs} is simple, and that for B_a is not complicated either. The dominant element is that of B_L , where L signifies "longitudinal." The expression we derived many years ago is in the form of B_t , the susceptance of a transverse aperture coupling two waveguides, plus a correction term. The correction term accounts essentially for the presence of the wall opposite the tee stub junction, and the absence of the top and bottom walls that would be present for the transverse aperture. In the slot-coupled tees analyzed years ago, the correction term was small relative to the other terms.

When the expressions taken from the report [21] are reduced appropriately to our case, and the notation changed to accommodate to our present notation, we obtain for the elements of Fig. 2.9:

$$n_{cs} = \sqrt{\frac{2b}{a'}} \left(\frac{2}{k_{ys} b} \right) \sin \frac{k_{ys} b}{2} \quad (2.97)$$

$$\frac{B_a}{Y_0} = - \frac{\pi}{16} k_{ys} b \left(\frac{b}{a'} \right) J_0^2 \left(\frac{k_{ys} b}{2} \right) \quad (2.98)$$

where J_0 is the Bessel function of order zero, and

$$\begin{aligned} \frac{B_L}{Y_0} = & \frac{k_{ys} a'}{2\pi} Q_n \csc \frac{\pi b}{a'} + \frac{k_{ys} a'}{2\pi} \left[Q_n 1.43 + \frac{1}{2} \left(\frac{k_{ys} a'}{2\pi} \right)^2 \right] \\ & + \frac{\pi}{32} k_{ys} b \left(\frac{b}{a'} \right) J_0^2 \left(\frac{k_{ys} b}{2} \right) \end{aligned} \quad (2.99)$$

From stored power considerations, we are able to identify the first term in (2.99) as equal to one half the susceptance of a transverse capacitive aperture in a waveguide when the aperture involves only a reduction in height. The third term is seen to be one half of B_a/Y_0 , and the second term is the "correction term."

For an ordinary rectangular waveguide E-plane tee junction, for which no slot is present and for which the stub and main guides are identical, the first term in B_L/Y_0 becomes zero, so that the correction term alone becomes equal to $B_L/Y_0 + (1/2)B_a/Y_0$. For the special values $a = 0.900''$, $b = 0.400''$, where a and b are the usual rectangular waveguide dimensions, and for a free space wavelength $\lambda_0 = 1.2606''$, the results of careful measurements are available for B_a/Y_0 and $B_L/Y_0 + (1/2)B_a/Y_0$. These two quantities follow directly from measurements because they correspond to what occurs when the network is bisected with an open circuit and a short circuit, respectively.

Comparisons between the measured results and the corresponding quantities computed using (2.98) and (2.99) are the following:

| | <u>Measured</u> | <u>Computed</u> |
|---|-----------------|-----------------|
| $\frac{B_L}{Y_0} + \frac{1}{2} \frac{B_a}{Y_0}$ | 0.29 | 0.246 |
| $\frac{B_a}{Y_0}$ | -0.096 | -0.108 |

These agreements are actually quite good, and would indicate that in this range of dimensional ratios the expressions (2.97) to (2.99) are valid. In particular, the correction term in B_L/Y_0 referred to above, which is always under suspicion, seems to be reasonably reliable. The measured values are taken from curves on pages 173 and 175 of reference [21].

Using these expressions, we may readily obtain the dispersion relation from the network in Fig. 2.9. By taking the input admittances looking in both directions from reference plane T in Fig. 2.9, and summing them to zero, we find

$$-j \frac{a'}{2b} \cot(k_{y_0} \frac{a-a'}{2}) + j \frac{B_L}{Y_0} + \frac{1}{2} (1 + j \frac{B_s}{Y_0}) = 0 \quad (2.100)$$

When expressions (2.97) to (2.99) are substituted into (2.100), we obtain for the dispersion relation

$$\begin{aligned} -j \frac{a'}{2b} \cot(k_{y_0} \frac{a-a'}{2}) + j \frac{k_{y_0} a'}{2\pi} \left[n \csc \frac{\pi b}{a'} + \frac{1}{2} \right. \\ \left. + j \frac{k_{y_0} a'}{2\pi} \left[n 1.43 + \frac{1}{2} \left(\frac{k_{y_0} a'}{2\pi} \right)^2 \right] \right] = 0 \end{aligned} \quad (2.101)$$

Since the equation is complex, a complex value will result for k_{y_0} , and the solution will correspond to that for a leaky mode. The real and imaginary parts of k_z , from (2.96), are the phase constant β and the leakage constant α .

We have not as yet systematically investigated the parametric dependence of α and β on the various dimensions, but we present in Fig. 2.10 curves of α/k_0 and β/k_0 as a function of b/a , when $a'/a = 0.6$, which was found in Sec. C, 1 to yield higher values of α than other ratios. The dispersion relation (2.101) is seen to yield very high values for α as compared to those found in Sec. C, 1. They are in fact not that much different from the values reported above, which were obtained from the Waveguide Handbook expressions, and which we felt we could not trust because they were valid only in the static limit.

The curve for α/k_0 in Fig. 2.10 was computed at the same frequency and the same value of a'/a as the one in Fig. 4 of the second short paper in Sec. B, 1, and it can therefore be compared with it. We must be careful about the scales, however. The range of b/a in the abscissa in the above-mentioned Fig. 4 is very wide, going from zero to 2.0, whereas the one in Fig. 2.10 only goes up to 0.4. Within the smaller range, however, the curve shapes are similar, although the maximum for α/k_0 moves to $b/a = 0.35$ from 0.20. Missing in Fig. 2.10 are the nulls that appear

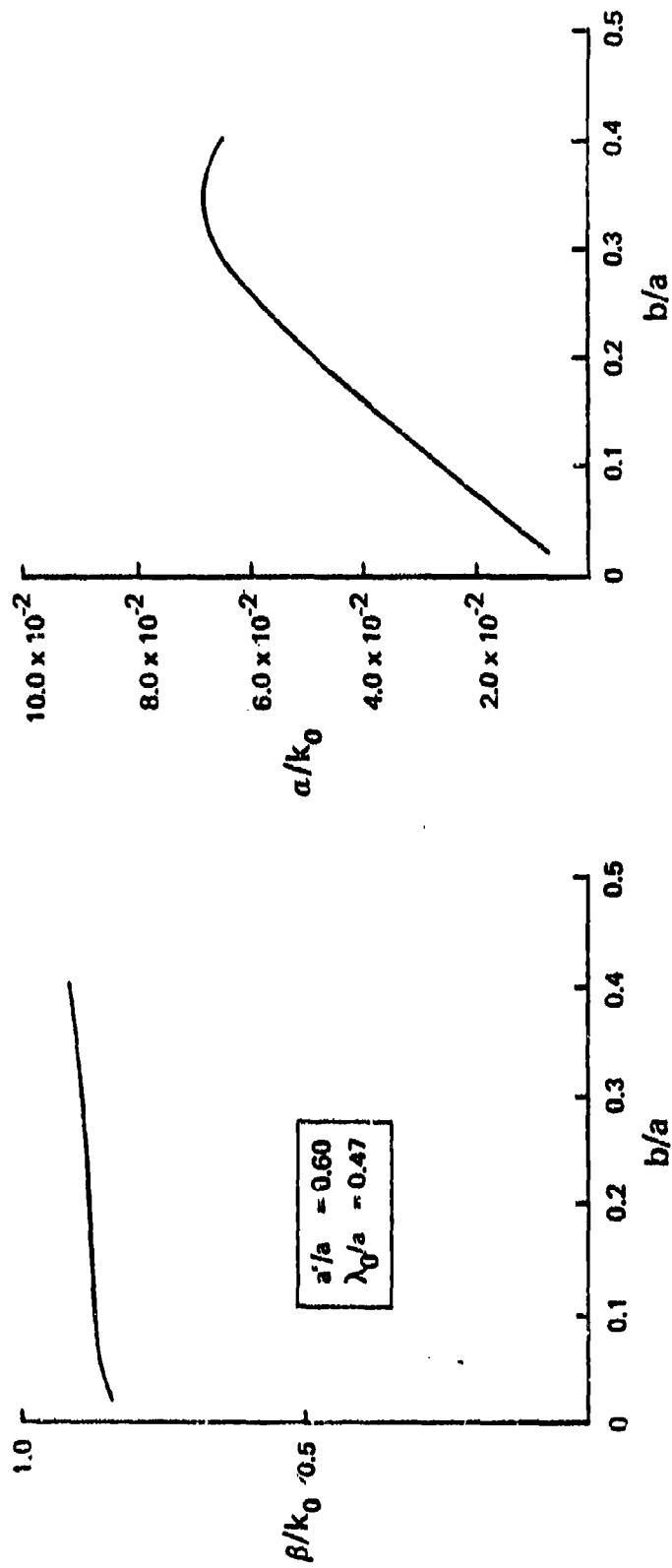


Fig. 2.10 Curves of phase constant β and leakage constant α as a function of the width b of the tee stub, using the transverse equivalent network of Fig. 2.9.

in Fig. 4 that we know must be correct, but the stub guide theory cannot yield them because those dimensional ratios are outside of that theory's range of validity.

Equally striking, but in a different way, is the behavior on the ordinate scale. Here, we find that the values of α are more than twenty times the values found in Fig. 4. It is difficult to understand the reason for such a large discrepancy. Upon noting these differences, we tried to use another equivalent network for the step junction, to see whether another and separate calculation may reveal different results. With respect to β/k_0 , the curves in Fig. 4 and in Fig. 2.10 appear to correlate reasonably well with each other, although one cannot be sure because of the scales involved; on the other hand, it is the contrasts in α/k_0 that are more interesting.

The yet-another transverse equivalent network referred to just above is shown in Fig. 2.11. It is in a simpler form than the one in Fig. 2.9 because the reference plane locations in the main guide have been shifted (although that does not affect the dispersion relation since the main guide arms are matched). It was used with dramatic success in its application to narrow radiating slots in the broad face of rectangular waveguide [22]. That range of dimensional parameters produces a different field in the slot than we would find in the open stub case we have now, so that it may not be safe to extrapolate the expressions to our case. Nevertheless, we know that the network was excellent there, and we shall see what it yields for us, giving us another comparison.

The expressions for the elements of the network, after modifying the notation appropriately to apply to our case, become

$$n_j = \sqrt{\frac{2b}{a'}} \quad (2.102)$$

$$\frac{B_j}{Y_0} = \frac{k_{y0} a'}{2\pi} \eta \csc \frac{\pi b}{a'} + \frac{k_{y0} a'}{2\pi} \left[\eta^2 + \frac{3}{8} \left(\frac{k_{y0} a'}{2\pi} \right)^2 \right] + \frac{k_{y0} b}{8} \quad (2.103)$$

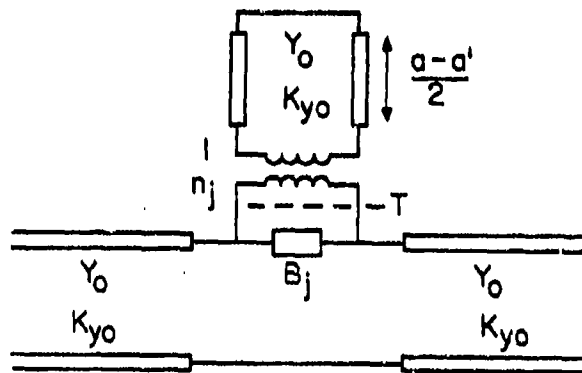


Fig. 2.11 A second transverse equivalent network corresponding to the structure in Fig. 2.8, containing a simplified form of network representation for the tee junction itself.

These expressions are a bit simpler than those in (2.97) to (2.99); in (2.103), the first term is the same as the first term in (2.99), but the last two terms here correspond to a "correction term."

When the transverse resonance relation is applied at reference plane T in Fig. 2.11, we find

$$j \frac{a'}{2b} \cot(k_{y0} \frac{a-a'}{2}) + j \frac{B_j}{Y_0} + \frac{1}{2} = 0 \quad (2.104)$$

which becomes, on use of (2.103),

$$- j \frac{a'}{2b} \cot(k_{y0} \frac{a-a'}{2}) + j \frac{k_{y0} a'}{2\pi} \left[\eta \csc \frac{\pi b}{a'} + \frac{1}{2} \right. \\ \left. + j \frac{k_{y0} a'}{2\pi} \left[\eta^2 + \frac{3}{8} \left(\frac{k_{y0} a'}{2\pi} \right)^2 \right] + \frac{k_{y0} b}{8} \right] = 0 \quad (2.105)$$

Numerical values for α/k_0 and β/k_0 computed via the dispersion relation (2.105) for the same parameters as the curves in Fig. 2.10 are shown in Fig. 2.12. Although there are small numerical differences due to the different network expressions, it is clear that the shapes and the dependences are very similar. The large values for α are also found now.

One feature that is mildly disturbing here is that, in the numerical calculations from both (2.101) and (2.105), the term contributing most strongly in each case is the "correction term," which is assumed to be small under most circumstances. If the correction term is not evaluated accurately, however, there could be a small numerical error introduced, such as the differences appearing between the curves in Figs. 2.10 and 2.12, but the major pattern should not be affected.

After the substantial efforts put into the topics discussed in Secs. C and D, we feel that we are still not completely sure of the validity of the various results, particularly because it is difficult to understand why the discrepancy is so large between the results obtained via the two different approaches (in Sec. C and in Sec. D). Some simple measurements should help greatly in this connection. The studies in Sec. D, on the other hand, are encouraging with respect to the potential utility of the leaky structure shown in Fig. 2.3. Its simplicity of form should enhance its attractiveness for millimeter wave antenna application, and its practicality would be assured if the numbers in Fig. 2.10 are indeed accurate.

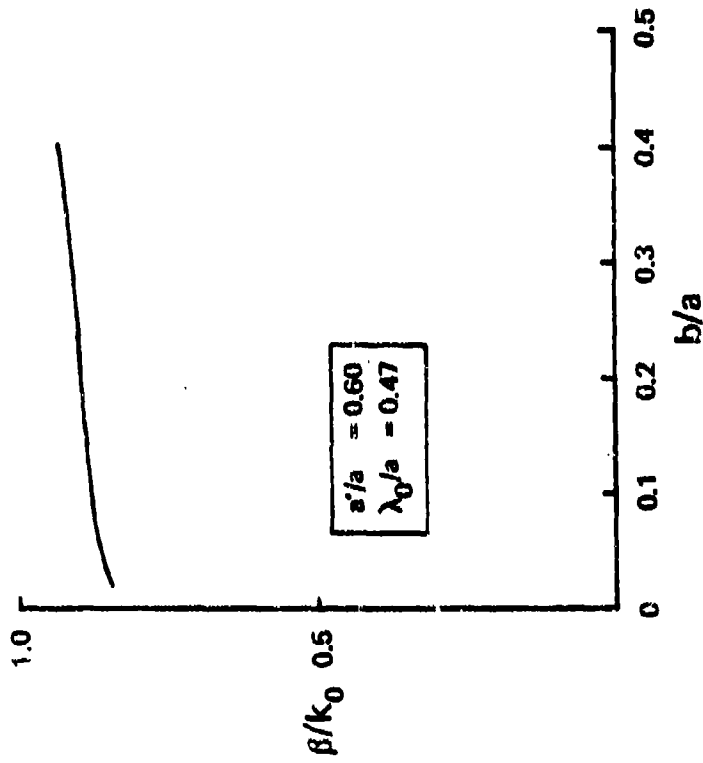
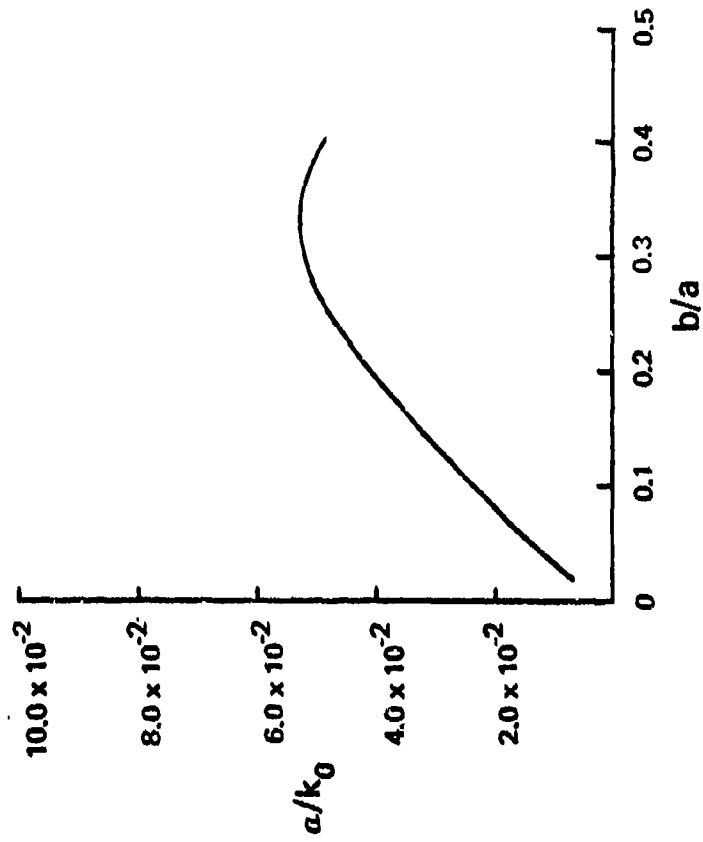


Fig. 2.12 Curves of phase constant β and leakage constant α as a function of the width b of the tee stub, using the alternative transverse equivalent network of Fig. 2.11.

PART III. ANTENNAS BASED ON NRD GUIDE

- A. THE FORESHORTENED-TOP ANTENNA: ACCURATE ANALYSIS AND NUMERICAL RESULTS
 - 1. Summary of Principal Features
 - 2. Derivations of the Constituents of the Transverse Equivalent Network
 - (a) The Modes Employed
 - (b) The Air-Dielectric Interface
 - (c) The Radiating Open End
 - (1) Summary of Weinstein's Formulation
 - (2) Analytic Continuations
 - (d) The Dispersion Relation for the Leaky Mode
 - 3. Numerical Results
- B. THE FORESHORTENED-TOP ANTENNA: PERTURBATION ANALYSES
 - 1. Procedure Based on the Transverse Equivalent Network
 - 2. Simpler, Reflection Coefficient, Procedure
 - 3. Comparisons with Accurate Analysis
- C. THE FORESHORTENED-TOP ANTENNA: MEASUREMENTS
 - 1. Measurement Procedure
 - 2. Measurements Taken by Yoneyama
 - 3. Comparisons with Theory
- D. NEW ASYMMETRIC ANTENNA
 - 1. Principle of Operation
 - 2. Analysis and Numerical Results

III. ANTENNAS BASED ON NRD GUIDE

The second basic low-loss waveguide on which new leaky wave antennas were designed is the NRD (or non-radiative dielectric) waveguide discussed in Sec. I, B. As indicated in Sec. I, A, two different approaches were used to produce the leakage; one involves foreshortening the top of the guide, whereas the other relies on asymmetry to cause the leakage. Although both approaches were employed with NRD guide, most of the time and effort was spent on the foreshortened type of antenna. The structure employing asymmetry was an outgrowth of an experimental difficulty originally encountered with measurements on the foreshortened structure, and its analysis took place only at the end of the contract period. Nevertheless, a discussion of the structure based on asymmetry, and some numerical results for it, are included here.

Although the original contract does not call for any measurements to be made, an experimental phase was introduced because our theoretical results differed by almost a factor of two with measurements taken a few years ago on a somewhat similar structure (actually, an H guide that radiated from both ends). Also disturbing was the fact that approximate theoretical calculations were made at that time which showed better agreement with those measurements than with our theory. Our theory is almost rigorous (with the "almost" explained later), but we could perhaps have made some inadvertent error. We were concerned by the discrepancies, and we therefore wished to perform our own careful measurements.

It turned out finally that our theory is indeed correct, and that the earlier measurements and approximate theories were wrong. We explain below why that was the case. Experimentally, our theoretical values were verified in two ways. One way involved our own measurements, which consisted of direct field probing along the length of the antenna aperture. The second, completely independent, measurements were taken at our request by Prof. T. Yoneyama of Tohoku University in Japan. Both sets of measurements agreed very well with our theoretical results, as we demonstrate below.

Before the results of our measurements and those of Prof. Yoneyama became known, we derived some perturbation expressions for the values of α and β of the foreshortened top antenna. Usually, a rigorous expression is derived to serve as a reliable result against which various approximate theories can be compared. Here, we did the inverse. We had an essentially rigorous result which we felt may be in question because of discrepancies with certain earlier measured and theoretical results (mentioned above). We therefore derived approximate expressions to see how far off they were from the essentially rigorous one. It turned out that numerical values obtained from these approximate, perturbation expressions agreed much better with our accurate results than with any of the earlier results, thus serving as an additional verification of the validity of our theoretical results.

Of course, these perturbation expressions are simpler to compute from than the almost rigorous expression, so that they may themselves be found useful for numerical calculations, at least in the early stages of a design. As expected, they are most accurate for smaller values of α and when the guide is not near to mode cutoff. These perturbation expressions are therefore of value in their own right.

A short presentation of the theory underlying the foreshortened-top NRD guide antenna appears in the Proceedings of the URSI International Symposium on Electromagnetic Theory [23]. Another short presentation, which stresses the microwave network features rather than the antenna aspects, is given in the Digest of the International Microwave Symposium [24]. A version similar to the first presentation, but slightly expanded, has been accepted for publication in Radio Science [25].

The first of these presentations is included in this Final Report because it provides an excellent summary of the principle of operation of the antenna, a discussion of the main features of the almost-rigorous transverse equivalent network, and a few typical numerical results. That paper is given as Sec. A, 1 here.

The work on the foreshortened-top antenna based on NRD guide is discussed here in Secs. A, B and C. The basic analysis together with numerical data are presented in Sec. A. In A, 1, we include the paper from the URSI Proceedings [23] because it provides a summary of the most important features. No derivations are contained in that paper, however, so that the derivations of the constituents comprising the transverse equivalent network are given in Sec. A, 2. The numerical data appearing in the paper are also necessarily limited, applying to one case, and presenting only the variation of α and β with d , the length of the foreshortened top section. Additional numerical data, corresponding to other cases, and illustrating the variation of α and β with other parameters, are contained in Sec. A, 3.

The perturbation expressions are presented in Sec. B, together with a summary of their derivations. Also included are curves showing comparisons between the basic almost-rigorous theory and the perturbation expressions. Two basically different perturbation procedures were adopted, one following the transverse equivalent network with both of its constituent transmission lines, and the other using only one transmission line and starting from a different basis. The two perturbation procedures are treated in Secs. B, 1 and B, 2, and they are evaluated and compared numerically with the almost-rigorous values in Sec. B,3.

Section C discusses the measurements, both the procedure and the results. We first review the earlier measurements and the associated approximate theory (both by H. Shigesawa and K. Takiyama) to demonstrate why we felt it was necessary to take these measurements. Then, in Sec. C, 1, we present the measurement procedure itself, together with the details of the structures that were measured, and the difficulties that we encountered. The measurement procedure employed by Prof. Yoneyama, which is the same as ours in principle, but which has a different feed mechanism, is described briefly in Sec. C, 2. Also in that section are Yoneyama's results and how they compare with our theoretical values. As will be seen, the agreement is very good. In Sec. C, 3, we present some of our own measured results, together with comparisons with our theoretical curves; the agreement is seen to be very gratifying.

Finally, in Sec. D, we describe the new antenna based on NRD guide that employs asymmetry to produce the desired leakage. The basic structure and the principle of operation are discussed in Sec. D, 1, together with alternative structures and limitations. The theoretical analysis and numerical values for a typical case are presented in Sec. D, 2. Some interesting performance features emerge, verifying their relationship in certain fundamental ways with the class of dielectric strip waveguides analyzed previously [26,27]. Some of these calculations were made after the end of the contract period, and it is these above-mentioned relationships that permitted us to continue these calculations under the support of our Joint Services Electronics Program, on which the novel leakage features of dielectric strip waveguides were originally found. These relationships are also discussed in Sec. D, 2.

A. THE FORESHORTENED-TOP ANTENNA: ACCURATE ANALYSIS AND NUMERICAL RESULTS

In Sec. A, 1, we reproduce a short paper that appeared in the Proceedings of the URSI International Symposium on Electromagnetic Theory, held in Santiago de Compostela, Spain, on August 23-26, 1983 [23]. That paper contains a summary of the main features of this antenna, including its structure, its principle of operation, the almost-rigorous transverse equivalent network, and results for one typical case.

Derivations of the constituents of the transverse equivalent network are presented in Sec. A, 2. One first begins with the choice of transverse modes that yields the simplest transverse equivalent network, not only in form but also in the expressions for the constituent discontinuities. Our choice, which we believe is the wise one, yields a dispersion relation in closed form. Next, we treat in succession the two basic constituent discontinuities, the air-dielectric interface and the radiating open end. A few additional remarks are then made regarding the complete transverse equivalent network and the corresponding dispersion equation.

Numerical data are included in Sec. A, 3 which illustrate the variations of α and β , the leakage and phase constants, with various geometric parameters and with the dielectric constant. The results show that a wide range of values of α can be achieved, so that one can select a wide radiated beam or a narrow one, and that the values of β remain fairly constant with most geometric variations, as one wishes for easy leaky wave antenna design.

1. Summary of Principal Features

ACCURATE THEORY FOR A NEW LEAKY-WAVE ANTENNA FOR
MILLIMETER WAVES USING NONRADIATIVE DIELECTRIC WAVEGUIDE

by A. Sanchez and A. A. Oliner

ACCURATE THEORY FOR A NEW LEAKY-WAVE ANTENNA FOR MILLIMETER WAVES USING NONRADIATIVE DIELECTRIC WAVEGUIDE

SANCHEZ A. (*). -OLINER A.A.

Polytechnic Institute of New York
333 Jay Street
Brooklyn, New York 11201, USA

*Present address: RCA Laboratories, Princeton, N. J. 08540

ABSTRACT. An almost-rigorous analysis is presented for a new leaky-wave antenna of simple configuration based on a recent nonradiative modification of H guide and suitable for millimeter wavelengths. The analysis employs a transverse equivalent network which yields a dispersion relation in closed form; numerical values are presented for the phase and leakage constants, and for a typical example of antenna performance.

INTRODUCTION

Two papers appeared recently [T. Yoneyama and S. Nishida, 1981a and b] which proposed a new type of waveguide for millimeter waves, and showed that various components based on it can be readily designed and fabricated. By a seemingly trivial modification, the authors, T. Yoneyama and S. Nishida, transformed the old well-known H guide, which had languished for the past decade and appeared to have no future, into a potentially practical waveguide with attractive features. The old H guide stressed its potential for low-loss long runs of waveguide by making the spacing between the metal plates large, certainly greater than half a wavelength; as a result, the waveguide had lower loss, but any discontinuities or bends in it would produce leakage of power away from the guide. Yoneyama and Nishida observed simply that when the spacing is reduced to less than half a wavelength all the bends and discontinuities become purely reactive; they therefore call their guide "nonradiative dielectric waveguide." As a result of this modification, many components can be constructed easily, and in an integrated circuit fashion, and these authors proceeded to demonstrate how to fabricate some of them, such as feeds, terminations, ring resonators and filters.

These papers [T. Yoneyama and S. Nishida, 1981a and b] treat only reactive circuit components, and no mention is made of how this type of waveguide can be used in conjunction with antennas. The present paper serves two functions. First, it shows that a leaky-wave antenna can be readily fabricated with "nonradiative dielectric waveguide," and, in fact, that it can be directly connected to the above-mentioned circuits in integrated circuit fashion, if desired. Second, it presents a very accurate theory for the leakage and phase constants of the antenna. A key feature of this theory involves an almost-rigorous transverse equivalent network, which requires two coupled transmission lines. Some subtle features are involved in the derivation of the elements of this equivalent network, including the best choice of constituent transverse modes, an analytic continuation into the below cutoff domain, and mode coupling at an air-dielectric interface. In the discussion below, we present the structure of the antenna, the principle of operation, an outline of the almost-rigorous theory, and a typical

numerical example for antenna performance.

The form of the antenna is also responsive to problems facing line-source antennas at millimeter wavelengths; that is, it is simple to fabricate since it is composed of a single continuous open slit, and it is fed by a relatively low-loss waveguide so that the leakage constant of the antenna dominates over the attenuation constant of the waveguide. The antenna is also simple to design because it is possible to vary the leakage constant without measurably affecting the phase constant, and because our theory yields closed-form expressions for the leakage and phase constants.

PRINCIPLE OF OPERATION OF THE LEAKY-WAVE ANTENNA

The new waveguide, shown in Fig. 1, looks like the old H guide except that the spacing between plates is less than half a wavelength to assure the nonradiative feature. In the vertical (y) direction, the field is of standing wave form in the dielectric region and is exponentially decaying in the air regions above and below. The guided wave propagates in the z direction. The leaky-wave antenna based on this waveguide is shown in Fig. 2. In Fig. 2(a) we see that the antenna is created simply by decreasing the distance d between the dielectric strip and the top of the metal plates. When distance d is small, the fields have not yet decayed to negligible values at the upper open end, and therefore some power leaks away. The upper open end forms the antenna aperture, and the aperture amplitude distribution is tapered by varying the distance d as a function of the longitudinal variable z. The polarization of the antenna is seen to be vertical in view of the electric field orientation in the waveguide.

The antenna is seen to be very simple in structure. A side view of the antenna, shown in Fig. 2(b), indicates that the taper in the antenna amplitude distribution is achieved easily by positioning the dielectric strip waveguide with respect to the upper open end, and also that the feeding strip can be readily connected to some other part of the millimeter wave circuit and therefore serve as the output from it.

The antenna is analyzed as a leaky waveguide which possesses a complex propagation constant $\beta - j\alpha$, where β is the phase constant and α is the attenuation or leakage constant. We thus establish a transverse equivalent network for the cross section of the antenna, and from the resonance of this network we obtain the dispersion relation for the β and α values. An almost-rigorous equivalent network is presented in Fig. 3, where it is seen that two coupled transmission lines are required in the representation. The reason for two lines is that the waveguide modes are hybrid, and possess all six field components in the presence of the radiating open end.

If we employ the usual TE and TM modes in these transmission lines which represent the constituent transverse modes, the lines will remain uncoupled at the air-dielectric interface but will be coupled together at the radiating open end. On the other hand, the open end is uniform longitudinally, and this geometrical arrangement suggests the use of $E^{(z)}$ -type and $H^{(z)}$ -type modes (alternatively called LSM and LSE modes, respectively, with respect to the xy plane). Transmission lines representing such modes will not couple at the radiating open end, but do become coupled at the air-dielectric interface. These two valid but alternative representations were considered, and we chose the second of these as the simpler approach for our antenna.

The transverse equivalent network in Fig. 3 thus corresponds to the $E^{(z)}$ -type and $H^{(z)}$ -type transverse modes mentioned above. The coupling network at the air-dielectric interface was obtained from an adaptation of a network presented earlier [P. J. B. Claricoats and A. A. Oliner, 1965] for cylindrical air-dielectric interfaces, and suitably transformed for planar interfaces.

The principal new feature in the transverse equivalent network in Fig. 3 relates to the terminal admittances representing the $E^{(z)}$ -type and $H^{(z)}$ -type modes incident on the radiating open end. Those admittances were not available in the literature but were derived by analytic continuation of expressions for reflection coefficient given by L. A. Weinstein [1969]. Those reflection coefficients applied to normal incidence of ordinary parallel plate modes; modifications were made to account for a longitudinal wavenumber variation (corresponding to oblique incidence) and then for modes below cutoff, the latter step producing results which appear totally different since the phases and the amplitudes of the reflection coefficients then become exchanged.

The terminal admittances in Fig. 3 assume that all the higher modes in the transmission lines decay exponentially to infinity. In principle, they "see" the air-dielectric interface distance d away. In practice, that distance is large; for example, for the first higher mode in a specific case the field at the air-dielectric interface was about 30 dB lower than its value at the radiating open end. Because of this feature, however, we have referred to this analysis as almost rigorous.

The dispersion relation for α and β of the leaky-wave antenna that was found from a resonance of the transverse equivalent network in Fig. 3 contains elements all of which are in closed form, thus permitting easy calculation. We have examined the various parametric dependences of α and β on the dimensions a , b and d , and on the dielectric constant ϵ , in order to clarify design information. Here we present only a single typical case, corresponding to certain geometrical parameters given by T. Yoneyama and S. Nishida [1981a]. The behavior of β and α are shown in Figs. 4 and 5 for this case as a function of distance d (see Fig. 2(a)). For distance $d > 2$ mm, one sees from Fig. 4 that the value of β remains essentially unchanged, as desired. It is seen in Fig. 5 that α increases as d is shortened, as expected since the field decays exponentially away from the dielectric region. Thus, the value of α that one can achieve spans a very large range.

Leaky-wave antennas are often designed so that 90% of the incident power is radiated, and the remaining 10% is dumped into a load. Following this criterion, if one selects $d = 2.0$ mm for this geometry, the length of the antenna will be about 40 cm, and the beam will radiate at an angle of about 35° from the normal, with vertical electric field polarization, and with a beam width of approximately 1° . A larger value of d will result in a narrower beam whose value can be calculated from the curve for α in Fig. 4.

A somewhat similar antenna has been analyzed and measured [H. Shigesawa and K. Takiyama, 1964; K. Takiyama and H. Shigesawa, 1967; and H. Shigesawa, K. Fujiyama and K. Takiyama, 1970]. An extrapolation from that study implies that our values for the leakage constant are somewhat lower than what they would predict. Their analysis is approximate, however, and the measurement procedure they use is indirect and subject to some question. We have recently taken some preliminary direct measurements which show good agreement with our theoretical calculations, but more careful measurements are in progress.

REFERENCES

- Claricoats, P. J. B. and A. A. Oliner, 1965, "Transverse-Network Representation for Inhomogeneously Filled Circular Waveguides," Proc. IEE, vol. 112, No. 5, pp. 883-894.
- Shigesawa, H. and K. Takiyama, 1964, "Study of a Leaky H-guide," Internat. Conf. on Microwaves, Circuit Theory and Information, Paper M1-7, Tokyo, Japan. More complete version in K. Takiyama and H. Shigesawa, March 1967, "On the Study of a Leaky H-guide," Science and Engineering Review of Doshisha University, vol. 7, No. 4, pp. 203-225, (in English).
- Shigesawa, H., K. Fujiyama and K. Takiyama, July 3, 1970, "Complex Propagation Constants in Leaky Waveguides with a Rectangular Cross Section," presented at a Japanese scientific conference.
- Takiyama, K. and H. Shigesawa, February 1967, "The Radiation Characteristics of a Leaky H-guide," J. Inst. Electrical Commun. Engrs. of Japan (J.I.E.C.E.), vol. 50, No. 2, pp. 181-188, (in Japanese).

Weinstein, L.A., 1969, "The Theory of Diffraction and the Factorization Method," pp. 29-50, The Golem Press, Boulder, Colorado (translated from Russian).

Yoneyama, T. and S. Nishida, November 1981, "Nonradiative Dielectric Waveguide for Millimeter-Wave Integrated Circuits," IEEE Trans. on Microwave Theory Tech., vol. MTT-29, No. 11, pp. 1188-1192.

Yoneyama, T. and S. Nishida, December 1981, "Non-radiative Dielectric Waveguide Circuit Components," International Conference on Infrared and Millimeter Waves, Miami, Florida.

ACKNOWLEDGMENT

The work described here was supported by the Rome Air Development Center at Hanscom AFB, Mass., under Contract No. F19628-81-K-0044.

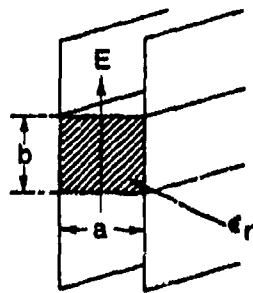


Fig. 1. Cross section view of nonradiative dielectric waveguide, where $a < \lambda_0/2$.

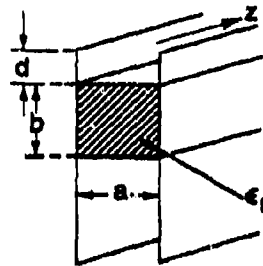


Fig. 2(a) Cross section view of leaky-wave antenna, where leakage is controlled by distance d .

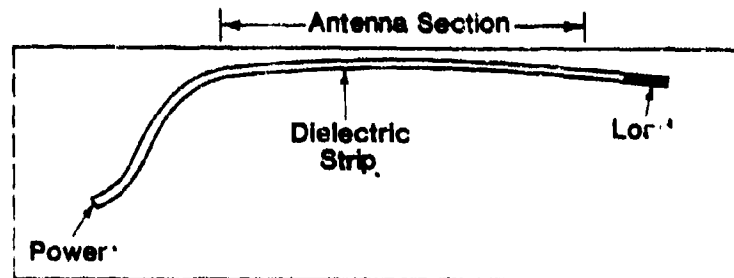


Fig. 2(b) Side view of antenna, where the antenna aperture distribution can be tapered by altering the position of the dielectric strip, and the strip can be connected to the rest of the millimeter-wave integrated circuit.

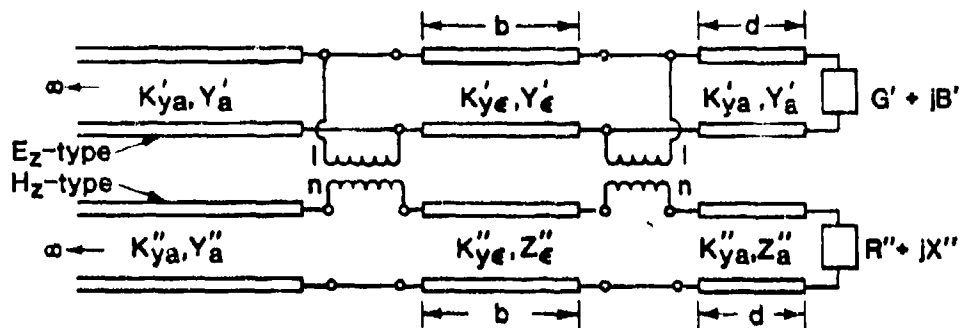


Fig. 3. Rigorous transverse equivalent network for the antenna shown in Fig. 2(a). The network is placed on its side for clarity.

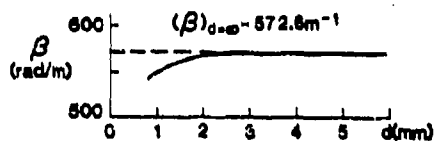


Fig. 4. Phase constant β in radians/meter of the leaky-wave antenna in Fig. 2(a) as a function of d in mm, showing that β is independent of d beyond some minimum value of d .

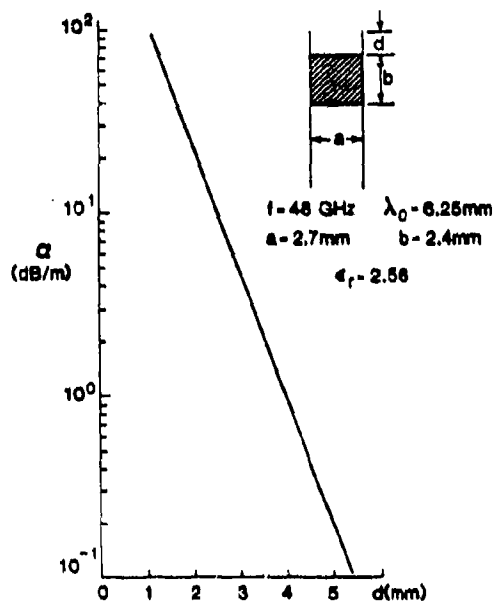


Fig. 5. Leakage constant α in dB/meter of the leaky-wave antenna in Fig. 2(a) as a function of the distance d in mm between the dielectric strip and the radiating open end.

2. Derivations of the Constituents of the Transverse Equivalent Network

The form of the transverse equivalent network is shown in Fig. 3 of the paper reproduced in Sec. A, 1. It is seen to consist of constituent elements that correspond to the various geometric discontinuities contained in the foreshortened-top leaky wave antenna structure shown in Sec. A, 1 as Fig. 2(a). The lengths of transmission line in the transverse equivalent network are representative of the transverse modes that propagate in the uniform regions of the cross section. In addition, the choice of modes modifies the form of the network in basic ways.

As mentioned in Sec. A,1, if ordinary TE (or H) and TM (or E) modes are used, then the air-dielectric interface remains a simple junction but these TE and TM modes become coupled together at the radiating open end. On the other hand, if H-type (LSE) and E-type (LSM) modes are employed, they become coupled together at the air-dielectric interface but remain uncoupled at the radiating open end. After careful consideration, we chose the E-type and H-type mode formulation as the simpler one on balance.

Expressions for the field components and the characteristic impedances for the E-type and H-type modes relevant to this geometry are presented in subsection (a) below.

These E-type and H-type modes become coupled together at the air-dielectric interfaces, but their coupling can be represented by a simple transformer network arrangement. Also, only the dominant modes are coupled, and no higher-order modes are excited, as at true geometric discontinuities. The derivation of the network form and the expressions corresponding to it appear in subsection (b). It should be recognized that this network form is an adaptation to planar geometry of a result previously given by Clarricoats and Oliner [28] for circular geometries, but that its derivation and utilization in planar form is new. This constituent result is therefore of interest in its own right.

The remaining discontinuity is the radiating open end. As shown in subsection (c), and as summarized in Sec. A, 1, the constituent terminal admittances representing the E-type and H-type modes incident on the open end are derived by making several necessary modifications of a result derived some years ago by L. A. Weinstein [29]. The original expressions of Weinstein were valid only for normal incidence; our situation contains a variation in the longitudinal direction, with the incident transverse modes below cutoff, thus requiring appropriate analytic continuation of these expressions. The details are contained in subsection (c).

Each of the constituent expressions has been derived in closed form, which is a significant virtue of this approach and these derivations. The complete transverse equivalent network thus yields a dispersion relation for the leaky wave that is likewise in closed form. The dispersion relation is summarized in subsection (d), together with some added remarks.

(a) The Modes Employed

The coordinate system to be used appears in connection with Fig. 2(a) in Sec. A, 1. The final leaky wave propagates in the axial (z) direction, and the transverse transmission line direction is the vertical (y) direction. The transmission direction of the transverse modes is thus the y direction. However, the structure is uniform with respect to the z direction. The E-type and H-type modes to be employed are therefore separable with respect to z, but propagating in y. It is accurate, therefore, to designate them as $E^{(z)}$ -type and $H^{(z)}$ -type modes (or alternatively as LSM and LSE modes with respect to the z direction).

We shall choose the E-type and H-type notation, and follow the formulation developed by Altschuler and Goldstone [19] but with our coordinate system. They have presented the derivations of the pertinent field relations and the orthogonality relations, so that we will not repeat them here. However, it is necessary for us to know the field components and the characteristic impedances for these modes, corresponding to our choice of coordinate system.

The constituent vertical guiding regions in our antenna structure (Fig. 2(a) in Sec. A, 1) are portions of parallel plate waveguide, either dielectric-filled or air-filled. We also recall that ordinary TM (or E) and TE (or H) modes would be characterized by the presence or absence of the y component of field, whereas the E-type and H-type modes are distinguished by the presence or absence of the appropriate z component.

The E-type modes shall be denoted by primed quantities and the H-type modes by double-primed quantities. The transmission direction is y, so that the components of the mode functions for the i th E-type modes are h'_{xi} , e'_{xi} and e'_{zi} , with $h'_{zi} = 0$. Correspondingly, the components of the mode functions for the i th H-type modes are h''_{xi} , e''_{xi} and h''_{zi} , with $e''_{zi} = 0$. For air-filled regions, the relations between them, and the expressions for the characteristic immitances Z'_i and Y''_i are:

E(z) - type modes

$$\begin{aligned} h'_{zi} &= 0 \\ h'_{xi} &= e'_{zi} \end{aligned} \quad e'_{xi} = \frac{1}{k_o^2 - k_{zi}^2} \frac{\partial^2 e'_{zi}}{\partial x \partial z} \quad (3.1)$$

$$Z'_i = \frac{k_o^2 - k_{zi}^2}{\omega \epsilon k_{yi}} \quad (3.2)$$

H(z) - type modes

$$\begin{aligned} e''_{zi} &= 0 \\ e''_{xi} &= h''_{zi} \end{aligned} \quad h''_{xi} = \frac{1}{k_o^2 - k_{zi}^2} \frac{\partial^2 h''_{zi}}{\partial x \partial z} \quad (3.3)$$

$$Y''_i = \frac{k_o^2 - k_{zi}^2}{\omega \mu k_{yi}} \quad (3.4)$$

Next, we present the explicit field components for the parallel plate waveguide constituent regions under the condition that a net traveling wave propagates along the z direction, so that $\partial/\partial z$ yields $-j\beta$, where $k_z = \beta$. We also particularize the expressions for the dominant mode of each mode type. It is straightforward to generalize the expressions for the i th mode. The parallel-plate geometry and the associated coordinate system are given in Fig. 3.1.

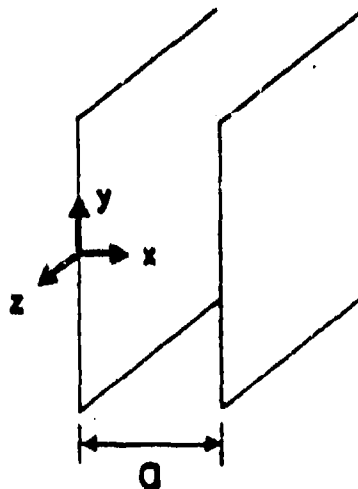


Fig. 3.1 Parallel plate waveguide and associated coordinate system.

$H_z^{(e)}$ - type modes

$$\begin{aligned}
 H_z^{(e)}(x, y, z) &= I'(y) h_z^{(e)}(x, z) \\
 &= I'(y) \sqrt{\frac{2}{a}} \sin \frac{\pi x}{a} e^{-j\beta z}
 \end{aligned} \tag{3.5}$$

$$\begin{aligned}
 E_z^{(e)}(x, y, z) &= V'(y) e_z^{(e)}(x, z) \\
 &= V'(y) \sqrt{\frac{2}{a}} \sin \frac{\pi x}{a} e^{-j\beta z}
 \end{aligned} \tag{3.6}$$

$$\begin{aligned}
 E_z^{(e)}(x, y, z) &= V'(y) e_z^{(e)}(x, z) \\
 &= -jV'(y) \sqrt{\frac{2}{a}} \frac{\pi}{a} \left[\frac{\beta}{k_0^2 \epsilon_r - \beta^2} \right] \cos \frac{\pi x}{a} e^{-j\beta z}
 \end{aligned} \tag{3.7}$$

$$\begin{aligned}
 H'_y(x, y, z) &= -\frac{1}{j\omega\mu} (\nabla \times E')_y = \frac{1}{j\omega\mu} \left(\frac{\partial E_z}{\partial x} - \frac{\partial E_x}{\partial z} \right) \\
 &= -jV'(y) \sqrt{\frac{2}{a}} \frac{\pi}{a} \left[\frac{\omega\epsilon_0\epsilon_r}{k_0^2\epsilon_r - \beta^2} \right] \cos \frac{\pi x}{a} e^{-j\beta z}
 \end{aligned} \tag{3.8}$$

$$\begin{aligned}
 E'_y(x, y, z) &= \frac{1}{j\omega\epsilon_0\epsilon_r} (\nabla \times H')_y = \frac{1}{j\omega\epsilon_0\epsilon_r} \frac{\partial H_z}{\partial z} \\
 &= -I'(y) \sqrt{\frac{2}{a}} \left[\frac{\beta}{\omega\epsilon_0\epsilon_r} \right] \sin \frac{\pi x}{a} e^{-j\beta z}
 \end{aligned} \tag{3.9}$$

$$\text{Or: } H'_y = \frac{\omega\epsilon_0\epsilon_r}{\beta} E'_z \tag{3.10}$$

$$E'_y = -\frac{\beta}{\omega\epsilon_0\epsilon_r} H'_z \tag{3.11}$$

$$\text{And: } Z' = \frac{k_0^2\epsilon_r - \beta^2}{\omega\epsilon_0\epsilon_r k'_y} \tag{3.12}$$

H⁽²⁾ - type modes

$$\begin{aligned}
 H''_x(x, y, z) &= \Gamma''(y) h''_x(x, z) \\
 &= \Gamma''(y) \sqrt{\frac{2}{a}} \cos \frac{\pi x}{a} e^{-j\beta z}
 \end{aligned} \tag{3.13}$$

$$\begin{aligned}
 E''_z(x, y, z) &= V''(y) e''_z(x, z) \\
 &= -V''(y) \sqrt{\frac{2}{a}} \cos \frac{\pi x}{a} e^{-j\beta z}
 \end{aligned} \tag{3.14}$$

$$\begin{aligned}
 H''_z(x, y, z) &= \Gamma''(y) h''_z(x, z) \\
 &= jI''(y) \sqrt{\frac{2}{a}} \frac{\pi}{a} \left[\frac{\beta}{k_0^2\epsilon_r - \beta^2} \right] \sin \frac{\pi x}{a} e^{-j\beta z}
 \end{aligned} \tag{3.15}$$

$$E''_y(x, y, z) = \frac{1}{j\omega\epsilon_0\epsilon_r} (\nabla \times H'')_y = -\frac{\omega\mu}{\beta} H''_z \tag{3.16}$$

$$H''_y(x, y, z) = -\frac{1}{j\omega\mu} (\nabla \times E'')_y = \frac{\beta}{\omega\mu} E''_z \tag{3.17}$$

$$\text{And: } Y'' = \frac{k_0^2\epsilon_r - \beta^2}{\omega\mu k''_y} \tag{3.18}$$

(b) The Air-Dielectric Interface

We note from the structure depicted in Fig. 2(a) in Sec. A, 1, that two air-dielectric interfaces appear in the cross section when viewed in the y direction. One of these interfaces is depicted in Fig. 3.2.

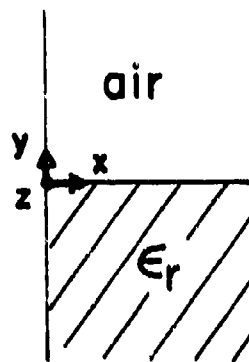


Fig. 3.2 An air-dielectric interface in a parallel plate region.

If ordinary TE and TM modes were employed in the y direction, the air-dielectric interface would represent a simple junction between transmission lines, and the TE and TM modes would not be coupled together at the interface. For the E-type and H-type modes we employ, however, these modes do couple at the interface, and the purpose of this section is to derive a simple network to describe this coupling.

A coupling network of this type was derived previously by Clarricoats and Oliner [28] for inhomogeneously filled circular waveguides. There, the geometry was radial, and the transmission lines were the so-called E-type and H-type radial transmission lines developed by N. Marcuvitz [50]. These radial transmission lines represent propagation in the radial direction,

but are found to be separable with respect to the axial direction. In our case, the geometry is planar rather than cylindrical; the modes propagate in y but are separable with respect to the z (axial) direction. The strong similarities present suggest that the procedure introduced there can be adapted for use here, and indeed this turns out to be the case.

The boundary conditions that must be satisfied at the air-dielectric interface are

$$\underline{E}_{t\epsilon} = \underline{E}_t \quad (3.19)$$

$$\underline{H}_{t\epsilon} = \underline{H}_t$$

that is, the tangential electric and magnetic fields must be continuous across the interface. In terms of components, relations (3.19) become

$$\begin{aligned} \underline{x}_0 (E_{y\epsilon}' + E_{y\epsilon}^*) + \underline{z}_0 E_{z\epsilon}' &= \underline{x}_0 (E_y' + E_y^*) + \underline{z}_0 E_z' \\ \underline{x}_0 (H_{y\epsilon}' + H_{y\epsilon}^*) + \underline{z}_0 H_{z\epsilon}' &= \underline{x}_0 (H_y' + H_y^*) + \underline{z}_0 H_z' \end{aligned} \quad (3.20)$$

where \underline{x}_0 and \underline{z}_0 are unit vectors, and the arguments of the components are dropped for simplicity. Expressing (3.20) in terms of mode functions, and equating the \underline{x}_0 components and the \underline{z}_0 components separately, we obtain

$$\begin{aligned} V^* e_{y\epsilon}^* + V' e_{y\epsilon}' &= V^* e_y^* + V' e_y' \\ V' e_{z\epsilon}' &= V' e_z' \end{aligned} \quad (3.21)$$

$$\begin{aligned} \Gamma^* h_{y\epsilon}^* + \Gamma' h_{y\epsilon}' &= \Gamma^* h_y^* + \Gamma' h_y' \\ \Gamma^* h_{z\epsilon}^* &= \Gamma^* h_z^* \end{aligned} \quad (3.22)$$

Upon examination of the mode functions presented in expressions (3.5) to (3.7) and from (3.13) to (3.15), we find that

$$\begin{aligned} e_{s1}^i &= e_s^i & h_{s1}^n &= h_s^n \\ h_{s1}^i &= h_s^i & e_{s1}^n &= e_s^n \\ e_{s1}^i &\neq e_s^i & h_{s1}^n &\neq h_s^n \end{aligned} \quad (3.23)$$

On use of (3.23), relations (3.21) and (3.22) reduce to

$$V_1^i = V^i \quad (3.24)$$

$$F_1^i = F^i$$

$$V_1^n - V^n = V^i \frac{e_s^i - e_{s1}^i}{e_s^n} \quad (3.25)$$

$$I_1^i - I^i = F^i \frac{h_s^n - h_{s1}^n}{h_s^i}$$

When the relations in (3.25) are divided by V^i and I^i , respectively, and use is made of (3.24), (3.25) becomes

$$\frac{V_1^n}{I_1^i} - \frac{V^n}{I^i} = \frac{V^i}{I^i} \frac{e_s^i - e_{s1}^i}{e_s^n} \quad (3.26)$$

$$\frac{I_1^i}{V_1^i} - \frac{I^i}{V^i} = \frac{F^i}{V^i} \frac{h_s^n - h_{s1}^n}{h_s^i}$$

The two equations in (3.26) can be multiplied together, eliminating the ratio V^i/I^i and yielding

$$\left(\frac{V_1^n}{F_1^i} - \frac{V^n}{F^i} \right) \left(\frac{I_1^i}{V_1^i} - \frac{I^i}{V^i} \right) = \frac{h_s^n - h_{s1}^n}{h_s^i} \cdot \frac{e_s^i - e_{s1}^i}{e_s^n} \quad (3.27)$$

Finally, (3.27) can be rewritten as

$$(Z_{\epsilon}^{\prime\prime} + Z^{\prime\prime}) (Y_{\epsilon}^{\prime} + Y^{\prime}) = \frac{h_x^{\prime\prime} - h_{x\epsilon}^{\prime\prime}}{h_x^{\prime}} \cdot \frac{e_x^{\prime} - e_{x\epsilon}^{\prime}}{e_x^{\prime\prime}} \quad (3.28)$$

where $Z_{\epsilon}^{\prime\prime}$ and Y_{ϵ}^{\prime} are the impedance of the H-type mode and the admittance of the E-type mode at the air-dielectric interface looking into the dielectric region, and $Z^{\prime\prime}$ and Y^{\prime} are the corresponding quantities looking into the air region. A change in sign results when an impedance or admittance is taken looking in the opposite direction.

A simple network form, shown in Fig. 3.3, can be drawn based on (3.28) which is representative of the coupling between the E-type and H-type modes at the air-dielectric interface. The turns ratio N in this network is then given by

$$N^2 = \left| \frac{h_x^{\prime\prime} - h_{x\epsilon}^{\prime\prime}}{h_x^{\prime}} \cdot \frac{e_x^{\prime} - e_{x\epsilon}^{\prime}}{e_x^{\prime\prime}} \right| \quad (3.29)$$

When expressions (3.6), (3.7), (3.14) and (3.15) are used for the mode functions in (3.29), we obtain for the turns ratio N

$$N = \frac{(\pi/a) k_0^2 \beta (\epsilon_r - 1)}{(k_0^2 - \beta^2) (k_0^2 \epsilon_r - \beta^2)} \quad (3.30)$$

The network in Fig. 3.3 can be used as a constituent in a transverse equivalent network that is representative of the H guide or NRD guide structure shown in Fig. 1 in Sec. A, 1. A transverse resonance equation can then be set up using E-type and H-type modes, utilizing relations (3.30) for N and (3.12) and (3.18) for the appropriate characteristic immittances of the transmission lines. A. Sanchez has shown in his Ph.D. thesis [31] that the dispersion relation derived in this fashion reduces readily to the one given in the literature and found by employing the usual TM mode in the y direction. It is a cumbersome method for that simple problem, but it is indeed mathematically equivalent.

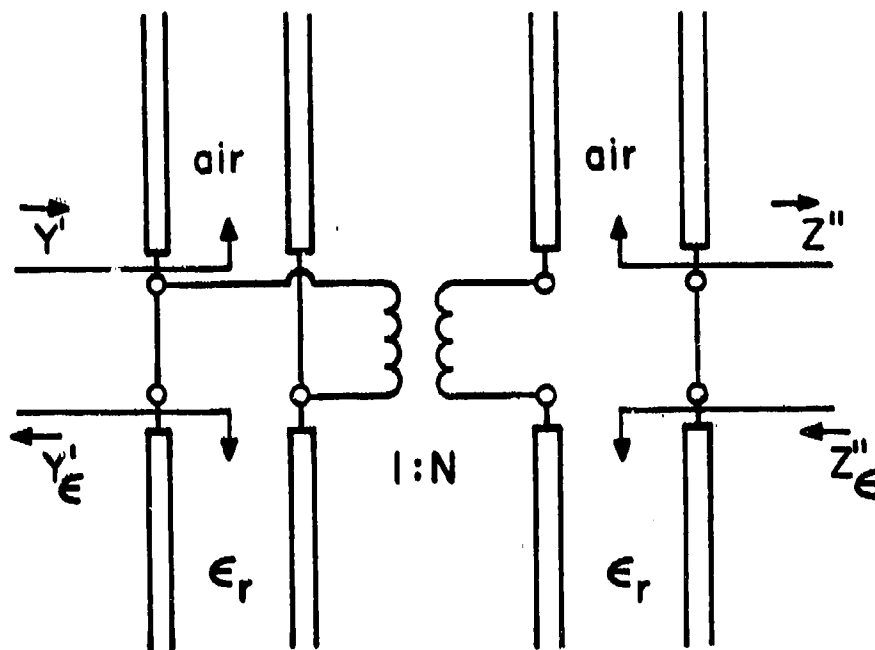


Fig. 3.3 Simple equivalent network that represents the coupling between the E-type and H-type modes at an air-dielectric interface of the type shown in Fig. 3.2.

(c) The Radiating Open End

If ordinary TE and TM modes with axial (z) variation are incident on the open end of parallel plate guide, they become coupled by the discontinuity. The modes remain uncoupled, though, when $E^{(z)}$ -type and $H^{(z)}$ -type modes are employed instead. In obtaining the terminal complex immittances for these modes, which are needed in the transverse equivalent network, we are able to make use of expressions for reflection coefficients derived by L. A. Weinstein [29] for a simpler situation.

His results apply to propagating TM_1 (or E_1) and TE_1 (or H_1) modes in parallel plate guide normally incident on the radiating open end. Our case involves modes with longitudinal variation along z which are below cutoff, so that it was necessary to analytically continue Weinstein's results in an appropriate manner. His expressions are of great value, however, since they were derived using the factorization, or Wiener-Hopf, method, and are therefore rigorous.

The analytic continuation required two steps. First, we recall that for NRD guide it is necessary to maintain the plate spacing less than a half wavelength so that the incident modes would be below cutoff even if there were no axial variation. This circumstance calls for an analytic continuation of Weinstein's reflection coefficients to modes below cutoff.

The next step accounts for the longitudinal variation of the incident $E^{(z)}$ -type and $H^{(z)}$ -type modes. These modes become the normally-incident TE_1 and TM_1 modes, respectively, when $\beta = 0$ in expressions (3.5) through (3.18). The paper [19] by Altschuler and Goldstone has also indicated how the reflection coefficients must be modified when a longitudinal variation is introduced into the E-type and H-type modes, provided that these modes remain uncoupled by the discontinuity in question, as is the case here. The modification is to replace k_0 , wherever it appears, by $(k_0^2 - \beta^2)^{1/2}$.

(1) Summary of Weinstein's Formulation:

Weinstein's rigorous analysis [29] applies to TM_1 and TE_1 modes normally incident on the open end of parallel plate guide. He solves for the reflection coefficients of the surface currents in each case, but we can relate these to the voltage and current reflection coefficients of interest in our problem. His coordinate system, time dependence, and other notation are also different.

In his notation, the reflection coefficients are written as

$$R_{1,1} = - |R_{1,1}| e^{-j\theta} \quad (3.31)$$

where

$$|R_{1,1}|_{H_1} = \sqrt{(q - \gamma)/(q + \gamma)} e^{-\pi\gamma} \quad (3.32)$$

and

$$|R_{1,1}|_{E_1} = \sqrt{(q - \gamma)/(q + \gamma)} e^{-\pi\gamma} \quad (3.33)$$

and

$$q = a/\lambda, \quad \gamma = k_y (a/2\pi) = \sqrt{q^2 - 1/4} \quad (3.34)$$

Quantity θ is also given for both mode types by

$$\begin{aligned} \theta = & 2(2 - C + \ln \frac{2}{q} - \frac{1}{2\gamma} \arcsin \frac{\gamma}{q} - \\ & - \frac{1}{\gamma} \arcsin \frac{\gamma}{\sqrt{2}} + \sigma - \sum_{m=1}^{\infty} A_{2m+1} S_m \gamma^{2m}) \end{aligned} \quad (3.35)$$

where

$$\begin{aligned} C = & 0.5772 \dots = \lim_{N \rightarrow \infty} \left(\sum_{n=1}^N \frac{1}{n} - \ln N \right) \\ \sigma = & 0.265 = \sum_{n=0}^{\infty} \left(\frac{1}{n+1} - \frac{1}{\sqrt{n(n+1)}} \right) \end{aligned} \quad (3.36)$$

and A_{2m+1} are the coefficients of the series

$$\arcsin z = \sum_{m=0}^{\infty} a_{2m+1} z^{2m+1} \quad (3.37)$$

where $A_1 = 1$, $A_3 = 1/6$, $A_5 = 3/40 \dots$, and S_m is given by

$$S_m = \sum_{n=0}^{\infty} \frac{1}{[n(n-1)]^{m+1/2}} \quad (3.38)$$

with $S_1 = 0.123$, $S_2 = 0.014$, ...

We find above what is customary in these factorization procedures, that the magnitudes are simple in form but the phase expressions are complicated.

We next need to relate these reflection coefficients for the wall current densities to the voltage and current reflection coefficients corresponding to our transmission line formulation. In this connection, we may write [32] for the TM_1 (or H_1) mode

$$j_z = H_y \Big|_{\text{wall}} = \frac{1}{j \omega \mu} \nabla_t \cdot (\underline{y}_0 \times \underline{E}_t) \quad (3.39)$$

where the time dependence is $\exp(j\omega t)$. Since

$$\underline{E}_t = V(y) \underline{e}_t(x)$$

we see that the reflection coefficient for the current density j_z is also the voltage reflection coefficient. Consequently,

$$R_v'' = - \left| R_{1,1}'' \right| e^{-j\theta} \quad (3.40)$$

for the TE_1 (or H_1) mode, where $\left| R_{1,1}'' \right|$ and θ are still given by (3.32) and (3.35), and the double prime is employed because of the mode involved.

For the TM_1 (or E_1) mode, we may write [32]

$$j_y = -H_z \Big|_{\text{wall}} = -I(y) h_z(x) \quad (3.41)$$

Therefore, the reflection coefficient for the current density for this mode corresponds to the current reflection coefficient

$$R_I' = |R_{1,1}'| e^{-j\theta} \quad (3.42)$$

where $|R_{1,1}'|$ and θ are still given by (3.33) and (3.35).

It was indicated in (3.34) how q and γ are related to frequency and wavenumbers in our notation. Elaborating further, we find

$$q = \frac{a}{\lambda_0} = \frac{k_0 a}{2\pi}, \quad \gamma = \frac{k_y a}{2\pi} \quad (3.43)$$

so that $\gamma = \sqrt{q^2 - 1/4}$ becomes

$$k_y = \sqrt{k_0^2 - (\pi/a)^2} \quad (3.44)$$

and factors found in (3.32) and (3.33) become

$$\frac{q \mp \gamma}{q \pm \gamma} = \frac{k_0 \mp k_y}{k_0 \pm k_y} \quad (3.45)$$

(2) Analytic Continuations

The first step is to analytically continue the expressions for the reflection coefficients so that they apply to modas below cutoff. The term γ (see (3.43)) is now imaginary and should be written as

$$\gamma = -j|\gamma|$$

The expression for the phase angle θ is not ambiguous if principal values are taken for the terms $\ln(2/q)$, arcsine (γ/q) and arcsine $(\gamma/\sqrt{2})$. We need only to be careful in the choice of branches in the complex plane for the reflection coefficient magnitudes.

In Fig. 3.4 we summarize the three mappings that are involved in ascertaining the choice of branches that correctly analytically continue the reflection coefficient magnitudes, $|R_{1,1}''|$ and $|R_{1,1}'|$.

1) The mapping $q \rightarrow \gamma$ maps the segments of the real axis $1/2 < q < 3/2$ and $0 < q < 1/2$ onto the segments $0 < \gamma < \sqrt{2}$ of the real axis of the γ plane and the segment of the imaginary γ axis between zero and $-(1/2)j$, respectively. We recognize that $q = 1/2$ corresponds to mode cutoff.

2) The mapping $q \rightarrow |R_{1,1}'|$ maps the segment of the real axis $1/2 < q < 3/2$ onto the segment of the real axis of the $|R_{1,1}'|$ plane between 1 and $C = [(3 + 2\sqrt{2}) / (3 - 2\sqrt{2})]^{1/2} > 1$, and the real segment $0 < q < 1/2$ onto the arcs of the unit circle subtended by the first and third quadrants.

3) In a similar manner, the mapping $q \rightarrow |R_{1,1}''|$ maps the segment of the real axis $1/2 < q < 3/2$ onto the segment of the real axis of the plane $|R_{1,1}''|$ between 1 and $C' = [(3 - 2\sqrt{2}) / (3 + 2\sqrt{2})]^{1/2} < 1$, and the real segment $0 < q < 1/2$ onto the arcs of the unit circle subtended by the second and fourth quadrants.

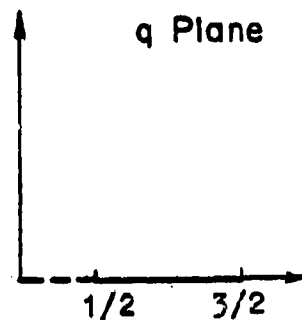
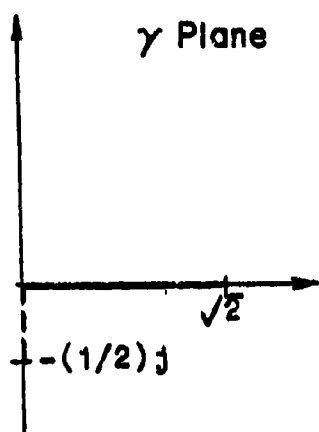
The continuity condition of the mappings $|R_{1,1}'|$ and $|R_{1,1}''|$ at $q = 1/2$ along the real axis of the q plane imposes the choice of the arcs of the unit circle situated in the first and fourth quadrants as the correct analytical continuation of the $|R_{1,1}'|$ and $|R_{1,1}''|$ quantities. Thus

$$\operatorname{Re} \left(\frac{\sqrt{(q \pm \gamma)}}{(q \mp \gamma)} \right) > 0$$

when the mode just goes below cutoff.

Up till now we have not taken into account the variation with z that is present in our problem. When we include this variation, the TM_1 and TE_1 modes treated above become the $H^{(z)}$ -type and $E^{(z)}$ -type modes of concern to us. To determine the effect of this variation with z we change q to q' , where

$$q = k_0 a / 2\pi, \quad q' = (k_0^2 - \beta^2)^{1/2} (a / 2\pi) \quad (3.46)$$



$$C = \sqrt{(3+2\sqrt{2})/(3-2\sqrt{2})} = 5.82$$

$$C = \sqrt{(3-2\sqrt{2})/(3+2\sqrt{2})} = 0.172$$

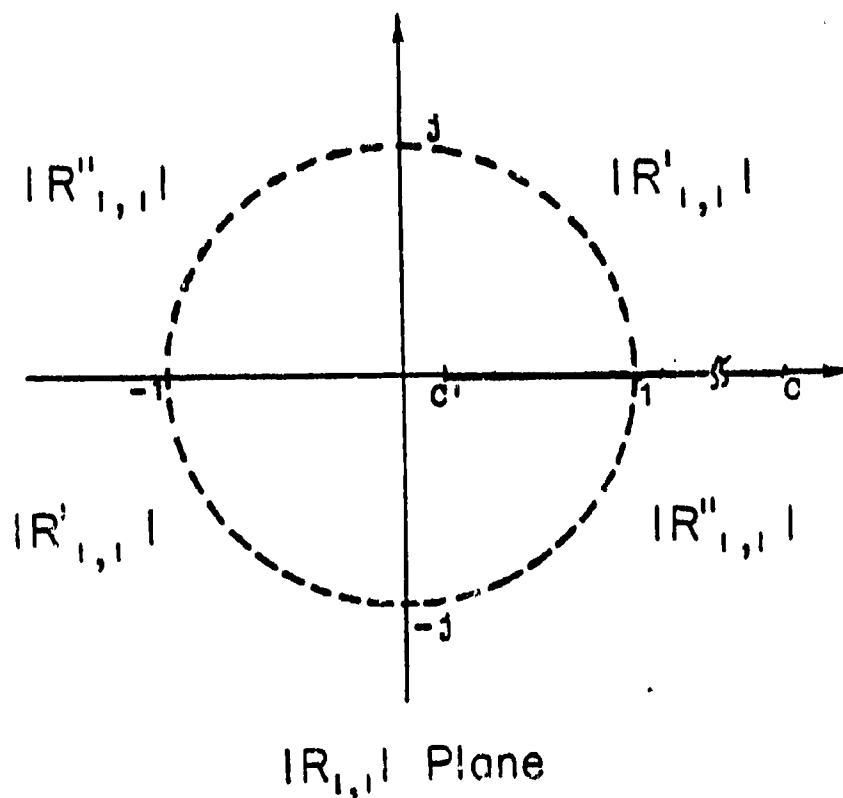


Fig. 3.4 Mappings of q into γ and q into $|R_{1,1}|$ required for analytic continuation.

From (3.40), bearing in mind that the voltage reflection coefficient is the negative of the current reflection coefficient, we have

$$-\Gamma_I = \Gamma_V = (R'_{1,1})_V \Big|_{z'} = -|R'_{1,1}| e^{-j\theta} \Big|_{z'} \quad (3.47)$$

while from (3.42) we obtain

$$-\Gamma^*_V = \Gamma^*_I = (R'_{1,1})_I \Big|_{z'} = -|R'_{1,1}| e^{j\theta} \Big|_{z'} \quad (3.48)$$

The terminal impedance for the $H^{(z)}$ -type mode and the terminal admittance for the $E^{(z)}$ -type mode corresponding to the radiating open end are therefore given by

$$Z^*_L = \frac{k_y}{\omega \epsilon_0} \frac{1 + \Gamma^*_V}{1 - \Gamma^*_V} = \frac{\sqrt{k_0^2 - (\pi/a)^2 - \beta^2}}{\omega \epsilon_0} \frac{1 + \Gamma^*_V}{1 - \Gamma^*_V} \quad (3.49)$$

and

$$Y'_L = \frac{k_y}{\omega \mu_0} \frac{1 + \Gamma'_I}{1 - \Gamma'_I} = \frac{\sqrt{k_0^2 - (\pi/a)^2 - \beta^2}}{\omega \mu_0} \frac{1 + \Gamma'_I}{1 - \Gamma'_I} \quad (3.50)$$

It should be remarked that the characteristic impedance and admittance appearing in the last two equations are the ones for the E_1 and H_1 modes when k_0^2 is replaced by $k_0^2 - \beta^2$ and not the ones corresponding to the $H^{(z)}$ -type and $E^{(z)}$ -type modes. In the transverse equivalent network given in Fig. 3 in Sec. A, 1, Z''_L and Y'_L are written respectively as $R'' + jX''$ and $G' + jB'$.

(d) The Dispersion Relation for the Leaky Mode

In subsection (a) above, we have presented expressions for the mode functions and the characteristic impedances of the $E^{(z)}$ -type and $H^{(z)}$ -type modes that propagate in the uniform regions of the cross section. We can therefore characterize exactly the properties of the various transmission lines in the transverse equivalent network. In subsections (b) and (c), we have derived rigorous expressions and network forms for the air-dielectric interface and the radiating open end, respectively. We therefore have all the constituents of the complete transverse equivalent network shown in Fig. 3 of Sec. A, 1.

The dispersion relation for the leaky wave behavior is then obtained by taking a free resonance of this transverse equivalent network. The resulting dispersion relation emerges in a straightforward manner but is somewhat messy in form. A simpler network form results if the structure is made symmetrical so that it leaks from both ends; we may then bisect the network with a short circuit. The dispersion relation for this simpler network may then be expressed in the following simple form.

$$[\bar{Z}'_i(\beta) + Z''_s(\beta)] [\bar{Y}'_i(\beta) + Y'_s(\beta)] = N^2(\beta) \quad (3.51)$$

where

$$\bar{Z}'_i(\beta) = j \frac{\omega \mu_0 k_{ye}}{\epsilon_r k_0^2 - \beta^2} \tan(k_{ye} b/2) \quad (3.52)$$

$$\bar{Y}'_i(\beta) = -j \frac{\omega \epsilon_0 \epsilon_r k_y}{\epsilon_r k_0^2 - \beta^2} \cot(k_{ye} b/2) \quad (3.53)$$

$$Z''_s(\beta) = Z''_a \frac{jZ''_a + Z''_L \cot(k_{ya} d)}{Z''_a \cot(k_{ya} d) + jZ''_L} \quad (3.54)$$

$$Y'_s(\beta) = Y'_a \frac{jY'_a + Y'_L \cot(k_{ya} d)}{Y'_a \cot(k_{ya} d) + jY'_L} \quad (3.55)$$

$$Z'_e = \frac{\omega \mu_0 k_{ya}}{k_0^2 - \beta^2} \quad Y'_e = \frac{\omega \epsilon_0 k_{ya}}{k_0^2 - \beta^2} \quad (3.59)$$

and $N^2(\beta)$, Z'_L & Y'_L are given by (3.30), (3.49) and (3.50), respectively.

(3) Numerical Results

Using the theoretical expressions derived above, we have obtained the values of the phase constant β and the leakage constant α as a function of various geometric parameters. These quantities are the ones we need in order to design the antenna in response to performance requirements.

In the short paper presented in Sec. A, 1, the variations of α and β are presented as a function of d , the distance between the air-dielectric interface and the radiating open end. These results appear there as Figs. 4 and 5, and they correspond to a set of geometric parameters given by Yoneyama and Nishida in their original paper [2] on NRD guide.

For simplicity in design, one desires that β remain constant while α varies greatly as a function of a specific parameter. In that way, the geometry can be changed to alter α without changing β , thereby permitting one to taper the amplitude distribution and simultaneously maintain the phase linear along the antenna aperture length. The variation of α and β with d satisfies this requirement provided that d remains less than about 2 mm for that set of dimensions. It is seen that for $d > 2\text{mm}$ β is essentially constant, whereas α varies over a large range.

This desirable behavior as a function of distance d allows us to build a tapered antenna in the manner shown in Fig. 2(b) of the short paper

in Sec. A, 1. The taper is achieved by adjusting the position of the dielectric strip relative to the open end.

Calculations were also made of the dependence of α and β on other geometric parameters and on the relative dielectric constant. In these calculations, the dispersion relation was solved by a numerical iterative procedure that requires a first estimate of the root searched for. In most cases, the estimate was taken from the value of β for the nonradiating case, for which the dispersion relation is simple and yields real roots. A typical number of five iterations was enough to achieve convergence, and double precision was required to obtain accurately the values of α .

The variations of α and β with the separation a between the plates is given in Fig. 3.5. Here we find an inverse situation, but as expected. As one varies the plate separation, the value of β changes greatly, but α changes only a little, except near cutoff. In fact, α remains flat over a reasonably wide range of a/λ_0 . These dependences permit the designer to vary spacing a to adjust β , and therefore the angle of the radiated beam, and to vary d to adjust α , and therefore the beam width. The variation of α vs. a in Fig. 3.5 also implies that a small variation in plate spacing will negligibly affect the side lobe distribution.

The dependences of α and β on the thickness b of the dielectric strip appear in Fig. 3.6. Here, both α and β change as b is varied. Most significantly, the leakage constant α decreases as the strip becomes thicker. This behavior is to be expected physically, since a thicker dielectric strip produces a greater field confinement to the region of the strip; as a result, the field amplitude at the radiating open end is less and, in turn, less leakage power is produced.

The last parameter that can be varied is the dielectric constant ϵ_r of the dielectric strip; the effects of ϵ_r on α and β are shown in Fig. 3.7. It is interesting that the leakage constant varies two orders of magnitude between cutoff and the onset of the slow-wave region, and that this whole range can be spanned by changing ϵ_r from 2.0 to only 3.4. Furthermore,

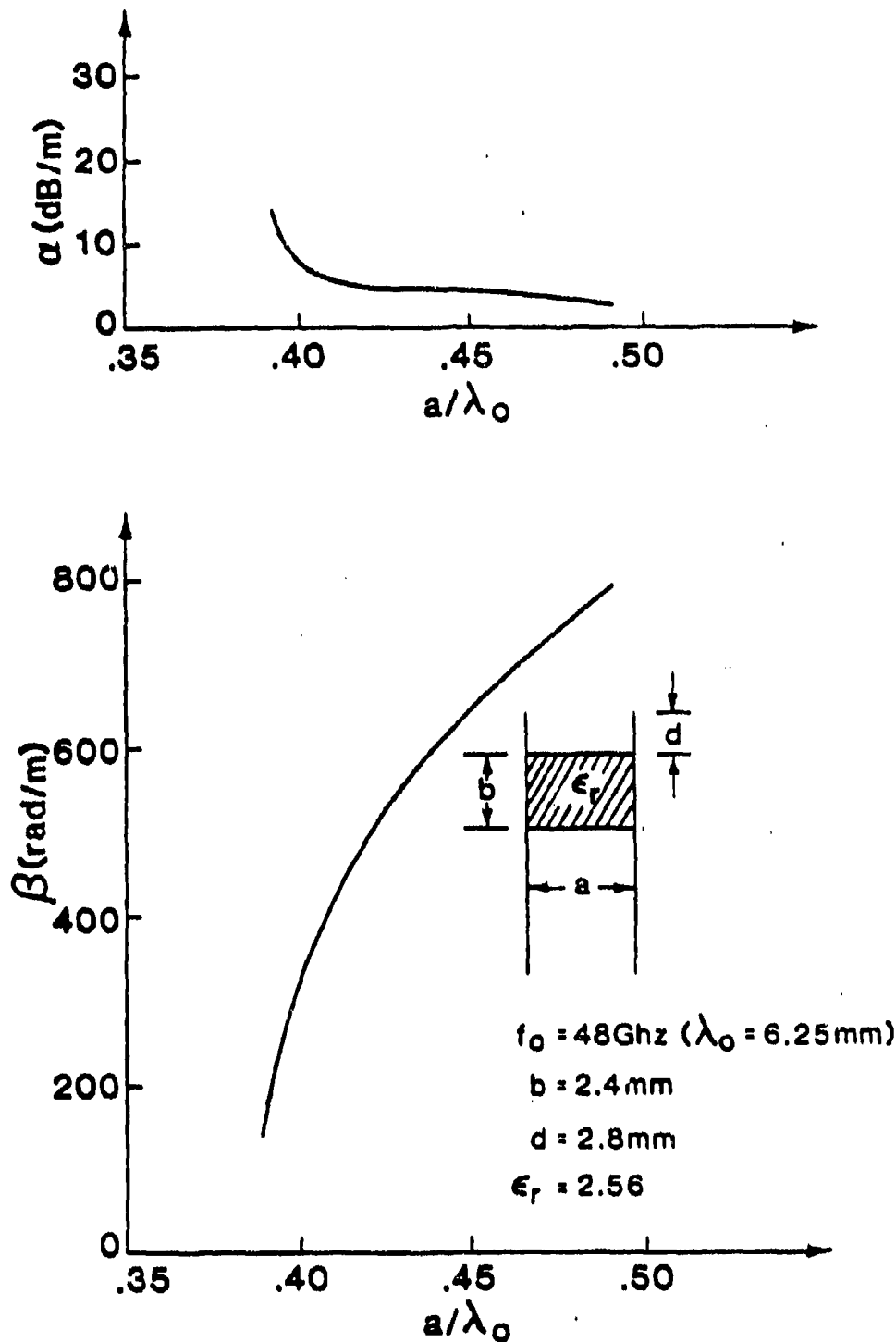


Fig. 3.5 Curves of leakage constant α and phase constant β as a function of the plate spacing a , for the foreshortened-top NRD guide antenna.

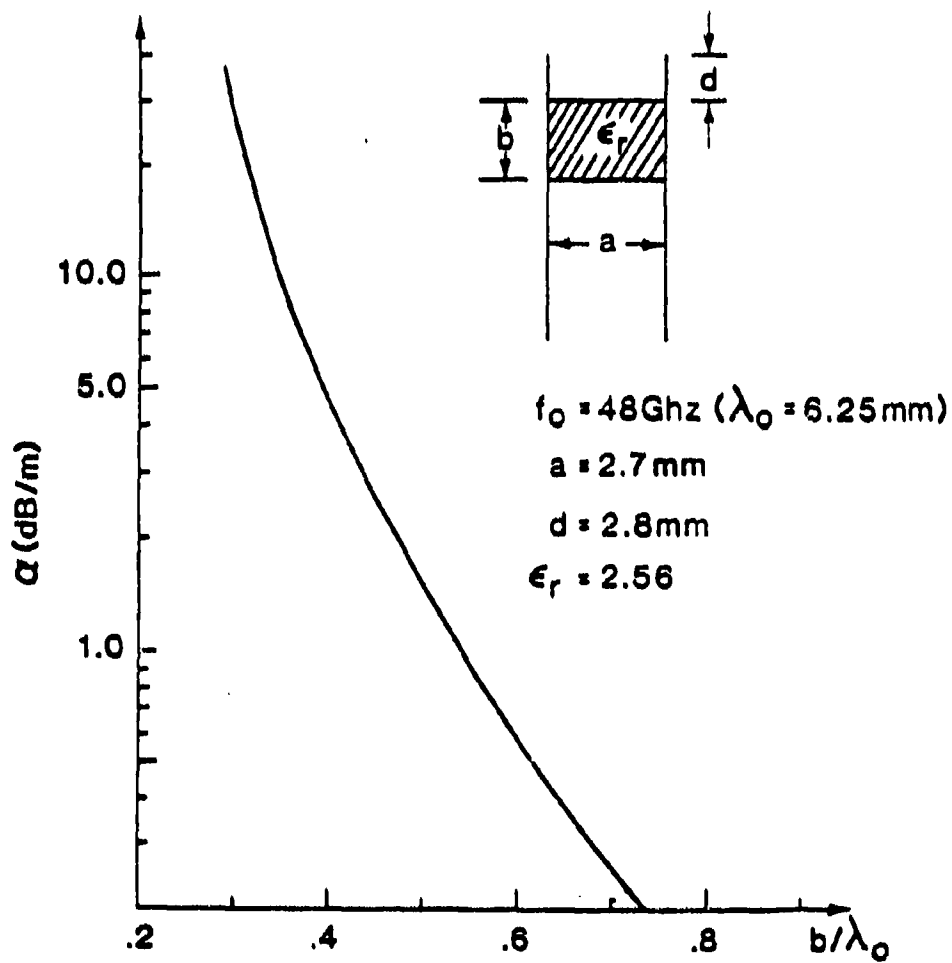
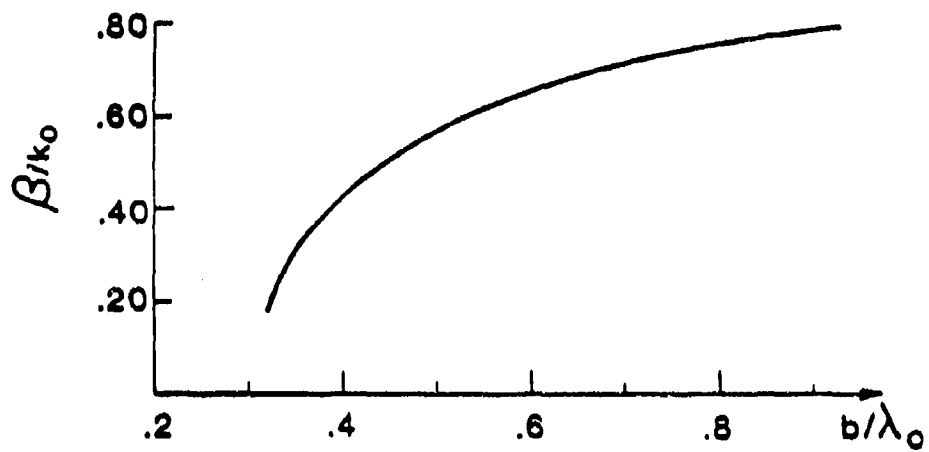


Fig. 3.6 Curves of phase constant β and leakage constant α as a function of the thickness b of the dielectric strip, for the foreshortened-top NRD guide antenna.

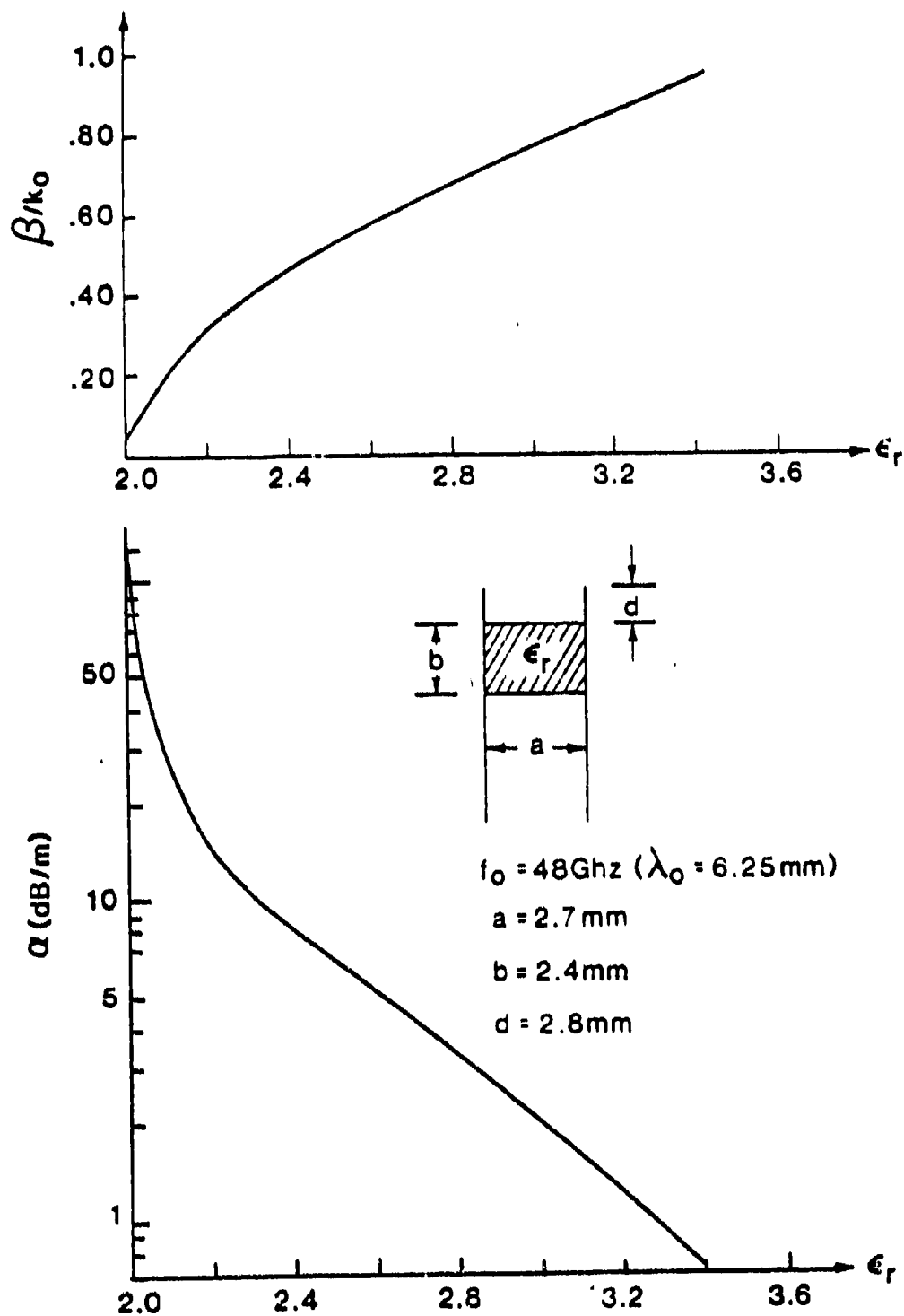


Fig. 3.7 Curves of phase constant β and leakage constant α as a function of the relative dielectric constant ϵ_r of the dielectric strip, for the foreshortened-top NRD guide antenna.

a strip with $\epsilon_r = 2.20$ can have roughly double the leakage of a strip of the same dimensions but composed of polystyrene, with $\epsilon_r = 2.56$. This decay of α with increasing ϵ_r is readily understood physically since the fields are more confined for higher ϵ_r values, so that less field arrives at the antenna aperture, and the leakage is reduced. We note that the phase constant β changes greatly with ϵ_r , as expected, but also that the variation is linear over a wide range of ϵ_r when the guide is away from cutoff.

B. THE FORESHORTENED-TOP ANTENNA: PERTURBATION ANALYSES

The perturbation analyses were originally conducted in order to check whether or not the accurate analysis discussed under Sec. A contained some inadvertent analytical or numerical error. Such errors are less likely in the simpler perturbation analyses, and they furthermore offer an alternative result. As mentioned in the introductory remarks to Part III, concern with respect to the validity of the accurate analysis arose when the same approach was applied to a somewhat similar, but simpler, problem for which both approximate theory and measurements were given (see Sec. C below); our theory differed by almost a factor of two from those measurements and theory.

Later, we also performed our own careful measurements and we received measured data from Professor Yoneyama, and all of those results agreed very well with our theory, thereby verifying that our theory is correct, and that the earlier measurements and theory that raised doubts were actually wrong. As we see below in this section, the perturbation calculations also agree well with our accurate theory.

We conducted two types of perturbation analysis. One type is based on the transverse equivalent network, with both of its constituent transmission lines; the second type is simpler, using a reflection coefficient directly and employing only one transmission line. Both approximate procedures yield good agreement with the accurate theory, as we show below.

Since these perturbation procedures yield good agreement with accurate results, and since they are simpler to compute from than the complete accurate theory, they are useful in their own right, no matter why they were derived originally. They can be used in many engineering situations when good approximate results are enough to form the basis for design.

The subsections 1 and 2 below derive the perturbation procedures, and subsection 3 numerically compares the perturbation results with those for the accurate theory.

1. Procedure Based on the Transverse Equivalent Network

One approximate approach that can be adopted is to assume that the radiation (or leakage) from the actual antenna, shown in Fig. 3.8(a), which radiates from the top only, is equal to one half the radiation from a symmetrical structure of the form seen in Fig. 3.8(b), which radiates from both ends. We have made numerical comparisons to determine the validity of this assumption, and it turns out that it is really very good unless the leakage is quite large. We shall therefore base our perturbation procedure on the dispersion relation (3.51), which holds for the structure in Fig. 3.8(b).

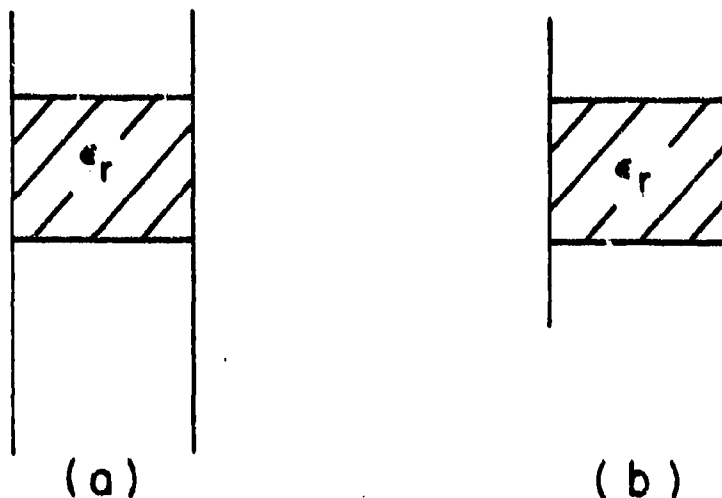


Fig. 3.8 Cross sections of (a) The actual asymmetric foreshortened-top NRD guide antenna, and (b) A symmetrical structure foreshortened at both top and bottom and therefore radiating from both ends.

Dispersion relation (3.51) accounts rigorously for the radiation and propagation characteristics of the leaky wave antenna shown in Fig. 3.8(b), when d , the distance between the air-dielectric interface and the open end,

is large enough to preclude higher $E^{(z)}$ -type and $H^{(z)}$ -type modes excited at the open end from reaching the air-dielectric interface. If d were not large enough, we would need additional transmission lines which would then become coupled at the air-dielectric interface, and the problem would become very involved. Therefore, d is kept within limits for which significant higher mode interaction between the two discontinuities does not occur. If, in addition, d is maintained within a limit such that the fields are small at the open end, we can expect small leakage to occur. In this instance, a perturbation procedure is in order.

If small leakage occurs, the propagation characteristics will be close to those of the nonradiating NRD guide, with infinitely long side walls. The phase constant will then be given closely by the solution for the nonradiating case, for which the dispersion relation is quite simple, and its deviation from it will be small, as will be the leakage constant. The solution for the nonradiating case will be called the unperturbed solution.

Let us call β_0 the phase constant corresponding to the unperturbed modal field. Then β_0 is the solution of

$$[\bar{Z}_e(\beta_0) + Z_e(\beta_0)] [\bar{Y}_e(\beta_0) + Y_e(\beta_0)] = N^2(\beta_0) \quad (3.57)$$

where Z_a'' and Y_a' are characteristic immittances, given by (3.18) and (3.12), respectively, since the air-filled regions are infinitely long. The terms Z_e'' and Y_e' are clearly

$$\bar{Z}_e'' = -j Z_e'' \tan(k_{ye} b/2) \quad (3.58)$$

$$\bar{Y}_e' = -j Y_e' \cot(k_{ye} b/2) \quad (3.59)$$

and N is given by (3.30). Inspection of (3.57) reveals that both parentheses on the left hand side are pure imaginary so that their product is real, as is N^2 . The solution for β_0 must therefore be real, conforming to the physical reality of absence of leakage.

If the NRD guide is now perturbed by terminating the parallel plates at a distance d from the air-dielectric interface, Z_a'' and Y_a' become Z_a'' and Y_a' , the arrows meaning that these immittances are not the characteristic ones but the equivalent impedance and admittance of the radiating open ends, seen through a length of transmission line. Z_a'' and Y_a' are now complex numbers that will produce a complex solution, denoted by

$$\beta = (\beta_0 + \Delta\beta) - j\alpha; \alpha, \Delta\beta \text{ small} \quad (3.60)$$

We therefore seek a solution of the form (3.60) for the equation

$$[\tilde{Z}''(\beta) + Z''_a(\beta)] [\tilde{Y}'(\beta) + Y'_a(\beta)] = N^2(\beta) \quad (3.61)$$

Solution of (3.61) by the perturbation procedure is equivalent to its linearization. Both sides of (3.61) are expanded around β_0 , the propagation constant of the unperturbed guide, and terms of order higher than the first are disregarded. We thus obtain

$$\begin{aligned} Z''(\beta_0) Y'(\beta_0) + \left[\left(\frac{d}{d\beta} Z'' \right) \Big|_{\beta_0} Y'(\beta_0) + Z''(\beta_0) \left(\frac{d}{d\beta} Y' \right) \Big|_{\beta_0} \right] d\beta = \\ N^2(\beta_0) + \frac{dN^2}{d\beta} \Big|_{\beta_0} d\beta \end{aligned} \quad (3.62)$$

where $Z''(\beta_0)$ and $Y'(\beta_0)$ stand for

$$\begin{aligned} Z''(\beta_0) &= \tilde{Z}''(\beta_0) + Z''_a(\beta_0) \\ Y'(\beta_0) &= \tilde{Y}'(\beta_0) + Y'_a(\beta_0) \end{aligned} \quad (3.63)$$

respectively. Solving for $d\beta$ in (3.62), one finds

$$d\beta = - \frac{Z''(\beta_0) Y'(\beta_0) - N^2(\beta_0)}{\tilde{Z}''(\beta_0) \Big|_{\beta_0} Y'(\beta_0) + Z''(\beta_0) \Big|_{\beta_0} \tilde{Y}'(\beta_0) - N^2(\beta_0) \Big|_{\beta_0}} \quad (3.64)$$

where the derivatives with respect to β are denoted by a dot on top of the corresponding magnitudes, the taking of the derivatives being prior to the evaluation of them at β_0 .

A more detailed elaboration of (3.64) allows the writing of

$$\Delta\beta - j\alpha = - \frac{(\dot{Z}_i^u + Z_a''(1 + \delta)) (\dot{Y}_i' + Y_a''(1 + \delta')) - N^2(\beta_0)}{(\dot{Z}_i^u + \dot{Z}_a'')_{\beta_0} \dot{Y}_i'(\beta_0) + \dot{Z}_i''(\beta_0) (\dot{Y}_i' + \dot{Y}_a'')_{\beta_0} - \frac{d}{d\beta} N^2} \quad (3.65)$$

where the new symbols are interpreted as

$$\dot{Z}_i^u |_{\beta_0} = j \frac{Z_i^u}{k_{yco}} \left[\frac{(\frac{\pi}{b})^2 - k_{yco}^2}{(\frac{\pi}{b})^2 + k_{yco}^2} \tan(k_{yco} \frac{b}{2}) + k_{yco} \frac{b}{2} (1 + \tan^2(k_{yco} \frac{b}{2})) \right] \left(- \frac{\beta_0}{k_{yco}} \right) \quad (3.66)$$

$$\dot{Y}_i' |_{\beta_0} = j \frac{Y_i'}{k_{yco}} \left[- \frac{(\frac{\pi}{b})^2 - k_{yco}^2}{(\frac{\pi}{b})^2 + k_{yco}^2} \cot(k_{yco} \frac{b}{2}) + k_{yco} \frac{b}{2} (1 + \cot^2(k_{yco} \frac{b}{2})) \right] \left(- \frac{\beta_0}{k_{yco}} \right)$$

$$\dot{Z}_a'' |_{\beta_0} = Z_a''(\beta_0) \left[\frac{b}{2} \frac{(\beta_0 \frac{b}{2})}{|k_{yco}|^2 (\frac{b}{2})^2} \frac{(\frac{\pi}{b})^2 + |k_{yco}|^2}{(\frac{\pi}{b})^2 - |k_{yco}|^2} \right] = Z_a''(\beta_0) W(\beta_0) \quad (3.67)$$

$$\dot{Y}_a'' |_{\beta_0} = Y_a''(\beta_0) \left[\frac{b}{2} \frac{(\beta_0 \frac{b}{2})}{|k_{yco}|^2 (\frac{b}{2})^2} \frac{(\frac{\pi}{b})^2 + |k_{yco}|^2}{(\frac{\pi}{b})^2 - |k_{yco}|^2} \right] = Y_a''(\beta_0) W(\beta_0)$$

$$\frac{dN^2}{d\beta} = \frac{1}{\beta_0} \left[2N^2\beta_0^2 \left(\frac{1}{\beta_0^2} + \frac{2}{k_0^2 - \beta_0^2} + \frac{2}{\epsilon_r k_0^2 - \beta_0^2} \right) \right] \quad (3.68)$$

and

$$1 + \delta(\beta_0) = \frac{jZ_a'' + Z_L'' \cot(k_{yco} d)}{Z_a'' \cot(k_{yco} d) + jZ_L''} |_{\beta_0} \quad (3.69)$$

$$1 + \delta'(\beta_0) = \frac{jY_a'' + Y_L'' \cot(k_{yco} d)}{Y_a'' \cot(k_{yco} d) + jY_L''} |_{\beta_0}$$

where Z_L'' and Y_L' have already been given in (3.49) and (3.50). The terms in δ'' , δ'' , δ' , and δ' have been neglected in the denominator of (3.65). They have been found small in all cases considered here, and their inclusion would unnecessarily complicate the formulation.

It is clear now that the denominator of (3.65) is real and therefore that (3.65) can be separated into real and imaginary parts in a simple manner. After use of (3.57), we can write

$$\Delta\beta = - \frac{(Y_2' / (\bar{Y}_2' + Y_2')) \delta_1' + (Z_2'' / (\bar{Z}_2'' + Z_2'')) \delta_1''}{(\bar{Z}_2'' + Z_2'') / (\bar{Z}_2'' + Z_2'') + (\bar{Y}_2' + Y_2') / (\bar{Y}_2' + Y_2')} - \frac{N^2}{N^2} \quad (3.70)$$

$$\alpha = - \frac{(Y_2' / (\bar{Y}_2' + Y_2')) \delta_1' + (Z_2'' / (\bar{Z}_2'' + Z_2'')) \delta_1''}{(\bar{Z}_2'' + Z_2'') / (\bar{Z}_2'' + Z_2'') + (\bar{Y}_2' + Y_2') / (\bar{Y}_2' + Y_2')} - \frac{N^2}{N^2} \quad (3.71)$$

where $\delta_1' = \delta_{1r}' + j\delta_{1i}'$ and $\delta_1'' = \delta_{1r}'' + j\delta_{1i}''$.

There are several important features embodied in the last two equations, namely:

a) The fact that they yield $\Delta\beta$ and α in an explicit fashion permits one to assess easily the influence of the different geometrical and constitutive parameters.

b) The effect of the open end discontinuity, which is included in δ_1' and δ_1'' , is clearly separated from other elements of the network.

c) The relative contributions of the $E^{(z)}$ -type and $H^{(z)}$ -type modes in the expression for the attenuation constant α are given by

$$\left[Y_1' / (\bar{Y}_1' + Y_1') \right] \delta_1' \quad \text{and} \quad \left[Z_2'' / (\bar{Z}_2'' + Z_2'') \right] \delta_2''$$

d) If the only parameter changed is d , the attenuation is linearly dependent on it since the δ 's depend exponentially on this parameter through terms of the form $\cot(k_{ya} d)$, as can be seen from equations (3.69).

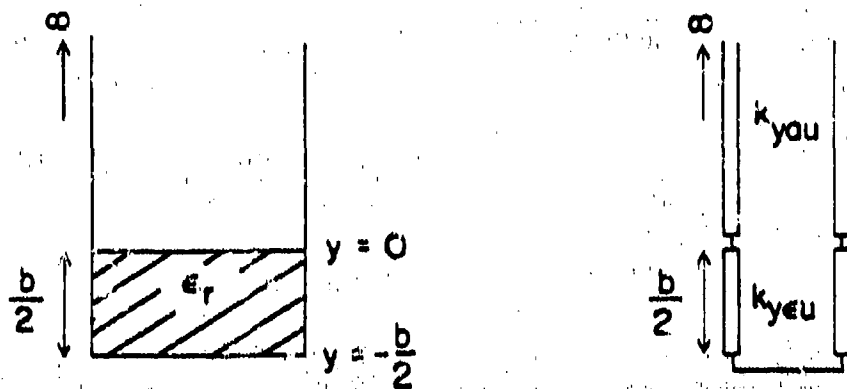
2. Simpler, Reflection Coefficient, Procedure

A simpler perturbation relation will be derived next, and it also is based on the symmetrical structure of Fig. 3.8(b). The unperturbed structure is again the nonradiating symmetrical NRD guide, with its side walls going to infinity. The perturbed structure is that of Fig. 3.8(b). The difference now is that we begin with a single transmission line supporting a TM mode in the y direction, rather than the two transmission lines supporting the $E^{(z)}$ -type and $H^{(z)}$ -type modes. The latter representation was rigorously correct in both the perturbed and unperturbed situations, whereas the former approach, employing only a single mode, is exact only for the unperturbed geometry, and approximate for the perturbed one. We expect, therefore, that the resulting expression will be simpler but less accurate.

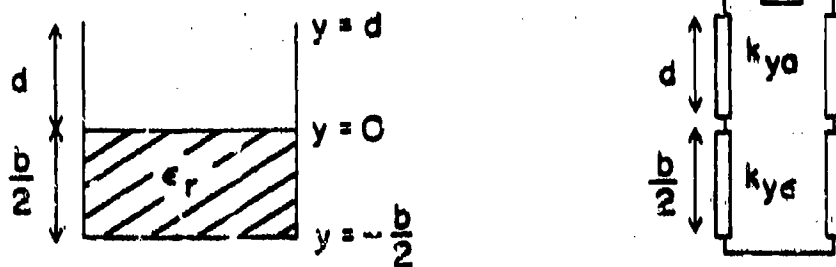
We also employ a different phrasing, one that begins directly with a perturbation relation:

$$\frac{\Delta Z'(-b/2)}{1 - [Z'_u(-b/2)]^2} = \frac{\Delta Y'(0)}{1 - [Y'_u(0)]^2} + j \frac{b}{2} \Delta k_y \quad (3.72)$$

The quantities in this relation are explained in terms of the unperturbed and perturbed transverse equivalent networks shown in Figs. 3.9 (a) and (b), respectively. The subscript u refers to unperturbed quantities, the primes signify quantities normalized to their characteristic immittances, and the



(a) unperturbed case



(b) perturbed case

Fig. 3.9 (a) Cross section of bisected nonradiating NRD guide and its transverse equivalent network, which is used as the unperturbed case in a perturbation analysis, and (b) Cross section of bisected radiating structure in Fig. 3.8(b), and an approximate transverse equivalent network for it that uses only one transmission line.

Δ 's describe directly the changes between the perturbed and unperturbed situations. The location $y = -b/2$ refers to the short-circuit bisection plane, $y = 0$ to the air-dielectric interface (which is a simple junction here because a TM (or E) mode is used now, rather than E-type or H-type modes), and $y = d$ corresponds to the location of the radiating open end in the perturbed case. The perturbation relation (3.72) applies to the dielectric-filled region.

In (3.72), $Z_{\text{u}}'(-b/2) = 0$, because the plane at $y = -b/2$ is a short-circuit plane; similarly, $\Delta Z'(-b/2) = 0$ because the plane remains a short circuit after the perturbation because of symmetry.

The term $Y_{\text{u}}'(0)$ is seen from Fig. 3.9(a) to be

$$Y_{\text{u}}'(0) = \frac{Y_{\text{a}}(0)}{Y_{\text{d}}} = \frac{Y_{\text{a}}}{Y_{\text{d}}} \quad (3.73)$$

which is just the ratio of characteristic admittances for the air and dielectric regions. For $\Delta Y'$, we write

$$\Delta Y'(0) = Y'(0) - Y_{\text{u}}'(0) \quad (3.74)$$

Thus, we need to know $Y'(0)$, where the termination at $y = d$ has been changed. We then write

$$Y'(b/2) = \frac{Y(b/2)}{Y_{\text{a}}} \approx \frac{Y(b/2)}{Y_{\text{d}}} \quad (3.75)$$

However, we know that

$$\frac{Y(b/2)}{Y_{\text{d}}} = \frac{1 - \Gamma(b/2)}{1 + \Gamma(b/2)} \quad (3.76)$$

where $\Gamma(b/2)$ is the input reflection coefficient at $y = b/2$ in the air region, and is related to $\Gamma(d)$ by

$$\Gamma(b/2) = \Gamma(d) e^{-2\beta_{\text{a}}(d-b/2)} \quad (3.77)$$

where

$$k_{ye} \approx -j |k_{ye}| \quad (3.78)$$

We therefore rephrase (3.77) as

$$\Gamma(b/\beta) \approx \Gamma(d) e^{-2|k_{ye}|(d-b/\beta)} \quad (3.79)$$

where $\Gamma(d)$ is the reflection coefficient at the radiating open end for the lowest TM (or E) mode.

Relation (3.79) can next be inserted into (3.76) which then becomes

$$\frac{Y(0)}{Y_0} = \frac{1 - \Gamma(d) e^{-2|k_{ye}|d}}{1 + \Gamma(d) e^{-2|k_{ye}|d}} \quad (3.80)$$

But $\Delta Y'(0)$ can be rephrased, on use of (3.75), as

$$\begin{aligned} \Delta Y'(0) &= \frac{Y(0)}{Y_{cs}} - \frac{Y_0}{Y_{cs}} = \frac{Y(0)}{Y_0} \frac{Y_0}{Y_{cs}} - \frac{Y_0}{Y_{cs}} \\ &= \frac{Y_0}{Y_{cs}} \left[\frac{Y(0)}{Y_0} - 1 \right] \end{aligned} \quad (3.81)$$

Inserting (3.80) into (3.81) yields

$$\Delta Y'(0) = -2 \frac{Y_0}{Y_{cs}} \left[\frac{\Gamma(d) e^{-2|k_{ye}|d}}{1 + \Gamma(d) e^{-2|k_{ye}|d}} \right] \quad (3.82)$$

Now that we have all the separate pieces we may return to (3.72) and insert (3.73) and (3.82) into it. We then obtain

$$\frac{\Delta k_{ye}}{k_{ye}} = -j \frac{2 Y_0 / Y_{cs}}{(k_{ye} b / \beta) [1 - (Y_0 / Y_{cs})^2]} \left[\frac{\Gamma(d) e^{-2|k_{ye}|d}}{1 + \Gamma(d) e^{-2|k_{ye}|d}} \right] \quad (3.83)$$

For TM (or E) modes, we have

$$\frac{Y_u}{Y_{ca}} = j \frac{k_{yca}}{\epsilon_r |k_{yca}|} \quad (3.84)$$

Use of (3.84) in (3.83) yields, finally,

$$\frac{\Delta k_{y\epsilon}}{k_{yca}} = \frac{2\epsilon_r |k_{yca}|}{(b/\beta) [\epsilon_r^2 |k_{yca}|^2 + k_{yca}^2]} \left[\frac{\Gamma(d) e^{-2|k_{yca}|d}}{1 + \Gamma(d) e^{-2|k_{yca}|d}} \right] \quad (3.85)$$

The expression for $\Gamma(d)$ to be used in (3.85) is the Γ_V'' in (3.48) since the H-type mode reduces to a TM mode in the limit.

The perturbed value of $k_{y\epsilon}$ is given by

$$k_{y\epsilon} = k_{yca} + \Delta k_{y\epsilon} \quad (3.86)$$

and it is related to the perturbed complex propagation wavenumber, namely,

$$k_z = \beta_u + \Delta\beta - j\alpha \quad (3.87)$$

by the sum of squares relation

$$k_z^2 = k_y^2 + k_x^2 + k_{y\epsilon}^2 \quad (3.88)$$

(β_u here is of course the same as β_o in Sec. B, 1.) The result (3.85) thus yields $\Delta k_{y\epsilon}$, which is placed into (3.86) and then into (3.88), from which the final β and α values, via (3.87), are obtained.

3. Comparisons with Accurate Analysis

Numerical calculations of the values of α and $\Delta\beta$ have been made using the two perturbation procedures derived above, and these results have been

compared with corresponding calculations made by means of the accurate theory discussed in Sec. A. In general, the comparisons indicate that the perturbation expressions are rather good. They are less valid near cutoff or when the leakage is quite strong. This last comment is especially true for the simpler formulation described in Sec. B, 2.

The next few figures indicate the comparisons found between the almost-rigorous theory and the more accurate perturbation formulation derived in Sec. B, 1. In Fig. 3.10, such a comparison is presented for values of α and β as a function of d , the distance between the air-dielectric interface and the radiating open end. The perturbation result, identified by the dashed line, is seen to track the almost-rigorous result very well over the whole range of α values. The deviation is slightly greater for values of d less than about 2 mm, where the values of α become large; similar behavior is found for β .

Comparisons as a function of plate spacing a are given in Fig. 3.11. The agreement for β is seen to be quite satisfactory over a large range of values of a/λ_0 ; near to cutoff and to the slow-wave region, the agreement begins to worsen. This behavior near the two ends is more pronounced for α , where the agreement is very good only over the central region.

The next comparisons are shown in Fig. 3.12 for variations as a function of b , the width of the dielectric strip. Here, the agreement for β is seen to be very good everywhere, and to be quite satisfactory for α over a wide range of values. The agreement worsens somewhat as α becomes large.

The comparisons as a function of ϵ_r appear in Fig. 3.13. The agreement for β is good over most of the range, but it gets noticeably less good as one approaches cutoff at one end and the onset of the slow-wave region, at $\beta/k_0 = 1$, at the other end. For α , a discrepancy of several percent between the perturbation and almost-rigorous results occurs for quite a range of values away from cutoff, and again near the slow-wave region.

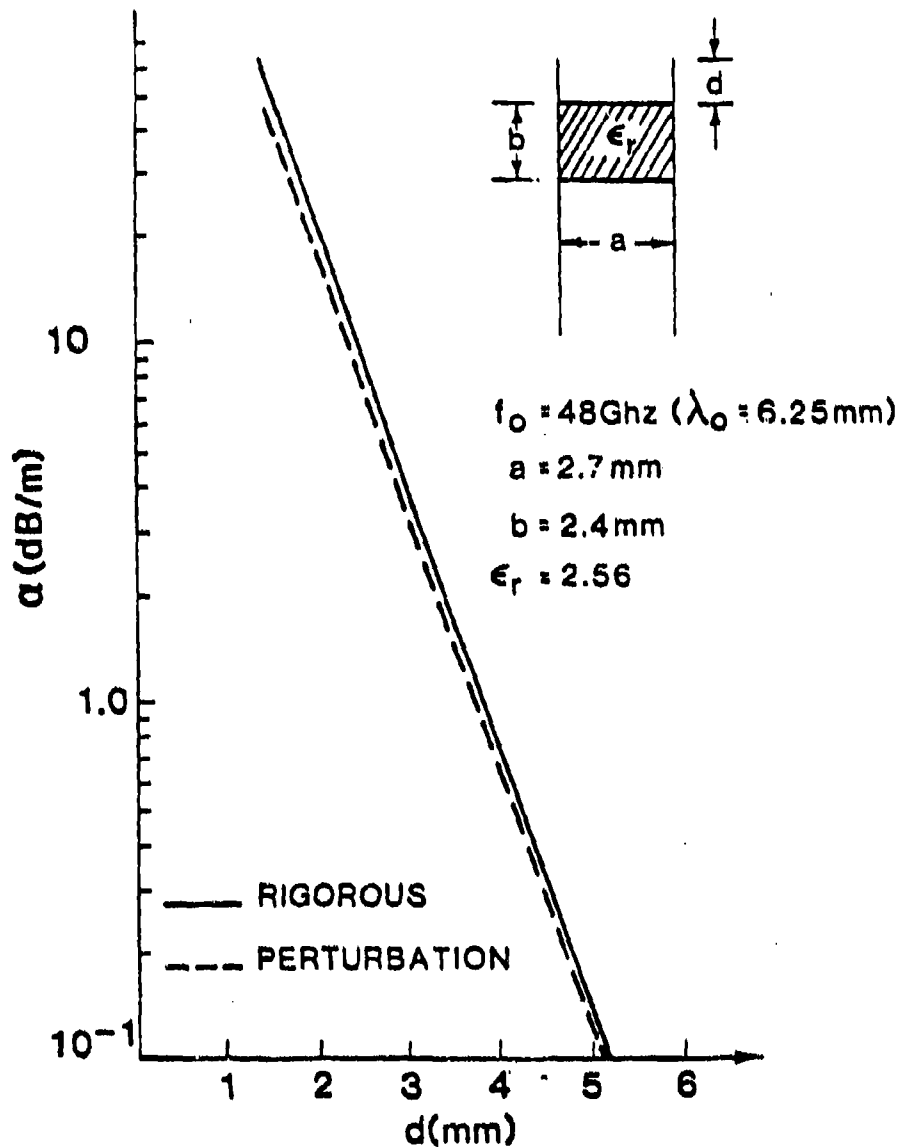
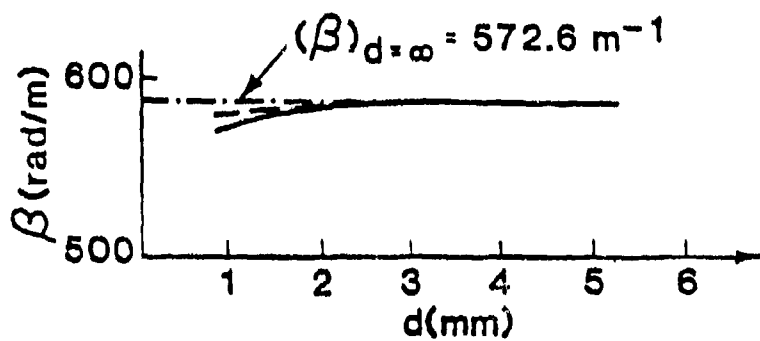


Fig. 3.10 Comparisons of results between the almost-rigorous theory and the first perturbation procedure for β and α as a function of d , the distance between the air-dielectric interface and the radiating open end.

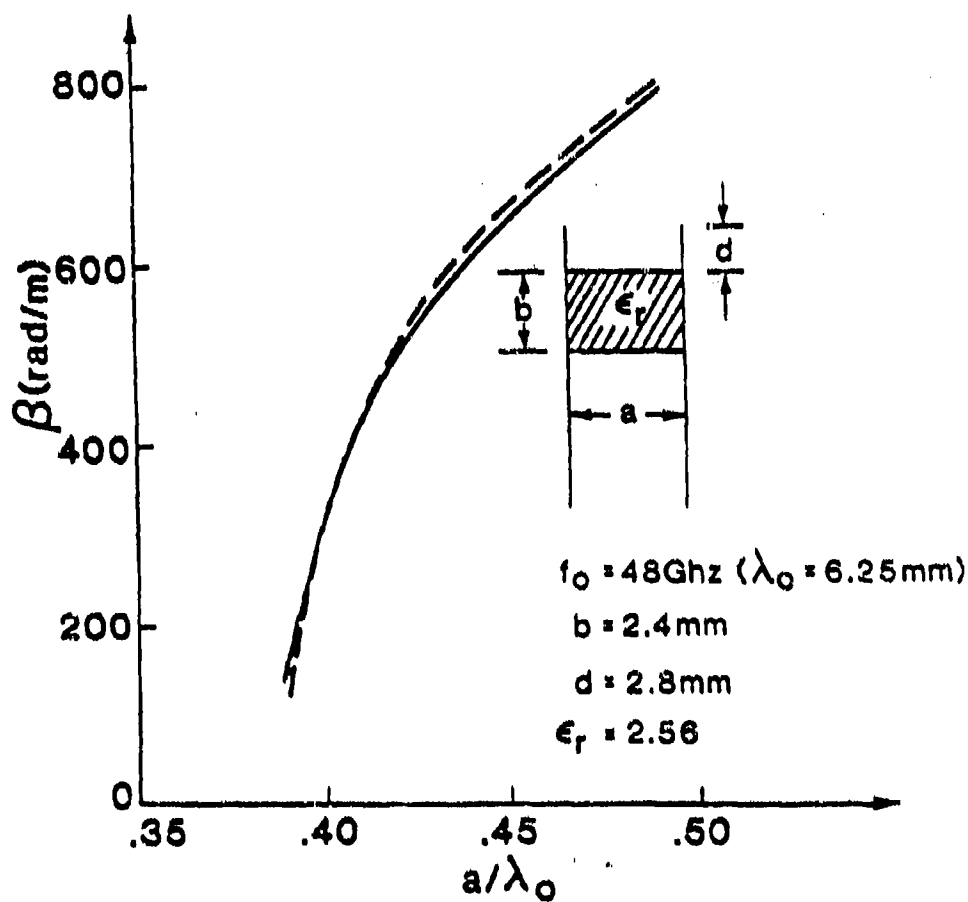
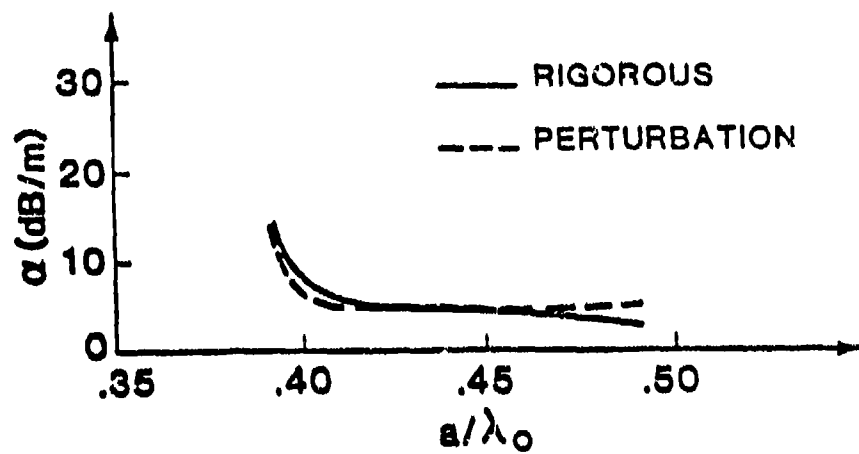


Fig. 3.11 Comparisons of results between the almost-rigorous theory and the first perturbation procedure for α and β as a function of plate spacing a .

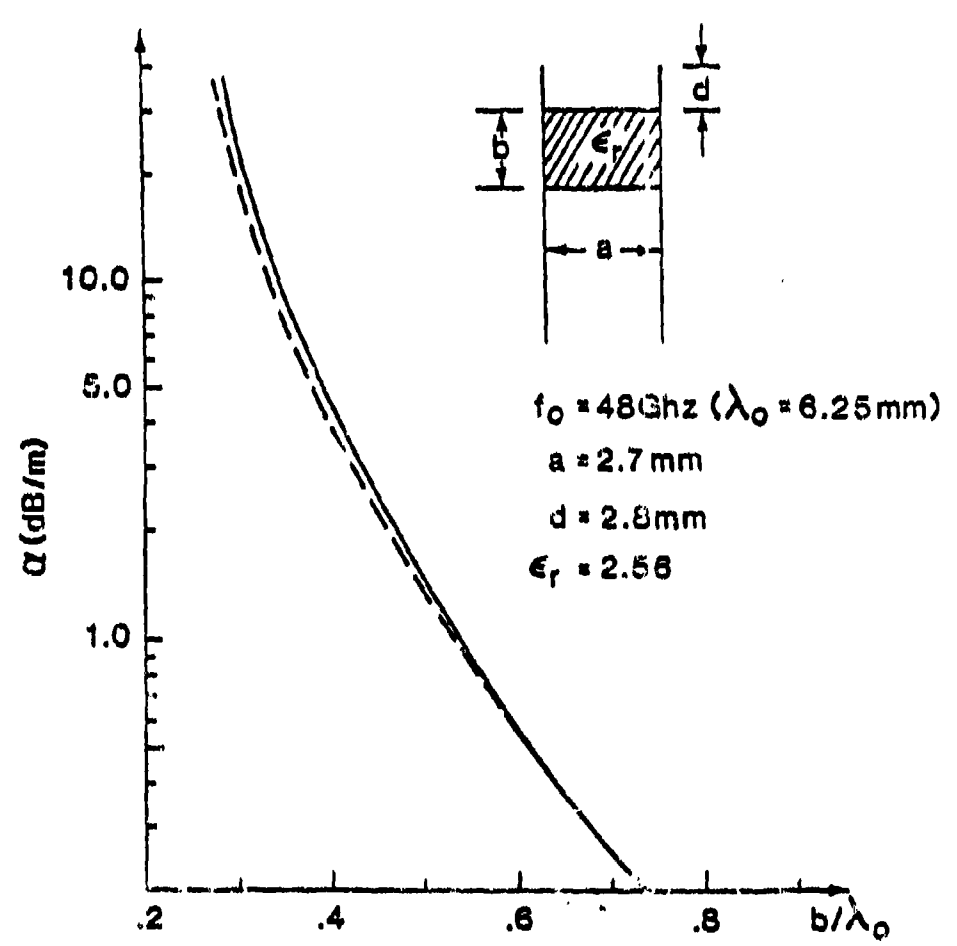
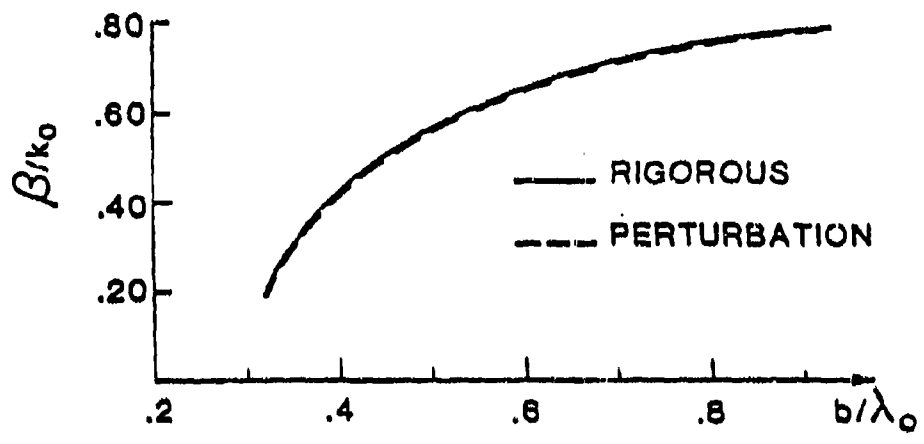


Fig. 3.12 Comparisons of results between the almost-rigorous theory and the first perturbation procedure for β and α as a function of the dielectric strip thickness b .

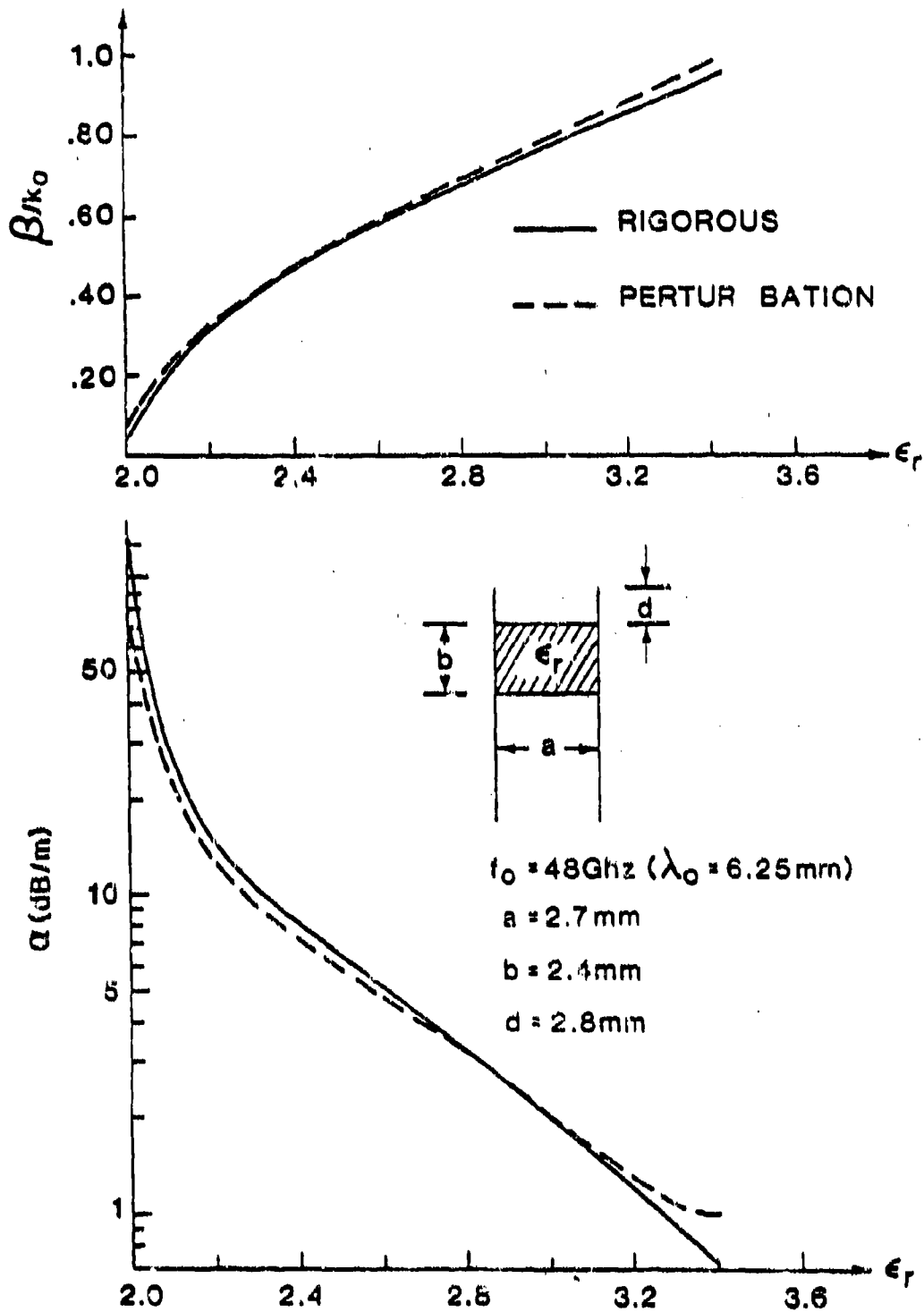


Fig. 3.13 Comparisons of results between the almost-rigorous theory and the first perturbation procedure for β and α as a function of the relative dielectric constant ϵ_r of the dielectric strip.

Even in Fig. 3.13, where the agreement is probably the worst, the perturbation results are certainly sufficiently good that they can be used for preliminary designs.

A comparison that illustrates how good the simpler perturbation procedure is appears in Fig. 3.14. The simpler perturbation method is the one derived in Sec. B, 2. That comparison, for α as a function of b , reveals some interesting behavioral differences between the two perturbation results. The procedure possessing greater rigor (the dashed line, corresponding to the theory in Sec. B, 1) tracks the almost-rigorous result quite well over a very wide range of values. The simpler method (points, corresponding to the theory in Sec. B, 2) appears to produce better agreement with the almost-rigorous theory than the other perturbation procedure when the values α are small. However, for larger values of α , the deviation from the almost-rigorous values is significantly greater for the simpler formulation. We have also found from other calculations that the simpler procedure becomes much poorer as cutoff is approached. However, if one stays far from cutoff, and is concerned with small values of α , the simpler perturbation formulation yields very good agreement with the almost-rigorous results.

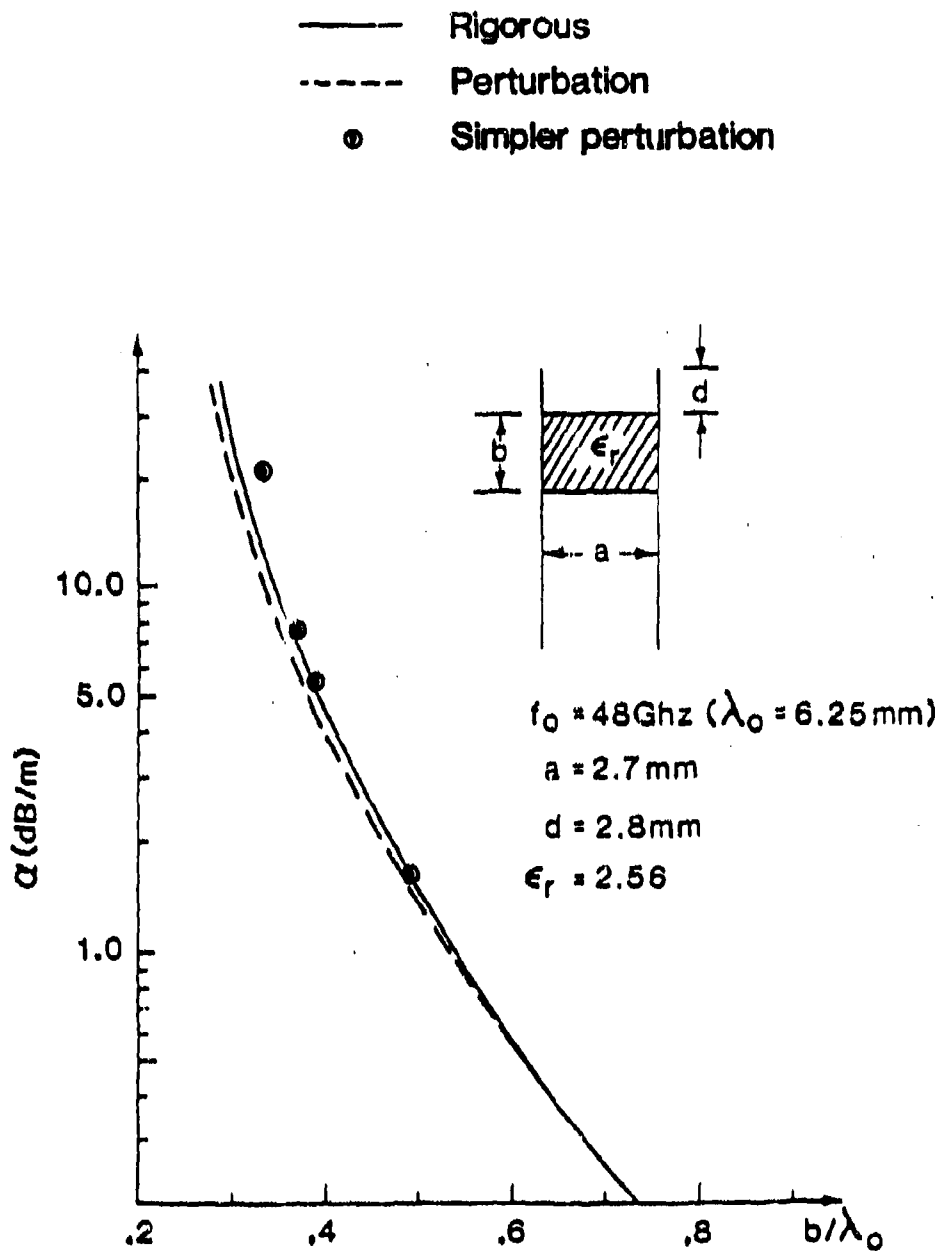


Fig. 3.14 Results comparing three theories: the almost-rigorous theory, the first perturbation procedure, and the second, simpler, perturbation procedure.

C. THE FORESHORTENED-TOP ANTENNA: MEASUREMENTS

It was mentioned earlier that a measurement phase was introduced into this research program even though the original contract did not call for any measurements. Before we discuss any of the measurement procedures or results, therefore, we should indicate why those measurements were taken.

A structure somewhat similar to ours was analyzed theoretically some years ago in Japan, and then measurements were made there to verify their theory. The structure was an H guide that was symmetrical and radiated from both ends, so that it is somewhat simpler than ours. (It is also not as versatile, and it produces unwanted radiation at every bend and junction.) However, our theory applies to that structure also, and we made calculations to compare with those made in Japan by Shigesawa and Takiyama [33-35]. The comparisons between our theory and their theory and measurements are shown in Fig. 3.15.

It is seen that the agreement between their theoretical and measured results is not bad, but that our theoretical values differ rather significantly from either their theory or their measurements, with discrepancies appearing that are almost a factor of two. These differences produced concern on our part.

We examined both their theoretical approach and their experimental procedure, and we found that both were subject to question. Two different theoretical approaches were used, and both were approximate. In one case, the radiating open end was treated in a Kirchhoff procedure, and in the second case, which is the one shown in Fig. 3.15, which yielded better agreement with their measurements, the parallel plate region was approximated by an elliptic cylinder. The measurements were also approximate, and open to question. They were insertion loss measurements, where a length of the antenna was placed between input and output rectangular waveguides. The input and output sections were connected to the radiating section by tapers, and the total power loss was measured. This

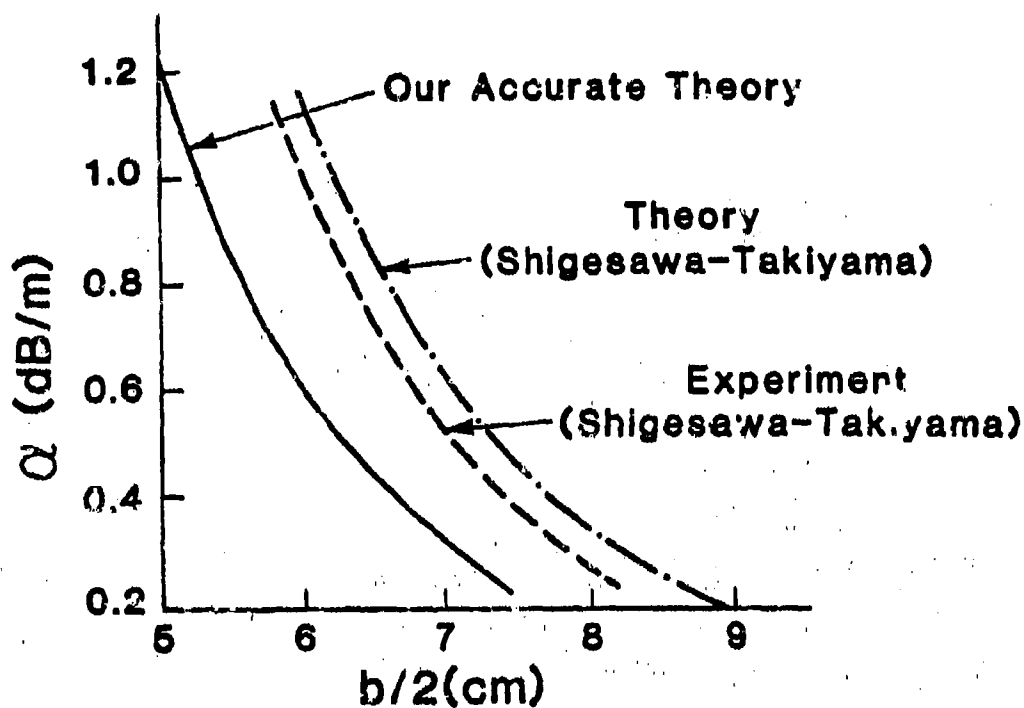


Fig. 3.15 Comparisons between our theoretical calculations and theoretical and measured results reported by Shigesawa and Takiyama on their structure.

total power loss was composed of three contributions: the actual leakage power, the intrinsic loss due to the metal and the dielectric material, and radiation (coupling losses) from the tapered junctions between the radiating section and the input and output sections. Approximate calculations were made for the metal and dielectric losses, and these values were subtracted from the total measured loss. The coupling loss was not taken into account, however. The amount of that loss is unknown, but it could be significant in view of the geometry involved.

Although neither their theory nor their measurements could be regarded as accurate, and the agreement between them could be fortuitous, we were nevertheless concerned because we could have made some inadvertent error in either our analysis or in our computer program. We therefore undertook

an experimental phase in our program, but we also designed the measurement procedure so as to avoid the possible errors introduced into the earlier measurements.

As stated in the introduction to Part III, we found later that our theoretical values were indeed correct, and that the early Japanese results were in error. Our theoretical values were confirmed experimentally in two ways. The first involved our own measurements, and the second was the result of independent measurements kindly taken by Prof. T. Yoneyama of Japan at our request. In Sec. C, 1, we describe our measurement procedure, with its advantages and possible pitfalls. The procedure employed by Yoneyama, and the results he obtained, are discussed in Sec. C, 2. The results of our own extensive measurements, and how they compare with our theoretical values, are presented in Sec. C, 3.

We should add only three points here:

(a) Both our measurements and those made by Yoneyama consisted of direct probe measurements along the length of the antenna aperture. The contributions from the intrinsic metal and dielectric losses were measured and subtracted out in both cases. The measurement method is therefore direct, and should yield accurate results.

(b) Yoneyama's measurements were taken at 50GHz, in the millimeter wave range. Our measurements were made in the frequency range between 10 GHz and 11 GHz, where the structures were scaled up in size to permit greater fabrication accuracy. We also took many more measurements than Yoneyama did.

(c) Both our measurements and those of Yoneyama showed very good agreement with our theoretical values, as we demonstrate in Secs. C, 2 and 3.

1. Measurement Procedure

In this section, we describe the set-up and measurement procedure employed in our own measurements. The frequency was lowered to the X-band range so that a structure with a larger cross section could be built for these measurements, thus assuring better accuracy. The only difficulty with scaling to a lower frequency is that the structure must then be made longer and the probing occur over a physically longer region.

The leaky structure has the cross section shown in Fig. 2(a) in Sec. A, 1, and it was made uniform along most of its length. The probe measurements were made along this uniform region. At its input end, the leaky structure was connected in a tapered fashion to rectangular waveguide, and, at its output end, it was originally bent gradually away from the radiating open end and terminated in lossy material meant to approximate a matched load. In a later, more sophisticated set-up, a taper was built into the output end identical to the one at the input end, and then followed by a true matched load.

The leaky structure was about 2.0 meters long, and was fabricated out of two architectural aluminum right angles of very rigid stock placed parallel to each other, and with the dielectric strip located appropriately between them. The dielectric strip was cut from a polystyrene rod (Stycast 0005, with $\epsilon_r = 2.56$ and $\tan\delta = 0.0005$). The separation between the plates was selected to be $a = 0.500$ inch to insure that the basic guide is nonradiative ($a/\lambda_0 > 1/2$) in the frequency range of our measurements, and yet to have low metallic losses. The dielectric strip thickness was made $b = 0.378$ inch so that only the lowest mode of the proper polarization can propagate. The relative dimensions chosen here were proposed by Yoneyama and Nishida in their first paper on NRD guide [2].

Spacers between the plates were placed well below the dielectric strip (on the nonradiating side) and along the length of the structure to keep the separation between plates constant and to hold the dielectric strip tightly. The spacers were located sufficiently far below the dielectric strip that they negligibly affected the fields.

The tapered feed end was designed very carefully so as to be nonradiating and also symmetrical, so that only the polarization desired would be present in the leaky structure. The feed arrangement consisted of three separate tapers in succession to insure that these requirements would be satisfied without undue fabrication difficulties. Maintaining symmetry is very important because actually three NRD guide modes can propagate in the frequency range of the measurements. These three modes are the desired mode with E vertical and two modes with H vertical; the latter two consist of the lowest mode, with no variation of field between the plates, and the next mode with a half-sine variation there. The cutoff frequencies of these three modes are, respectively, $f = 9.67$ GHz, $f = 0$ and $f = 8.74$ GHz. If any asymmetry is present in the feed tapers, therefore, the incident wave from the rectangular feed guide would excite in the leaky structure not only the desired mode with E vertical, but the other two as well, thereby introducing a strong interference pattern along the leaky structure itself, and substantial cross polarization in the radiated field.

In addition to the leaky structure itself, we require a probe arrangement to be responsive to the square of the electric field amplitude, and to be moveable along the length of the radiating aperture. A miniature coaxial probe with an extended center conductor, and with the outer conductor covered with absorbing material, was introduced into the radiating end of the cross section; it was maintained at a constant distance from the metallic plates as it was moved down the structure by means of a heavy gear arrangement. At first, we introduced the probe from the other (nonradiating) end of the cross section because the probe would then not perturb the radiation. The probe then samples the evanescent field beneath the dielectric strip. The approach was valid in concept but it turned out to be too sensitive, since the probe was located in a field that was exponentially decaying at a rapid rate.

A block diagram of the complete set-up is shown in Fig. 3.16. If one were to make probe measurements alone, it would not be necessary to have another transition after the leaky guide nor to have the two power meters

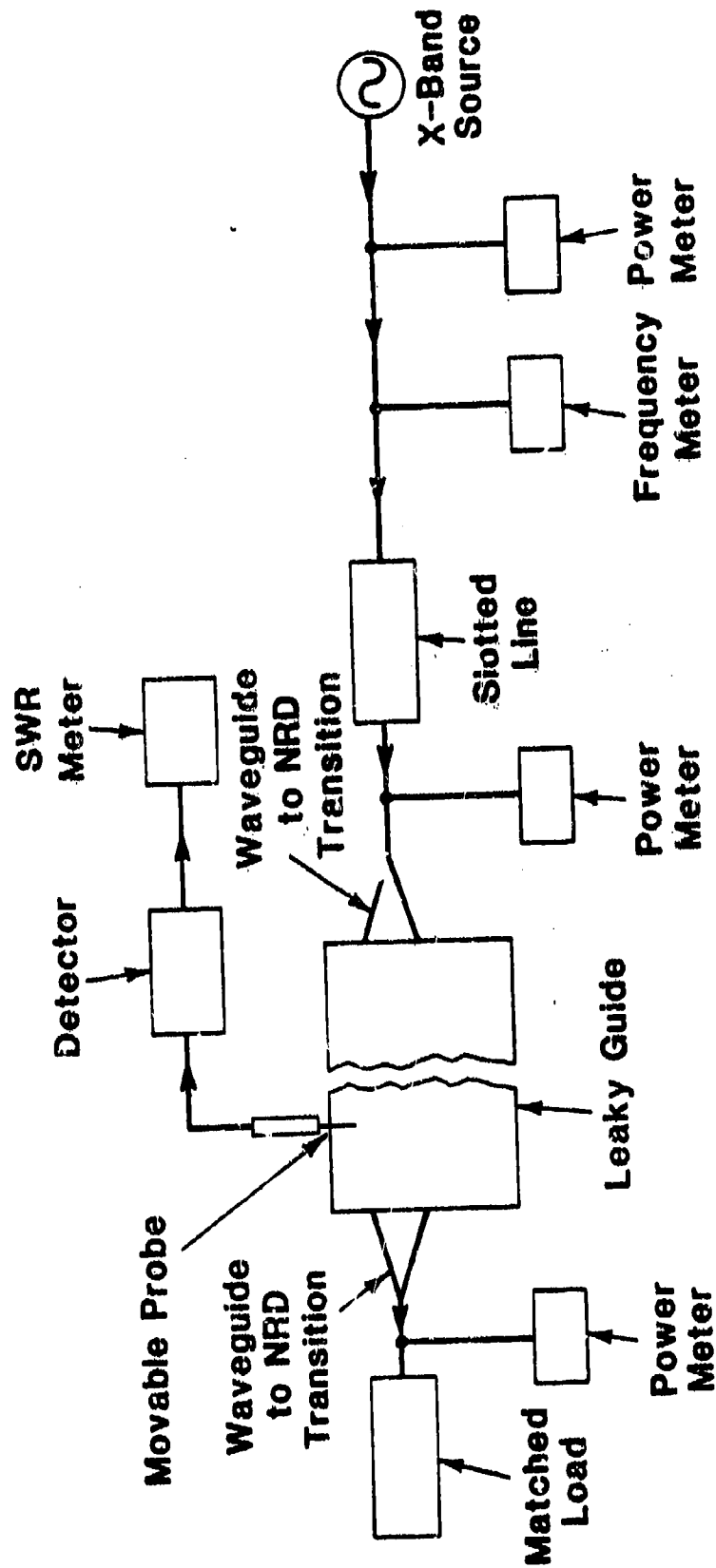


Fig. 3.16 Block diagram of experimental set-up for the probe measurement of the leakage constant of foreshortened-top NRD guide.

before and after the two transitions. The additional transition and power meters were placed there in order to permit us to take insertion loss measurements, as a back-up in case the probe measurements were not successful. It turned out that the probe results were very good, and we therefore did not conduct any insertion loss measurements.

The measurement procedure consists of probing the amplitude of the leaky wave along the length of the leaky structure, and therefore the aperture of the leaky wave antenna. When the structure is longitudinally uniform, as in these measurements, the value of α is readily determined from a semilog plot of the probe output as a function of position along the leaky structure. The value of α is then 1/2 of the measured slope on the semilog plot.

An example of such a semilog plot is given in Fig. 3.17; actually, this is a linear plot of the power in dB, but it is equivalent. These data hold for a specific frequency, $f = 10.20$ GHz, and for a specific distance between the air-dielectric interface and the radiating open end, $d = 0.25$ inch. The other parameters are as given above: $a = 0.500$ inch, $b = 0.378$ inch and $\epsilon_r = 2.56$. The whole probe run thus corresponds to a single set of dimensions at only one frequency.

It is also seen that the actual data correspond to a rippled curve, because of some spurious mode conversion or reflections from the end or what have you. It is not that regular, so that it is a mixture of several contributions, and it cannot be eliminated entirely. On the other hand, the straight line that must be drawn through its average can be determined quite accurately.

Different values of d were obtained by shifting the position of the dielectric strip relative to the radiating open end. The values of d chosen were $d = 0.150, 0.200, 0.250, 0.300,$ and 0.378 , all in inches. The values of a, b and ϵ_r were maintained the same. Also, for each setting of d , measurements were taken at a series of frequencies: $10.1, 10.2, 10.4, 10.6,$ and 10.8 , all in GHz. For each of these 25 different combin-

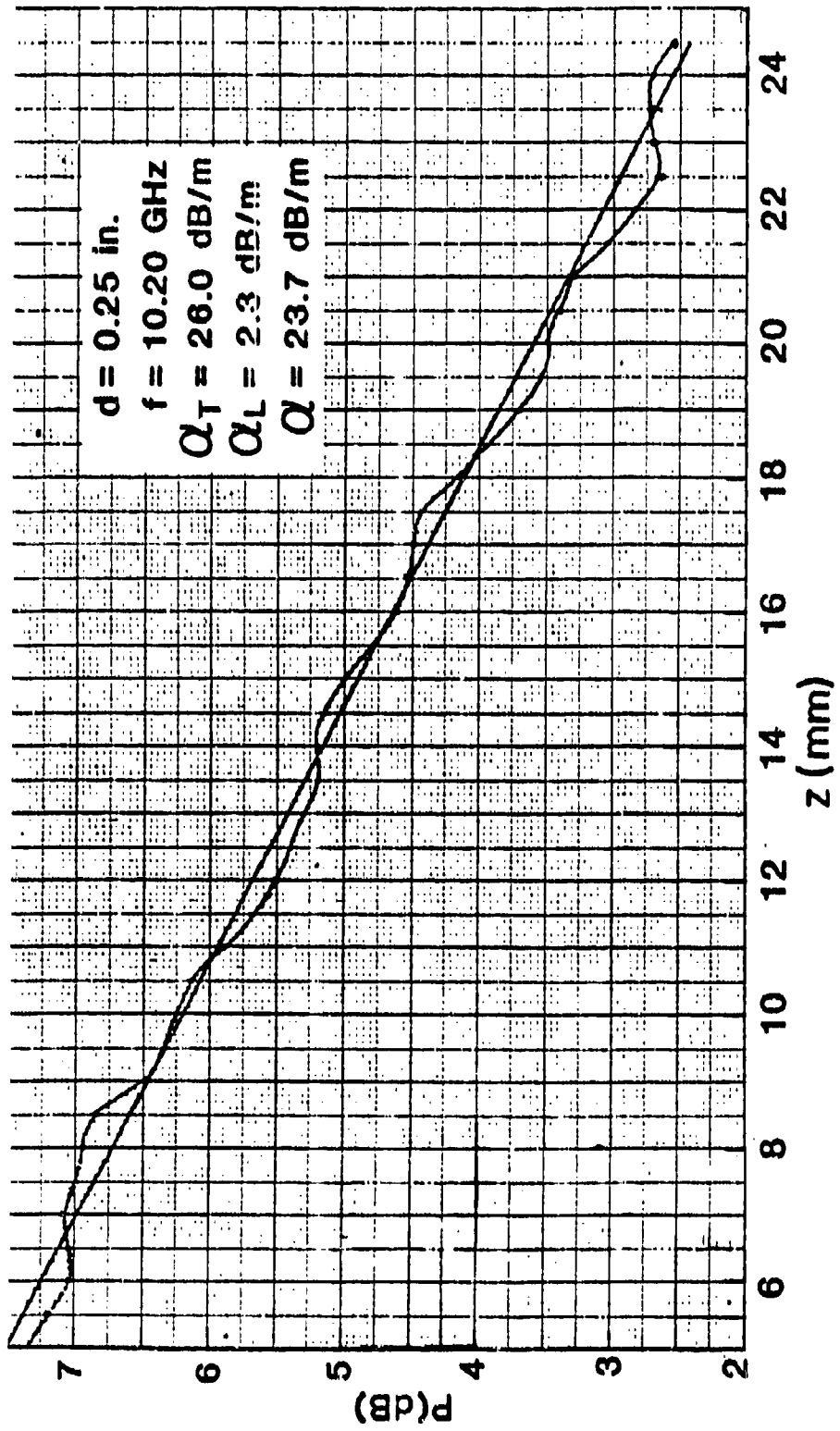


Fig. 3.17 Typical semilog plot of the probe pickup ($|E|^2$) as a function of position along the length of the radiating aperture. A separate plot of this type was obtained for every frequency and every change in guide dimensions.

ations, a plot similar to that in Fig. 3.17 was obtained, and the value of α was determined from the slope of the straight line through the average of the curve.

That value of α is the total loss α_T , to which we have two contributions: the leakage loss α , which we seek, and the intrinsic metal and dielectric loss α_L . The value of α_L for each of the selected frequencies was measured by applying the same procedure to the structure when d is made so large that no radiation results. Subtraction of the appropriate value of α_L from each determination of α_T yields the desired series of values of leakage constant α . In Fig. 3.17, the value of α_L is 2.3 dB/m compared to a measured value of 26.0 dB/m for α_T .

In the discussion above, we have described in some detail the basically straightforward measurement set-up that we designed, the feed taper being the only complicated and sophisticated part, and the simple and direct measurement procedure based on probing the field along the aperture length. Before moving on and describing the measurements taken by Yoneyama, we should mention some difficulties that arose in the early stages of our measurements. It is desirable to include some comments about these difficulties because they led both to our request to Prof. Yoneyama for measurements to be taken by him and to our recognition that the asymmetric leaky wave antenna described below in Sec. D should work well.

When we designed the first leaky structure, we did not have available a dielectric strip of sufficient thickness, but we did have many strips of half that thickness. We therefore took two strips and glued them together longitudinally, by placing dabs of some dielectric glue more or less periodically all along the length. The actual process was conducted by our machine shop personnel who said they had used this glue previously with success. We had no reason to suspect that any problem would arise, and we thought no more about it.

Although the design of the rest of the structure was conducted carefully, we encountered large ripples in the probe pattern and we found

cross-polarization effects everywhere, within the guide and in the radiated field. Nothing that we did improved matters much. We redesigned the feed taper, making it quite complex, with three independent successive taper sections, we refined the probe arrangement, we eliminated any possible gaps between metal and dielectric, and so on. All this took a great deal of time, but we were unable to locate the source of the problem. Although everything was maintained to be symmetrical, something was producing asymmetry with the resultant mode conversion and cross polarization. We finally discovered that the difficulty was due to the glue that was used to hold the two dielectric strips together longitudinally. Not only did the glue possess a different dielectric constant, but it seeped unevenly into the dielectric strips producing asymmetrical blobs.

We then purchased some new dielectric rods of larger diameter, and cut the strips from them. When we employed those new dielectric strips (without the need for glue), the situation improved dramatically. We were finally able to take decent measurements (Fig. 3.17 presents a sample), and we then did so in a short time.

During the period of difficulty and frustration, we met with Prof. Yoneyama at the International Microwave Symposium in Boston in June 1983; we described our research on the foreshortened-top leaky wave antenna, including both the theoretical and experimental aspects, and we described our measurement dilemma as well. We hinted that we would appreciate it if he could make such measurements for us, and he responded very favorably. It turned out that he was able to take such measurements rather quickly, and that they agreed well with our theory. Further details are given in the next section (C, 2).

During the process of examining all possible sources of asymmetry in our measurement structure, we noted that sometimes the dielectric strip separated from the metal walls, producing a small air gap. If the air gap occurs on only one side, producing asymmetry, then leakage of the opposite polarization is produced. In our set-up, such gaps were too small to cause much of a problem, and anyway no effect was noticed when the gaps

were closed. However, this observation led to the realization that a sufficiently large gap could form the basis of a new leaky wave antenna, of simple configuration, that radiates horizontal, instead of vertical, polarization. That structure is discussed in Sec. D.

2. Measurements Taken by Yoneyama

It was mentioned above that some measurements on the foreshortened-top leaky wave antenna were kindly taken at our request by Prof. T. Yoneyama of Tohoku University in Japan. Prof. Yoneyama, together with Prof. S. Nishida, had originally proposed the NRD guide in 1981, and he had designed many successful components in that guide type. He was therefore already set up to take the measurements we requested and he sent us the results within a short time [36]. We compared his measurements with our theory, found very good agreement, and then knew for sure for the first time that our results were correct and that those of Shigesawa and Takiyama (see Fig. 3.15) were wrong. The approximations in their theory were evidently not good ones, and the coupling losses that they neglected in their measurements must have been sizeable.

Yoneyama took measurements at only a single frequency, at $f = 50.0$ GHz in the millimeter wave range. The structure on which he took measurements, and the details of his feed arrangement, are shown in Fig. 3.18. He employed a directional coupler arrangement to excite one end of the antenna, so that the power picked up by the probe first increases over a short distance and then decreases in the expected exponential fashion.

A semilog plot for one of his cases is shown in Fig. 3.19, where the above-mentioned short rise appears. One sees that he also obtained a ripple, but he was able to draw a straight line through its average, and to deduce a value of α from it. He also measured the intrinsic (metal and dielectric) loss, and subtracted that value from the measured α value. The plot in Fig. 3.19 corresponds to our $d = 1.5$ mm (his d' in Fig. 3.18 is equal to

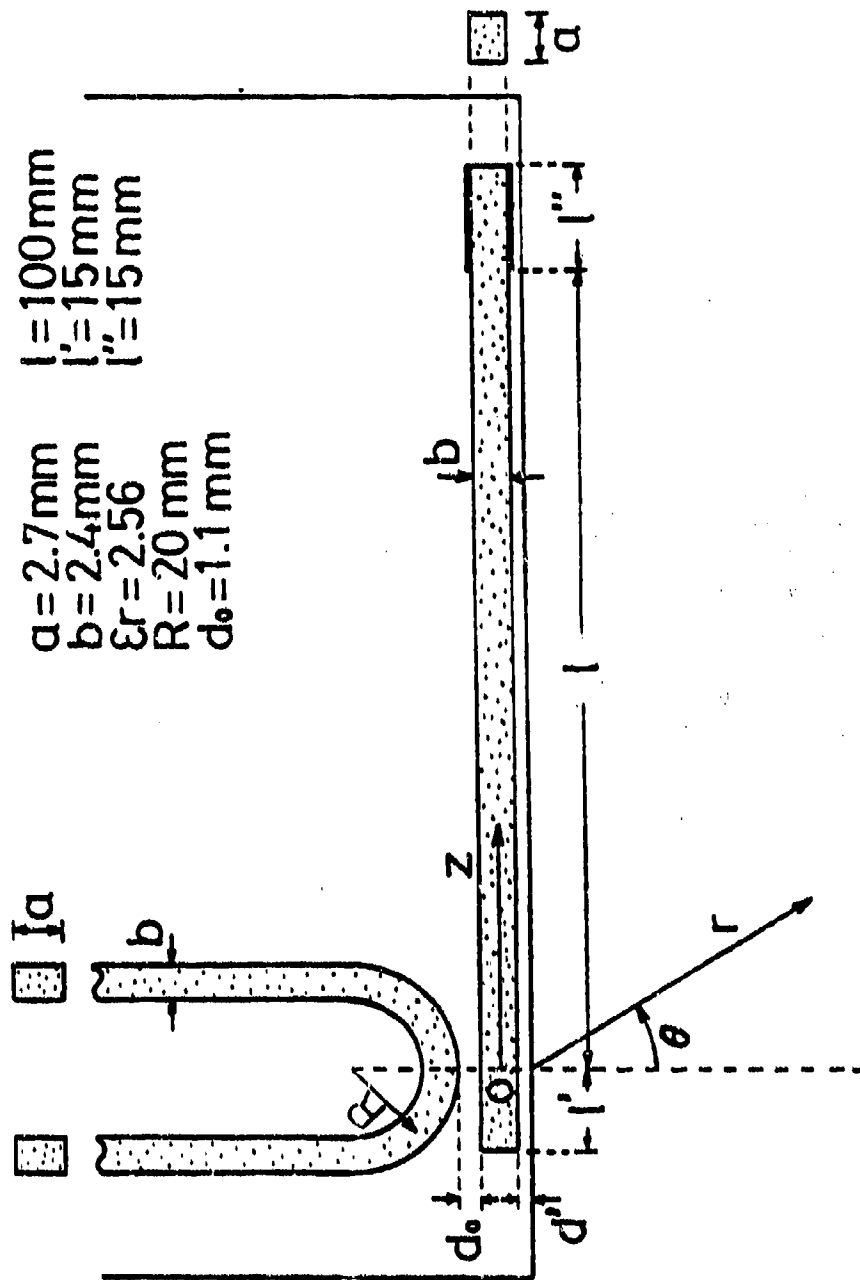


Fig. 3.18 Sketch of experimental set-up employed by T. Yoneyama in the measurement of leakage constant.

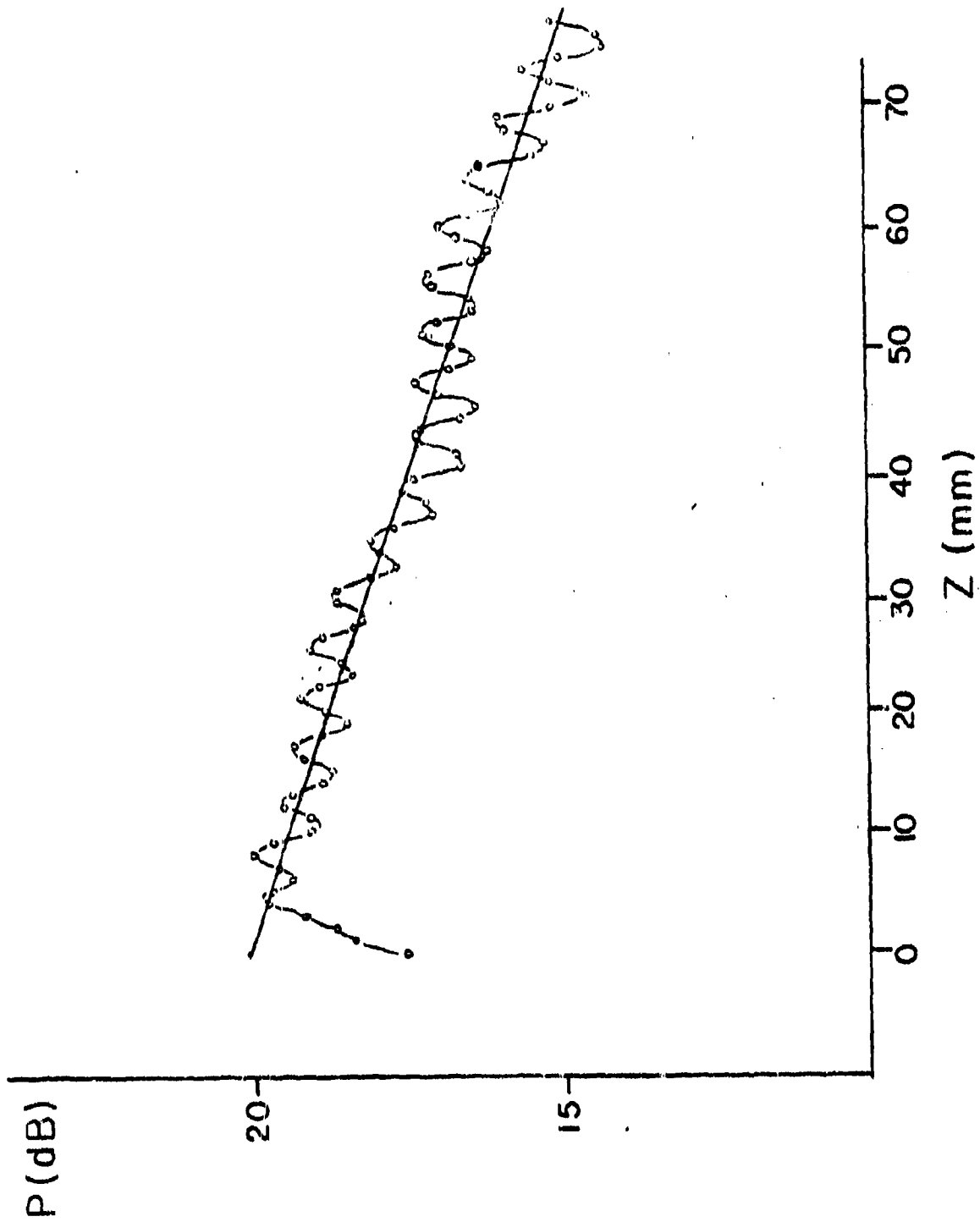


Fig. 3.19 Semilog plot, comparable to that in Fig. 3.17, obtained by T. Yoneyama in his probe measurements.

our d). An important difference between his measurements and ours is due to the difference in frequency. His structure is electrically much longer than ours; that is why the period of the ripples seems much smaller in Fig. 3.19 than in Fig. 3.17.

In Fig. 3.20 we present a comparison between Yoneyama's measured values and our theoretical results for the leakage constant α as a function of d . Even though his measurements were taken at a frequency of 50 GHz and our calculations were made at 48 GHz, the frequencies are close enough together to permit comparison. It is seen that the agreement is quite good, demonstrating that the discrepancy in Fig. 3.15 is not due to an error in our theoretical results.

3. Comparisons With Theory

The measurement procedure and the measurement set-up were described in Sec. C, 1. The measurements that were taken were of the leakage constant α as a function of the distance d between the air-dielectric interface and the radiating open end. The values of plate separation a , dielectric strip width b , and relative dielectric constant ϵ_r were maintained the same throughout the measurements; these values are $a = 0.500$ inch, $b = 0.378$ inch, and $\epsilon_r = 2.56$. The different values of d were $d = 0.150$, 0.200 , 0.250 , 0.300 , and 0.378 , all in inches. For each value of d , measurements were made at the following frequencies: 10.1, 10.2, 10.4, 10.6, and 10.8, all in GHz.

For each of these 25 different cases, probe measurements were made as a function of distance along the structure, and a plot similar to that in Fig. 3.17 was obtained. As explained in Sec. C, 1, the value of α was then determined from the slope of the straight line through the average of the curve. However, the intrinsic loss, comprised of the metal and the dielectric losses, must be subtracted from the α determined from the plot

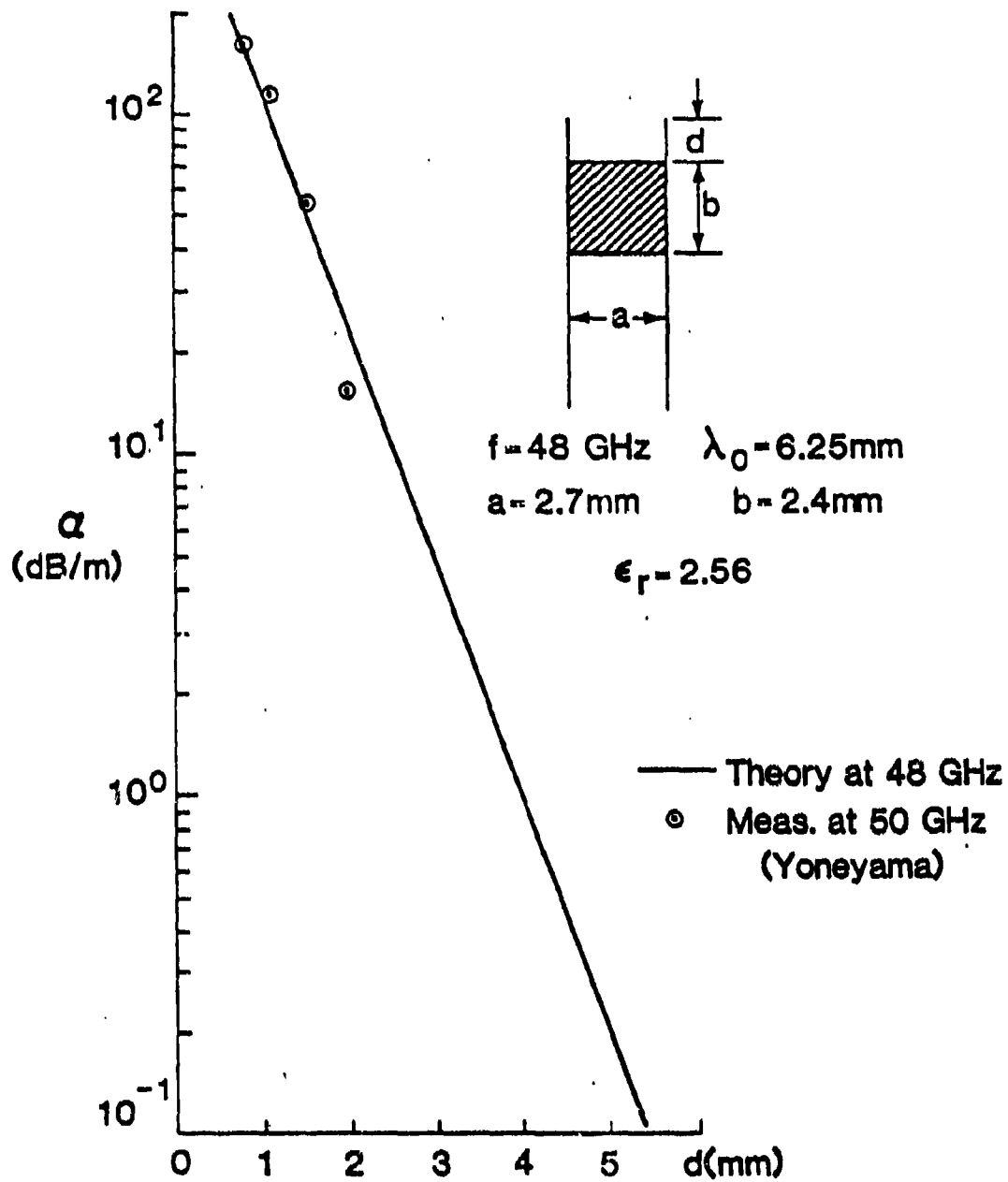


Fig. 3.20 Comparison between our theoretical calculations at 48 GHz and measurements taken by T. Yoneyama at 50 GHz for the leakage constant α as a function of distance d between the air-dielectric interface and the radiating open end.

in order to obtain the leakage loss itself.

Following the method described in Sec. C, 1 for measuring the intrinsic loss, the following values as a function of frequency were found for the structure indicated above (d is then essentially infinite):

| | | | | | | |
|------------------------|---|------|------|------|------|------|
| frequency (GHz) | : | 10.1 | 10.2 | 10.4 | 10.6 | 10.8 |
| intrinsic loss (dB/m): | | 2.2 | 2,3 | 2.5 | 2.7 | 2.9 |

In the values for α reported below, it is understood that these values were subtracted from the directly measured ones.

In Figs. 3.21 through 3.25, we present comparisons between theoretical curves and these measured results. The solid lines in these figures all represent numerical data computed using the almost-rigorous theory derived in Sec. A, 2; the measured points are indicated by x's. In each figure, the leakage constant α is plotted as a function of the distance d; the different figures correspond to different values of frequency. We therefore present in these figures five different theoretical curves, and 25 different experimental points.

The agreement is seen to be very good over the whole range of values of d and over all the frequencies. The theory is essentially rigorous, and systematic care was taken with respect to the measurements, so that the agreement found is highly gratifying.

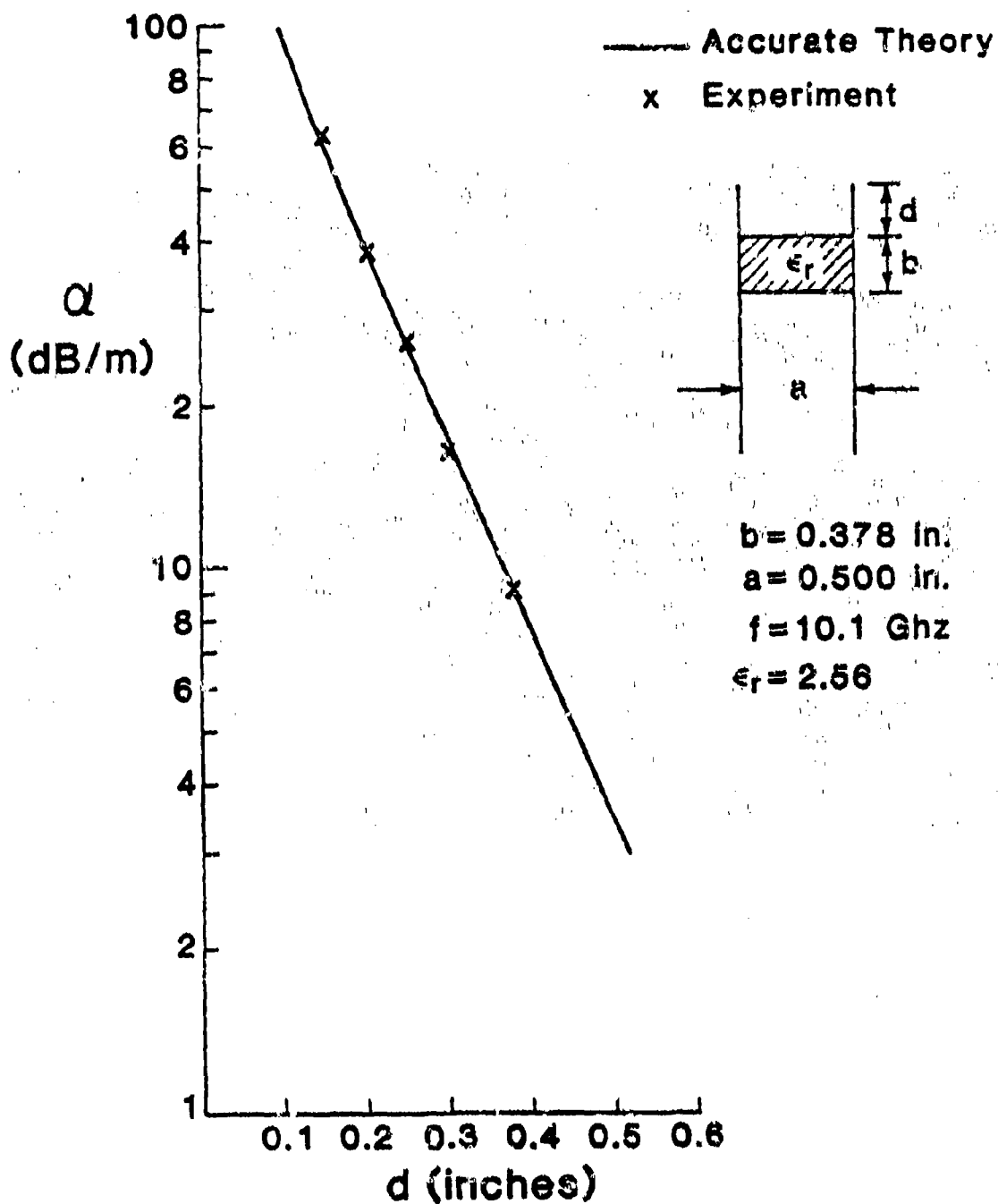


Fig. 3.21 Comparison between our theoretical calculations and our measured results for the leakage constant α as a function of distance d , at a frequency of 10.1 GHz.

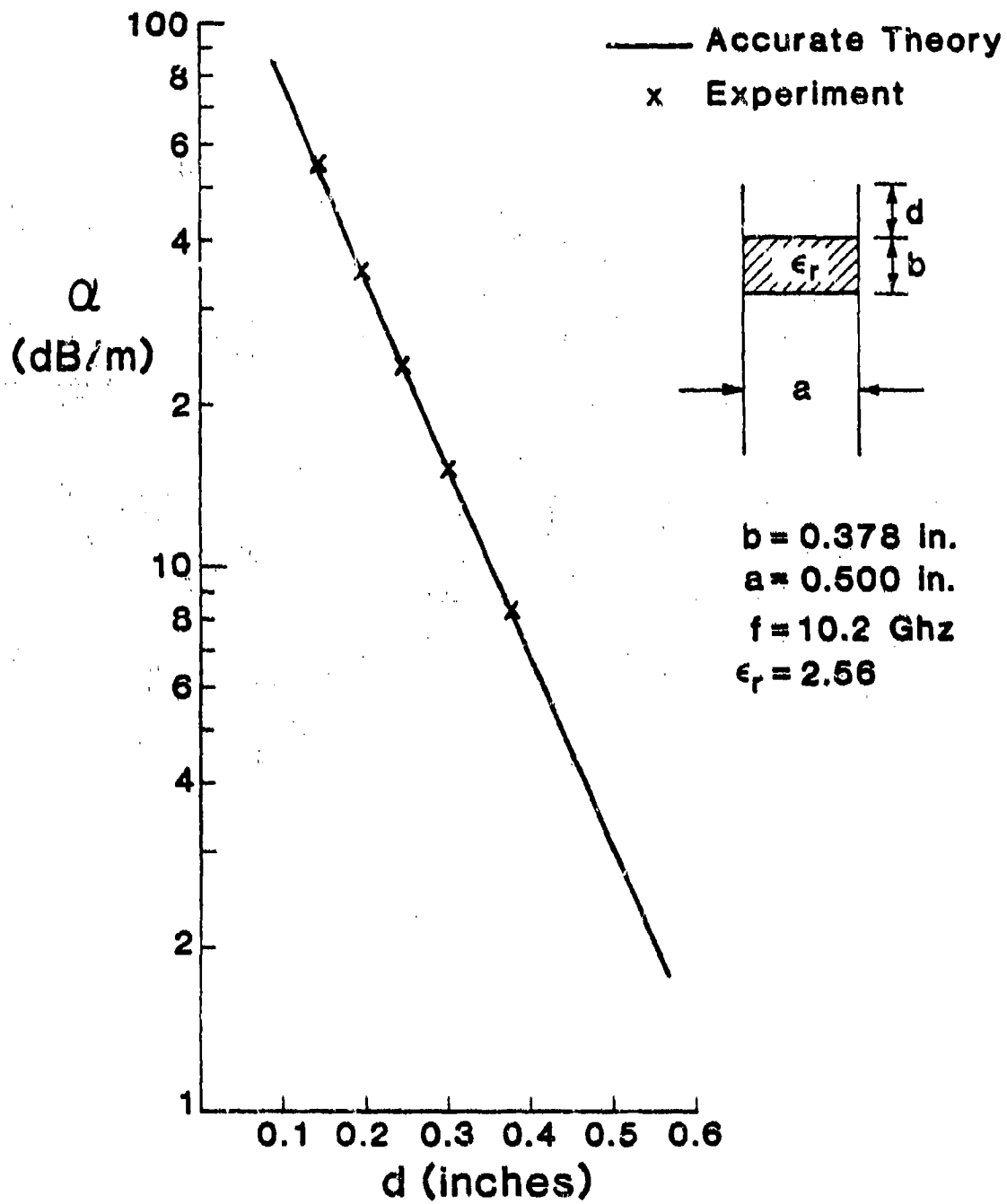


Fig. 3.22 Same as Fig. 3.21, but at a frequency of 10.2 GHz.

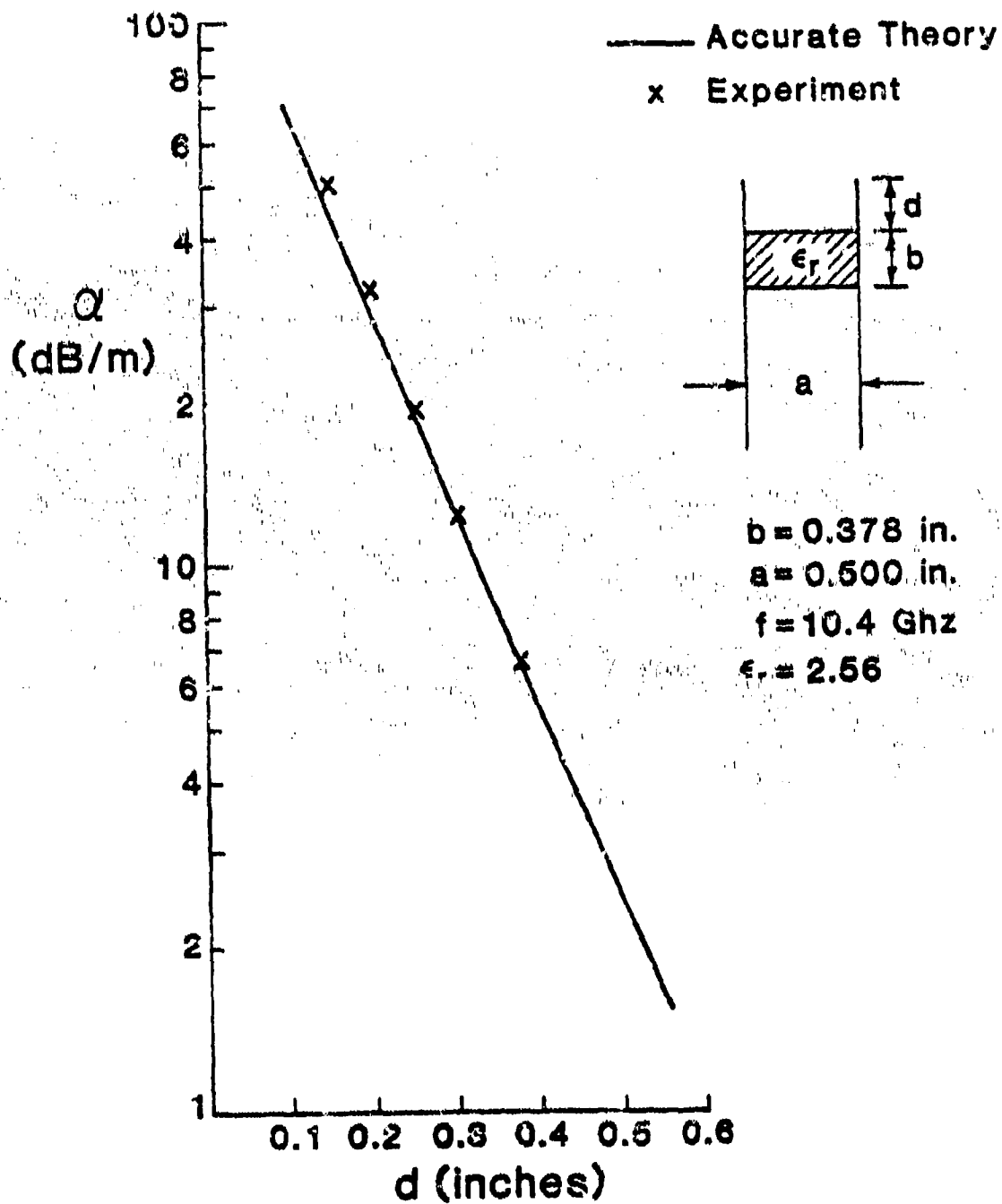


Fig. 3.23 Same as Fig. 3.21, but at a frequency of 10.4 GHz.

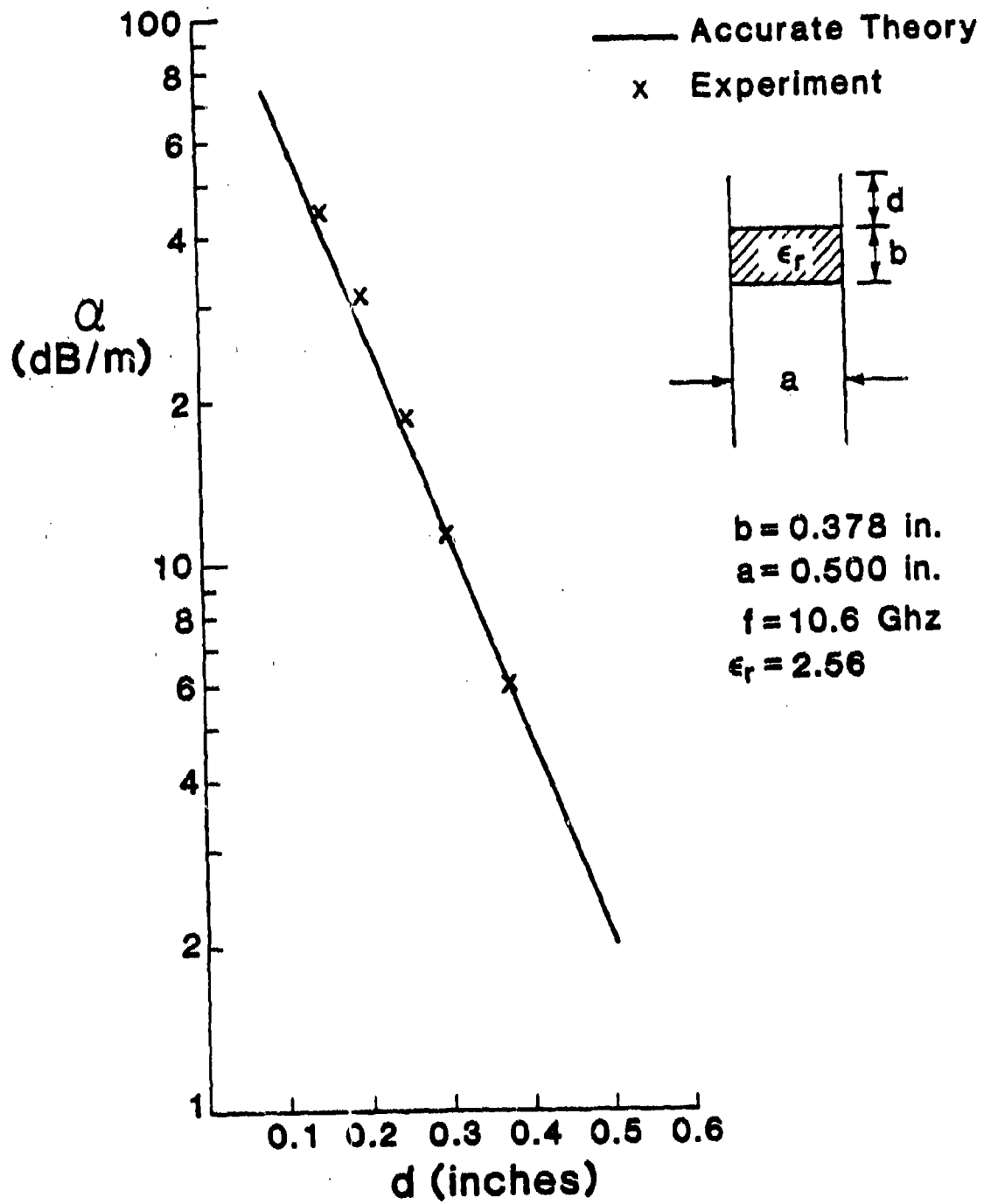


Fig. 3.24 Same as Fig. 3.21, but at a frequency of 10.6 GHz.

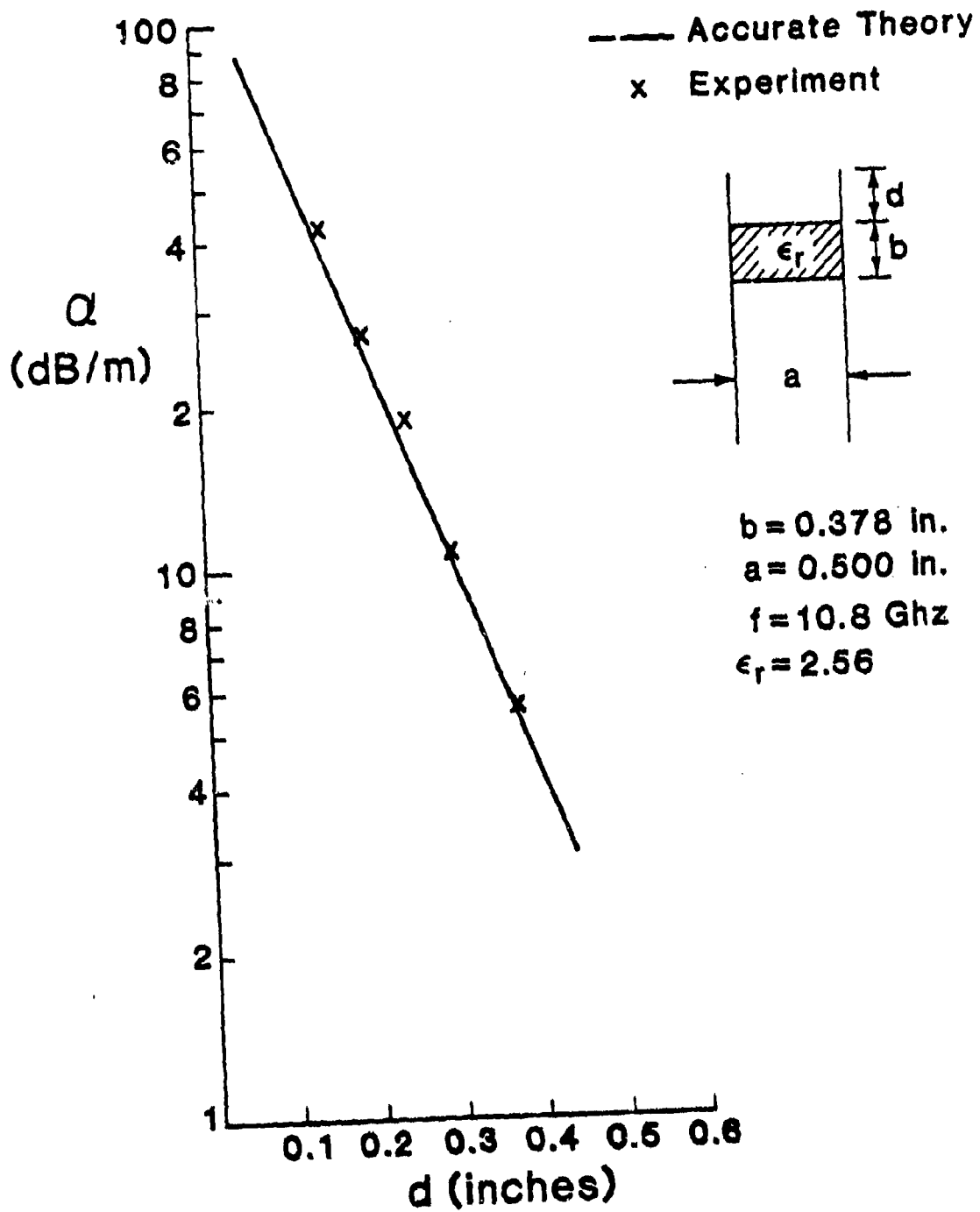


Fig. 3.25 Same as Fig. 3.21, but at a frequency of 10.8 GHz.

D. NEW ASYMMETRIC ANTENNA

It was mentioned in Sec. C, 1, that during the course of our measurements on the foreshortened-top leaky wave structure we found that a small air gap sometimes developed between the dielectric strip and the metal plates. We overcame the potential difficulty by employing a very thin double-backed adhesive strip, but we speculated about what effect such an air gap might have, and these thoughts led to the new asymmetric antenna described here. The principle of operation of the new antenna is described in Sec. D, 1.

While deciding how best to analyze the basic structure, we recognized that there are features about this structure that strongly resemble those of the family of dielectric strip waveguides. Those guides can also become leaky under appropriate circumstances, but they are not generally suitable as antennas. Because of this recognition, however, we analyzed the new antenna structure by employing the mode-matching procedure that we developed previously [26] under the Joint Services Electronics Program contract at the Polytechnic [37]. We even found that the computer program developed in that context could be applied here after appropriate modifications. Also, the analysis of the new leaky wave structure in NRD guide began near the end of the present contract. The kinship to the family of dielectric strip guides in fact permitted us to logically and legitimately continue the analysis of this structure under JSEP sponsorship after the present contract ended.

The main features of the analysis, and some numerical results, are presented in Sec. D, 2. In the context of these results, we indicate further the close relation of the new structure to leaky dielectric strip guides. Most striking is the presence of sharp dips in the curve of α as a function of strip width; that uncommon phenomenon also occurs for the dielectric strip guides, and the explanation for it there is valid here as well. Some other similarities and certain differences between the structures are also discussed. The section ends with some comments on what work still needs to be done in connection with this new type of antenna.

1. Principle of Operation

The leakage mechanism can best be understood by examining the basic structure. Let us refer to Figs. 3.26 (a) and (b), which show, respectively, the nonradiating NRD guide and the guide containing an asymmetric air gap. The structures are placed horizontally, rather than vertically, to permit direct comparison later with dielectric strip waveguides.

The first structure, in Fig. 3.26(a), is that of NRD guide itself, but with side walls of finite length. The length is sufficiently great, however, that the evanescent field of the lowest mode with the electric field polarization shown has negligible amplitude at the open ends. As a result, the guide does not leak, in contrast to the leaky wave antenna discussed in detail in Secs. A, B and C above, where one side of the NRD guide was foreshortened substantially.

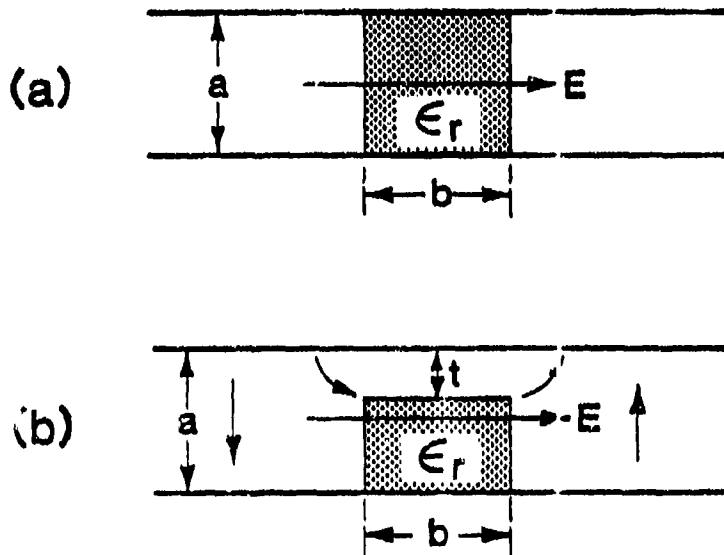


Fig. 3.26 Cross sections of (a) Nonradiating NRD guide, and (b) NRD guide containing an asymmetric air gap, which produces leakage. The structures are placed on their sides to permit later comparison with open dielectric strip waveguides.

In the second structure, that in Fig. 3.26(b), the asymmetrically placed air gap introduces new field components, as is shown in the figure for the electric field. As is seen, the distortion of the electric field lines produces a net vertical electric field, thereby exciting the TEM mode in the parallel plate region away from the dielectric strip. Since the TEM mode will propagate at all frequencies, it will carry power away from the dielectric strip region at an angle toward the openings at the sides, thereby producing power leakage. Because of the symmetry of the structure, power leaks away on both sides, but with opposite phase, as shown in Fig. 3.26(b) by the vertical electric field line on each side of the center strip.

Although the NRD guide will operate satisfactorily as a waveguide whether the guided mode is fast or slow, the antenna with the asymmetric air gap will radiate only when the guided wave is fast. This requirement follows readily from observing the wavenumbers. For the TEM mode, which is the $n = 0$ transverse mode,

$$k_o^2 = k_z^2 + k_{y0}^2, \text{ or } k_{y0} = [k_o^2 - k_z^2]^{1/2} \quad (3.89)$$

where k_z is the wavenumber of the guided wave (in the axial direction), and k_{y0} is the transverse wavenumber in the y direction in the outer air regions. If the guided wave is a fast wave, $k_o > k_z$, so that k_{y0} is real; for a slow wave, k_{y0} is imaginary, and the wave is evanescent transversely. (Actually, k_z and k_{y0} will possess small imaginary parts when leakage occurs, so that k_z and k_{y0} are really complex, but the simple physical idea presented above is still valid.)

For an actual leaky wave antenna, the antenna aperture amplitude distribution is tapered to control the side lobes. In this structure, such a taper can be produced easily by simply changing the thickness of the air gap, beginning with it completely closed and then gradually (in distance) opening it. For a practical antenna to be achieved, the structure would also have to be closed by a metal wall on one side, so that the radiation occurs from one side only. Additional comments in this regard are given at the end of the next section.

2. Analysis and Numerical Results

A dielectric step junction is present at each side of the dielectric strip in Fig. 3.26(b). At each such junction, all the higher transverse modes are excited in both the air region and the partially dielectric-filled region. In the air region, only the TEM transverse mode is above cutoff; in the partially dielectric-filled region, both the lowest TE and TM transverse surface wave modes are above cutoff. The remaining modes on both sides are evanescent, and are therefore stored in the vicinity of the junctions and contribute to their reactive nature.

The propagation characteristics of the leaky wave structure were obtained by a mode-matching procedure in the transverse direction similar to that described in detail for the analysis of leakage from dielectric strip waveguides [26,27]. Numerical values for a specific case for the leakage constant α as a function of the dielectric strip width b are presented in Fig. 3.27.

We should first note that the leakage values are quite large, being equivalent at the maximum value to about 1/2 dB per wavelength. The most dramatic behavior, however, concerns the series of sharp dips in α . This seemingly odd behavior also occurs in the leakage from dielectric strip waveguides, and it was explained in that context [27].

Examples of dielectric strip guides for millimeter waves are the rectangular dielectric image line, the "insular" image line, and the inverted strip guide, illustrated in Fig. 3.28. The dielectric image line, the topmost guide, never leaks, but the other two can because they possess dielectric wings that can carry away power in surface wave form. On the other hand, it can be shown [27] that the dominant mode on any of these dielectric strip guides does not leak, but that the lowest mode of the opposite polarization can leak, and that higher modes almost always leak.

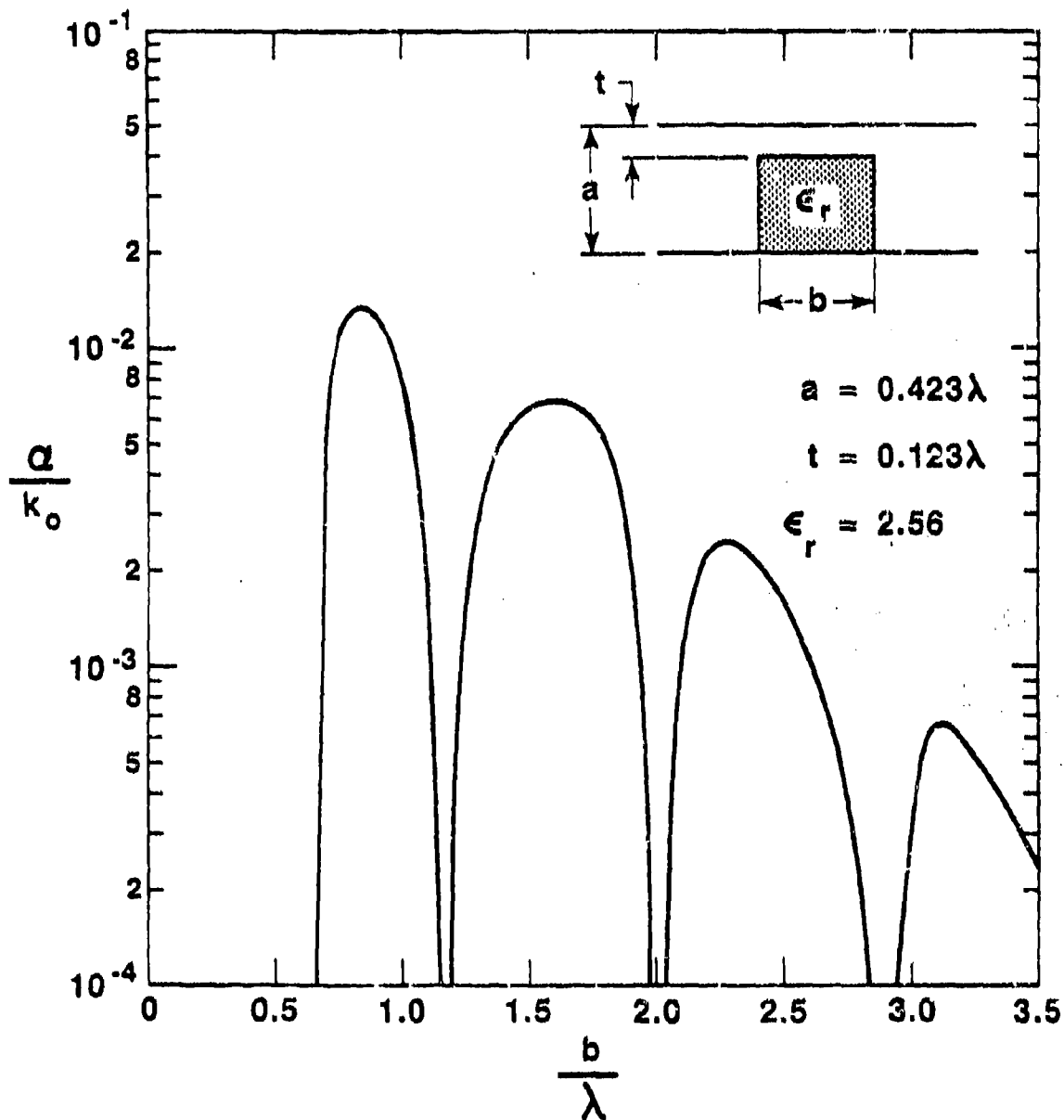


Fig. 3.27 Curve of leakage constant α as a function of dielectric strip width b for the new leaky wave structure shown in Fig. 3.26(b). Note the unusual sharp dips, characteristic of leakage from open dielectric strip waveguides.

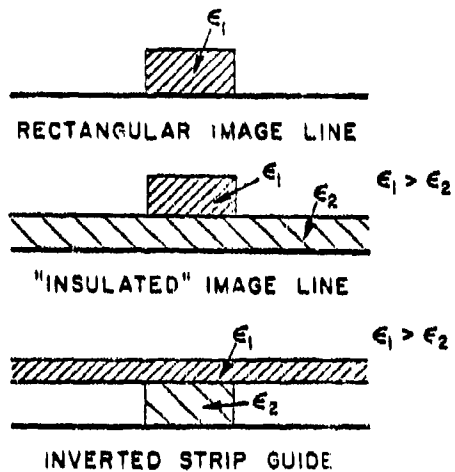


Fig. 3.28 Examples of open dielectric strip waveguides for millimeter waves.

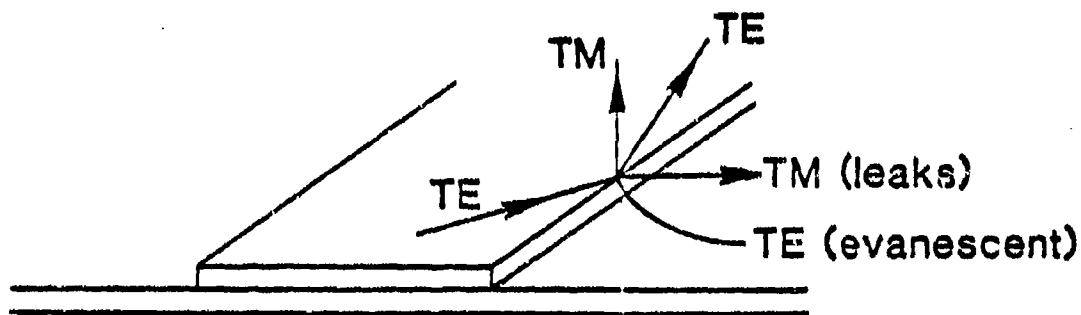


Fig. 3.29 Pictorial representation of TE-TM mode conversion effects at one side of an open dielectric strip waveguide that give rise to leaky modes.

We may now draw the first parallel between the dielectric strip guides and the structure in Fig. 3.26(b). The lowest mode on that structure possesses a vertical electric field, and may be viewed as a perturbation of the lowest mode on the dielectric image line. Even with asymmetry, that mode will not radiate. The mode shown in Fig. 3.26(b) is indeed the lowest mode of the opposite polarization, with the electric field horizontal instead of vertical. (It is also the mode we want for millimeter wave use, because the electric field is basically parallel to the walls so that the metal wall losses decrease with increasing frequency.)

The next basic point of similarity involves the mode conversion that occurs at the dielectric step junctions in each of these structures. The nature of this mode conversion for dielectric strip waveguides is shown pictorially in Fig. 3.29. Suppose first that no mode conversion occurs. Then, an incident TE surface wave ray produces only a reflected TE surface wave ray inside the strip and a "transmitted" TE ray outside that is evanescent, in keeping with the requirement that the mode be bound. When mode conversion at the dielectric step junction is taken into account, we find in addition a TM surface wave ray inside the strip region and a TM surface wave ray outside of it. Depending on the wavenumber conditions, the TM ray outside may or may not be propagating; if it is, it corresponds to the leakage of power in the form of a surface wave. The next interesting point to observe is that the polarization of that leaking TM surface wave outside of the strip region is opposite to that of the incident TE surface wave inside the strip region. Thus the power that leaks away has a polarization opposite to that possessed by the main portion of the guided mode.

If we were to draw a pictorial representation for the asymmetric NRD guide structure similar to that in Fig. 3.29 for dielectric strip guides, we would need to replace the outside dielectric layer by an air-filled parallel plate guide. The modes in the outside region would then not be surface waves but parallel plate modes instead. We would again have an incident TE surface wave ray, as before, with a reflected TE ray inside and an evanescent TE parallel plate mode outside. We would also have a

mode-converted TM surface wave ray inside, as before, but outside we would now need a mode-converted TEM ray. This TEM ray would or would not be propagating transversely depending on conditions, but we earlier noted that propagation would occur if the guided wave were fast. We also note that the polarization of the leaking TEM wave is opposite to that of the incident TE surface wave ray, in agreement with the situation found for dielectric strip waveguides.

The final correspondence relates to the strong dips found in the curve of α vs. b (Fig. 3.27). Similar dips are found in corresponding curves for dielectric strip guides. These dips are "resonances" or "cancellation effects" due to the mode-converted TM surface wave that bounces back and forth inside the dielectric strip region. That mode-converted contribution is also present in the asymmetric NRD guide antenna structure, so that we should indeed expect to find similar strong dips present.

We therefore see that there are very strong correspondences in physical behavior between the asymmetric NRD guide antenna and the leaky dielectric strip waveguides. They are similar in that a mode-converted TM surface wave is produced inside the strip region, that the polarization of the leakage power is opposite to that in the main guided wave, and that strong dips are found in the attenuation plots. One difference between the structures is that the leakage power is carried by a TEM mode in parallel plate guide rather than by a surface wave. It is interesting that the α is caused by the TEM mode outside of the strip region, but that the resonant dips in the values of α relate to the mode-converted TM surface wave inside.

Another important difference is present between these structures. In the dielectric strip guides, the outside region can always support a surface wave in some direction, so that its effective dielectric constant for the basic mode is real and positive. In contrast, the outside region in the asymmetric NRD guide structure, corresponding simply to the parallel plates, is below cutoff for the basic mode (the TE_1 mode), so that its

effective dielectric constant in that region is negative real. As a result, the lowest longitudinal guided mode for the overall structure is above cutoff for any value of dielectric strip width in the case of dielectric strip guides, whereas, for the structure in Fig. 3.26(b), the longitudinal guided mode will go below cutoff if the strip width b becomes sufficiently small. This feature explains why the curve in Fig. 3.27 stops at a non-zero value of width b .

For most millimeter wave applications, it is desirable to restrict the radiation from the leaky wave antenna to one side only. That modification as applied to the structure of Fig. 3.26(b) can be accomplished by placing a short-circuiting metal plate some distance away from the dielectric strip on one side and leaving the other side open or attaching it to a ground plane. This more complicated cross section still remains to be analyzed. Two problems will require attention. The first is that the leakage rate α will be affected by the precise location of the short-circuiting plate, so that its position must be optimized. The second is that the cross section is no longer symmetrical, so that additional modal solutions become possible. The added complications introduced by these additional solutions must be examined and then taken into account.

This new NRD guide leaky wave antenna, based on asymmetry, is of interest because of its simple configuration, its large maximum leakage rate (so that a large range of beam widths can be achieved), its ease of connection with NRD guide integrated circuitry, and the fact that its width is less than half a wavelength. This last point is of particular interest if the antenna is used as a line source in a phased array of such line sources, since grating lobes would then automatically be eliminated. An additional virtue of this antenna is that the polarization of its radiation is the opposite of that obtained from the foreshortened-top NRD guide antenna.

R E F E R E N C E S

1. W. Rotman and A. A. Oliner, "Asymmetrical Trough Waveguide Antennas," IRE Trans. Antennas and Propag., vol. AP-7, No. 2, pp. 153-162, April 1959.
2. T. Yoneyama and S. Nishida, "Nonradiative Dielectric Waveguide for Millimeter-Wave Integrated Circuits," IEEE Trans. on Microwave Theory Tech., vol. MTT-29, No. 11, pp. 1188-1192, November 1981.
3. T. Yoneyama and S. Nishida, "Nonradiative Dielectric Waveguide Circuit Components," International Conference on Infrared and Millimeter Waves, Miami, Florida, December 1981.
4. T. Yoneyama, M. Yamaguchi and S. Nishida, "Bends in Nonradiative Dielectric Waveguide," IEEE Trans. Microwave Theory Tech., vol. MTT-30, pp. 2146-2150, December 1982.
5. T. Yoneyama, N. Tozawa and S. Nishida, "Coupling Characteristics of Nonradiative Dielectric Waveguides," IEEE Trans. Microwave Theory Tech., vol. MTT-31, pp. 648-654, August 1983.
6. T. Yoneyama, F. Kuroki and S. Nishida, "Design of Nonradiative Dielectric Waveguide Filter," Digest of IEEE International Microwave Symposium, pp. 243-244, San Francisco, CA May 30 - June 1, 1984.
7. T. Nakahara, Polytechnic Institute of Brooklyn, Microwave Research Institute, Monthly Performance Summary, Report PIBMRI-875, pp. 17-61, 1961.
8. T. Nakahara and N. Kurauchi, "Transmission Modes in the Grooved Guide," J. Inst. of Electronics and Commun. Engrs. of Japan, vol. 47, No. 7, pp. 43-51, July 1964.
9. T. Nakahara and N. Kurauchi, "Transmission Modes in the Grooved Guide," Sumitomo Electric Technical Review, No. 5, pp. 65-71, January 1965.
10. H. Shigesawa and K. Takiyama, "Transmission Characteristics of the Close Grooved Guide," J. Inst. of Electronics and Commun. Engrs. of Japan, vol. 50, No. 11, pp. 127-135, November 1967.
11. H. Shigesawa and K. Takiyama, "On the Study of a Close Grooved Guide," Science and Engineering Review of Doshisha University, Japan, vol. 9, No. 1, pp. 9-40, May 1968.
12. F. J. Tischer, "The Groove Guide, a Low-Loss Waveguide for Millimeter Waves," IEEE Trans. on Microwave Theory Tech., vol. MTT-11, pp. 291-296, September 1963.

13. J.W.E. Griemsmann, "Groove Guide," Proc. Sympos. on Quasi-Optics, Polytechnic Press of Polytechnic Institute of Brooklyn, pp. 565-578, 1964.
14. N. Y. Yee and N. F. Audeh, "Wave Propagation in Groove Guides," Proc. National Electronics Conf., vol. 21, pp. 18-23, 1965.
15. D. J. Harris and K. W. Lee, "Groove Guide as a Low-Loss Transmission System for Short Millimetric Waves," Electron. Lett., vol. 13, No. 25, pp. 775-776, 8 December 1977. Professor Harris and his colleagues have published many papers on this topic, of which this is one of the first. One of their late works is given as ref. 16.
16. D. J. Harris and S. Mal, "Groove-Guide Microwave Detector for 100 GHz Operation," Electron. Lett., vol. 17, No. 15, pp. 516-517, 23 July 1981.
17. J. Meissner, "Calculation of Coupling of Two Grooves in a Parallel Plate Guide," Electron. Lett., vol. 22, No. 18, pp. 956-958, 28 October 1982.
18. J. Meissner, "Radiation Losses of E-Plane Groove-Guide Bends," Electron. Lett., vol. 19, No. 14, pp. 527-528, 7 July 1983.
19. H. M. Altschuler and L. O. Goldstone, "On Network Representations of Certain Obstacles in Waveguide Regions," IRE Trans. Microwave Theory Tech., vol. MTT-7, pp. 213-221, April 1959.
20. N. Marcuvitz, Waveguide Handbook, vol. 10 in the MIT Radiation Laboratory Series, McGraw-Hill Book Co., New York, 1951.
21. A. A. Oliner, "Equivalent Circuits for Slots in Rectangular Waveguide," Report R-234, Microwave Research Institute, Polytechnic Institute of Brooklyn, for the Air Force Cambridge Research Center, under Contract AF19(122)-3, August 1951. This comprehensive report also contained contributions by J. Blass, L. B. Felsen, H. Kurss and N. Marcuvitz.
22. A. A. Oliner, "The Impedance Properties of Narrow Radiating Slots in the Broad Face of Rectangular Waveguide, Part I: Theory, Part II: Comparison with Measurement," IRE Trans. Antennas and Propag., vol. AP-5, No. 1, pp. 4-20, January 1957.
23. A. Sanchez and A. A. Oliner, "Accurate Theory for a New Leaky-Wave Antenna for Millimeter Waves Using Nonradiative Dielectric Waveguide," Proc. URSI International Symposium on Electromagnetic Theory, pp. 397-400, Santiago de Compostela, Spain, August 23-26, 1983.
24. A. Sanchez and A. A. Oliner, "Microwave Network Analysis of a Leaky-Wave Structure in Non-radiative Dielectric Waveguide," Digest of IEEE International Microwave Symposium, pp. 118-120, San Francisco, CA, May 30 - June 1, 1984.

25. A. Sanchez and A. A. Oliner, "Accurate Theory for a New Leaky-Wave Antenna for Millimeter Waves Using Nonradiative Dielectric Waveguide," Radio Science, accepted for publication.
26. S. T. Peng and A. A. Oliner, "Guidance and Leakage Properties of a Class of Open Dielectric Waveguides, Part I: Mathematical Formulations," IEEE Trans. Microwave Theory Tech. vol. MTT-29 (Special Issue on Open Guided Wave Structures), pp. 843-855, September 1981. Invited paper.
27. A. A. Oliner, S. T. Peng, T. I. Hsu and A. Sanchez, "Guidance and Leakage Properties of a Class of Open Dielectric Waveguides, Part II: New Physical Effects," IEEE Trans. Microwave Theory Tech., vol. MTT-29 (Special Issue on Open Guided Wave Structures), pp. 855-869, September 1981. Invited paper.
28. P.J.B. Clarricoats and A. A. Oliner, "Transverse-Network Representation for Inhomogeneously Filled Circular Waveguides," Proc. IEE, vol. 112, No. 5, pp. 883-894, 1965.
29. L. A. Weinstein, The Theory of Diffraction and the Factorization Method, pp. 29-50, The Golem Press, Boulder, Colorado, 1969 (translated from Russian).
30. N. Marcuvitz, "Radial Transmission Lines," Chapter 8 of book by C. G. Montgomery, R. H. Dicke and E. M. Purcell, Principles of Microwave Circuits, vol. 8 in the MIT Radiation Laboratory Series, McGraw-Hill Book Co., New York, 1948.
31. A. Sanchez, "A Leaky-Wave Antenna for Millimeter Waves Using Nonradiative Dielectric Waveguide," Ph.D. Thesis, Polytechnic Institute of New York, June 1983.
32. N. Marcuvitz, Waveguide Handbook, vol. 10 in the MIT Radiation Laboratory Series, McGraw Hill Book Co., New York, 1951. See p. 4.
33. H. Shigesawa and K. Takiyama, 1964, "Study of a Leaky H-guide," Internat. Conf. on Microwaves, Circuit Theory and Information, Paper MI-7. Tokyo, Japan. More complete version in K. Takiyama and H. Shigesawa, March 1967, "On the Study of a Leaky H-guide," Science and Engineering Review of Doshisha University, vol. 7, No. 4, pp. 203-225, (in English).
34. H. Shigesawa, K. Fujiyama and K. Takiyama, July 3, 1970, "Complex Propagation Constants in Leaky Waveguides with a Rectangular Cross Section," presented at a Japanese scientific conference.
35. K. Takiyama and H. Shigesawa, February 1967, "The Radiation Characteristics of a Leaky H-guide." J. Inst. Electrical Communic. Engrs. of Japan (J.I.E.C.E.), vol. 50, No. 2, pp. 181-188, (in Japanese).
36. T. Yoneyama, private communication, July 4, 1983.
37. Joint Services Electronics Program, Contract No. F49620-82-C-0084.

APPENDIX A

THE DOMINANT MODE PROPERTIES OF
OPEN GROOVE GUIDE: AN IMPROVED SOLUTION

by

A. A. Oliner and P. Lampariello

TABLE OF CONTENTS

| | <u>Page</u> |
|---|-------------|
| Preface | iii |
| A. INTRODUCTION | 1 |
| 1. Background | 1 |
| 2. The Properties of Groove Guide | 2 |
| B. THE TRANSVERSE EQUIVALENT NETWORK | 5 |
| 1. Transverse Resonance Approach | 5 |
| 2. The Transverse Mode Functions | 6 |
| 3. The Equivalent Network for the Step Junction | 9 |
| (a) The Transformer Turns Ratio | 9 |
| (b) The Shunt Susceptance | 11 |
| 4. The Complete Transverse Equivalent Network | 12 |
| C. NUMERICAL RESULTS | 16 |
| 1. Comparison with Measurements | 16 |
| 2. Additional Numerical Results | 18 |
| D. CONCLUSIONS | 25 |
| E. REFERENCES | 26 |

MISSION
of
Rome Air Development Center

RADC plans and executes research, development, test and selected acquisition programs in support of Command, Control Communications and Intelligence (C³I) activities. Technical and engineering support within areas of technical competence is provided to ESD Program Offices (POs) and other ESD elements. The principal technical mission areas are communications, electromagnetic guidance and control, surveillance of ground and aerospace objects, intelligence data collection and handling, information system technology, solid state sciences, electromagnetics and electronic reliability, maintainability and compatibility.

Printed by
United States Air Force
Hanscom AFB, Mass. 01731